Investigation of the role of Nrf2 in hepatic stellate cells during liver fibrosis using *in vitro* models.

Inauguraldissertation

zur

Erlangung der Würde eines Doktors der Philosophie

vorgelegt der

Philosophisch-Naturwissenschaftlichen Fakultät

der Universität Basel

von

Vincenzo Prestigiacomo

aus Italien

Basel, 2020

Genehmigt von der Philosophisch-Naturwissenschaftlichen Fakultät
auf Antrag von Prof. Dr. Alex Odermatt (Fakultätsverantwortlicher), Prof. Dr. Laura Suter-Dick (Dissertationsleiterin) und Prof. Dr. Christopher Goldring (Korreferent).

Basel, den 24. April 2018

Prof. Dr. Martin Spiess
Dekan der Philosophisch-Naturwissenschaftlichen Fakultät

Table of Contents

Abbreviations

2D:	two-dimensional
3D:	three-dimensional
αSMA:	Smooth muscle α-actin
APAP:	Acetaminophen
ARE:	Antioxidant response element
ECM:	Extracellular matrix
GSH:	Glutathione
GST:	Glutathione S-transferases
HSC:	Hepatic stellate cell
hTERT-HSC:	Immortalized HSC
KC:	Kupffer cell
Keap1:	Kelch-like ECH-associated protein 1
LAP:	Latency-associated peptide
LPS:	Lipopolysaccharide
LSEC:	Liver sinusoidal endothelial cell
MAPK:	Mitogen-activated protein kinase
MMP:	Metalloproteinase
MT:	3D microtissue
MTX:	Methotrexate (MTX)
NPC:	Non-parenchymal cell
Nrf2:	Nuclear factor E2-related factor 2
PDGF:	Platelet-derived growth factor
PDGFRα:	PDGF receptor type alpha
PDGFRβ:	PDGF receptor type beta
R-Smad:	Receptor-regulated Smad
ROS:	Reactive oxygen species
TβRI:	TGF beta kinase receptor type I

TβRII:	TGF beta kinase receptor type II
TAA:	Thioacetamide
TGF-β1:	Transforming growth factor beta 1
TNF-α:	Tumour necrosis factor alpha

1. Summary

Liver fibrosis, known to be a consequence of various acute or chronic cellular insults, is a reversible wound-healing response characterized by fibroblast proliferation and extracellular matrix (ECM) remodelling. In particular, fibrosis results from exposure to liver toxicants or chronic liver diseases, including viral hepatitis and alcohol consumption. If the injury persists, fibrosis leads to portal hypertension, cirrhosis, liver failure, and increased risk of cancer. The development of fibrosis involves several intermediate steps, including hepatocyte injury and cell death, oxidative stress, activation of Kupffer cells (KC), activation of hepatic stellate cells (HSC), and chronic inflammation. Particularly, HSCs have been identified as the primary effector cells of fibrosis, since they orchestrate the deposition of extracellular matrix in normal and fibrotic liver. Following liver injuries, HSCs trans-differentiate into smooth muscle α-actin (αSMA) positive myofibroblasts-like cells in response to several factors released by the other liver cells. Among these factors, transforming growth factor beta 1 (TGF-β1), platelet-derived growth factor (PDGF) and oxidative stress, have been shown to play a critical role.

The present thesis is subdivided into two main projects that focused on the development of a suitable model system to study fibrosis and on the role of TGF-β1, PDGF and Nuclear factor E2-related factor 2 (Nrf2) on HSCs. Currently, most liver fibrosis research is performed *in vivo* since suitable *in vitro* system are lacking. This is due to short longevity of liver cells in culture and inadequacy of cell composition in currently available systems. The first two articles focus on the design and development of three-dimensional (3D) *in vitro* liver fibrosis models: a rat primary cell-based model and a human cell line based model. For the generation of the rat liver model hepatocytes, KC and HSC were isolated from healthy livers whereas the human model contained HepaRG, differentiated THP-1 (macrophages) and immortalized HSCs (hTERT-HSC). These three relevant hepatic cell types were cultured in 3D scaffold-free microtissues. The multicellular models responded to treatment with proinflammatory cytokine TGF-β1 and endotoxin lipopolysaccharide (LPS), displaying hepatocellular damage as demonstrated by decrease in albumin expression, and HSC activation as demostrated by increased αSMA expression and deposition of ECM. In addition, the human model displayed a fibrotic phenotype after exposure to methotrexate (MTX) and thioacetamide (TAA), characterized by the activation of HSC, upregulation of genes involved in the development of fibrosis and the secretion and deposition of extracellular matrix. MTX and TAA also elicited the upregulation of Nrf2 and Kelch-like ECH-associated protein 1 (Keap1) suggesting oxidative defence pathway activation during early stages of fibrosis. This human model is able to reproduce key events, generating a clinically relevant fibrotic phenotype. Both systems represent suitable cell culture-based alternatives to the widely used animal models for the investigation of liver fibrosis, as well as for pharmaceutical testing and anti-fibrotic therapy research.

The second part of the thesis aimed to elucidate the role of key factors TGF-β1 and PDGF as well as the potential role of Nrf2 pathway in HSC activation and to assess the potential of hTERT-HSC as an *in vitro* model to identify these roles. Although many studies have already reported the role of both TGF-β1 and PDGF in human HSCs, is not yet clear to which extent they act on the main cellular processes that characterize activation, such as proliferation, migration and differentiation. The aim of this work was not only to elucidate the effect on these cellular events of each single cytokine, but also the effect of the simultaneous exposure to both factors. Upon exposure to TGF-β1, both primary and hTERT-HSCs activated, differentiating into myofibroblasts-like cells, characterised by αSMA and collagen production. Contrarily, PDGF-AB-treatment did not affect cellular activation and fibrogenic capacity, but induced proliferation and cell migration in a concentration-dependent manner. Simultaneous exposure of HSCs to both factors showed a synergistic effect leading to full cell activation, with increases in both proliferative and fibrogenic capacities. The results obtained in this study may contribute to the design of novel drugs focused on the inhibition of these two key factor in HSC activation as well as to the use of the hTERT-HSC as surrogate of primary HSCs.

Finally, given the crucial role of Nrf2 in maintaining hepatocyte identity and homeostasis as well as the evidence showing its involvement in liver fibrosis, identifying its function in HSCs may be of relevant therapeutic importance. In this work, activation markers, as well as proliferation and migration, were assessed in both human primary and hTERT-HSCs following Nrf2 or Keap1 repression by siRNAs. Knocking down Nrf2 induces αSMA production as well as induction of ECM components, clearly indicating an induction of HSC activation. This induced activation was depended on the TGF-β1/Smad pathway, as the two Smad inhibitors SB431542 hydrate and SB525334 successfully suppressed the effect of the knockdown. HSC with reduced Nrf2-levels also showed an increase in migration and a decrease in proliferation. Moreover, TGF-β1 elicited a stronger induction of HSC activation markers in Nrf2 deficient cells than in wild type cells. These data point to a novel role of Nrf2 in HSCs, where it acts as a repressive factor for HSC activation through the inhibition of the TGF-β1/Smad pathway. This led to the hypothesis that its depletion may be a contributing factor to HSC activation and fibrosis.

In summary, the studies discussed in this thesis deliver contributions addressing two of the limiting factors of liver fibrosis research: the lack of a suitable 3D model and the discovery of potential pathways on which act in order to revert HSC activation. Firstly, novel and well-suited 3D liver models, able to recapitulate the key fibrotic events, were developed. Secondly, the roles of TGF-β1 and PDGF were further clarified in both primary and hTERT-HSCs. Finally, this thesis describes a novel role for Nrf2 as a suppressor of HSC activation. The results underlines the importance of the Nrf2 defence pathway, which may play important roles in many cell types and may thus be involved in several liver diseases.

2. Introduction

2.1 Liver fibrosis and cirrhosis

Fibrosis and consequent cirrhosis are the end-stages of the perpetuation of the normal wound healing response, triggered by chronic liver injury, including chronic viral hepatitis infection, non-alcoholic steatohepatitis, non-alcoholic fatty liver disease, alcoholic liver disease, cholestasis, in-born errors and autoimmune liver disease [1,2]. After acute liver injury, liver parenchymal cells (i.e. hepatocytes) are able to regenerate and replace the necrotic or apoptotic cells [3]. This process is associated with the transient activation of liver non-parenchymal cells (NPCs, i.e. Kupffer, endothelial and stellate cells), resulting in an inflammatory response and a limited deposition of extracellular matrix (ECM) [3]. However, if the injury persists, liver regeneration fails and chronic inflammation and excessive deposition of ECM occur, leading to a progressive substitution of hepatic parenchyma by scar tissue [4]. Fibrosis represents the first stage of liver scarring; however, the accumulation of ECM, extremely enriched in fibrillar collagens (predominantly collagen types I and III), distorts the normal liver architecture resulting in pathophysiologic damage to the organ [5,6]. The resulting cirrhotic liver is characterized by nodule formation and organ contraction with fibrotic septa surrounding regenerating nodules of hepatocytes [6]. The clinical manifestations of cirrhosis vary widely, from no symptoms at all, to physical and mental symptoms when liver damage is extensive [7]. Up to 40% of patients with cirrhosis are asymptomatic and may remain so for more than a decade, but the development of complications (including ascites, variceal haemorrhage or encephalopathy) inevitably induces a progressive deterioration of the liver, resulting in a 50% 5-year mortality rate, with approximately 70% of these deaths directly attributable to liver disease [8]. In addition, this condition led to hepatic insufficiency and portal hypertension with an increased risk for developing hepatocellular carcinoma [9]. Liver fibrosis and cirrhosis have a wide geographic distribution and are important causes of morbidity and mortality worldwide. Global deaths due to cirrhosis have increased since 1980, reaching the 1.95% of the global total deaths in 2010 and 1.8 % of total deaths in Europe in 2013 [10,11].

Currently, no treatments or therapies are available to cure cirrhosis or repair liver scarring that has already occurred. The only effective curative remedy is liver transplantation, but this intervention still presents many disadvantages, such as donor organ deficiency, surgical complications, immunological rejection, high medical costs and high mortality rate of transplanted patients [12,13]. For these reasons, in the last 20 years, there has been an increasing interest in understanding the pathogenesis of liver fibrosis in order to identify the main cellular effectors of this disease as well as the key cytokines and determinants of ECM turnover involved in the fibrotic process. Researchers focused on the development of new therapeutic approaches based mainly on cellular model systems, as more convenient tools to study the molecular mechanisms behind the onset of liver fibrosis and cirrhosis.

2.2 Histological organization of liver

The functional unit of the liver is a well-defined structure known as lobule. When viewed in cross section, each lobule presents a hexagonal shape, consisting of linear cords of hepatocytes which radiate out from a central vein (Figure 1 a and b) [14,15]. The hepatocytes represent the main cell type of the liver, occupying almost 80% of the total liver volume and performing the majority of numerous liver functions, such as metabolism, detoxification, storage and bile production [16]. Liver NPCs (liver sinusoidal endothelial cells LSEC, Kupffer cells KC, and hepatic stellate cells HSC) contribute only to 6.5% to the liver volume, but 40% to the total number of liver cells [16]. To carry out all their functions, the hepatocytes form an epithelial-like structure and are in close contact to vascular channels called sinusoids, of which the fenestrated walls are lined by LSEC, KC and HSC cells [16]. On the apical side of the hepatocytes, tiny bile collection vessels known as bile canaliculi run parallel to the sinusoids on the other side of the hepatocytes and drain into the bile ducts of the liver [15] (Figure 1 b). Situated around the perimeter of the lobule are branches of the hepatic artery, hepatic portal vein (which deliver oxygen and nutrients into the blood in the sinusoids) and bile duct. These three ducts cluster together forming the so called portal triad at the “corner” of the liver lobule [17]. On the other side of the hepatic epithelium, the area between endothelium and hepatocytes, is known as Space of Disse which collects lymph for delivery to the lymphatic capillaries [17,18]. The space of Disse also hosts KC and HSC, where they are in close contact with both hepatocytes and LSEC (Figure 1 c). Dendritic cells and other immune cells are also present in the Space of Disse, containing also ECM components such as collagen I and pro-collagen III, non-collagen glycoproteins, glycosaminoglycans, proteoglycans and matrix-bound growth factors which play an important role in the regulation of cell function in the healthy and fibrotic liver [19,20]. The ECM is in fact an essential histological component of all organs, as it can directly influence the function and behaviour of surrounding cells via interactions with cell surface receptors (including integrin and non-integrin matrix receptors). It also indirectly affects cell function via release of soluble cytokines, which in turn are controlled by local metallo-proteinases (MMPs) [5]. After liver injury, the space of Disse is the first affected liver region, since the HSC are the main ECM producing cells in the normal and injured liver. Hepatic ECM under-goes a transformation and enrichment of fibrillar components, primarily collagen I and collagen III. Similar to other tissues, the fibrotic component of the liver’s wound healing response is medi-ated by myofibroblasts, which are mainly derived from the HSCs [5].

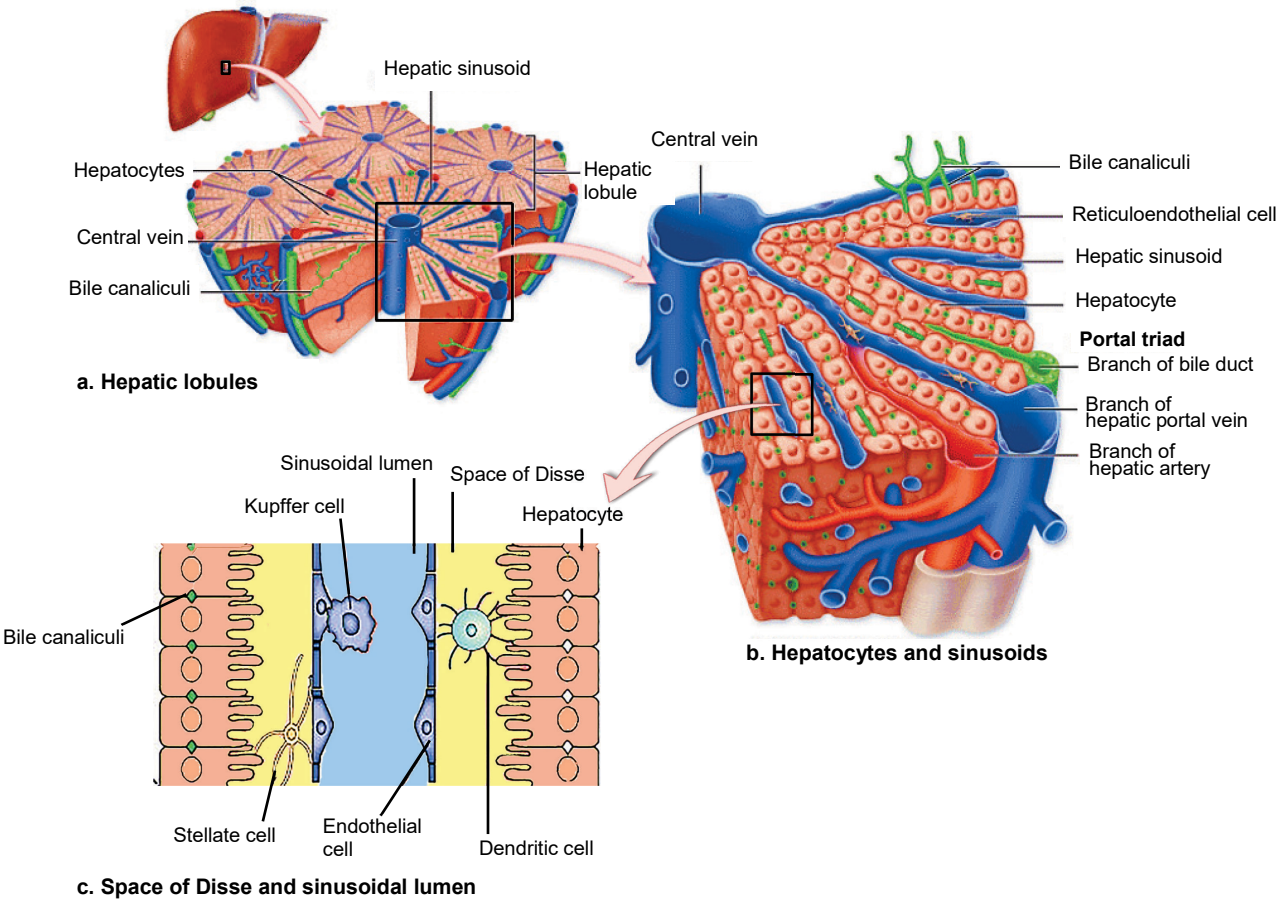

Figure 1. Representation of the histological microstructure of the liver. (a) When viewed in cross section, the liver shows a regular organization in hexagonal structures called liver lobule. (b) A more detailed visualization of the liver lobule shows the hepatocytes organised in an epithelial layer with the hepatic portal vein and hepatic arteries branching among them. (c) Detailed visualization of Space of Disse and sinusoids. The sinusoids are lined by morphologically and phenotypically unique endothelial cells that are characterized by the absence of tight junctions, the absence of a recognizable basement membrane and the presence of open fenestrae that are organized into sieve plates. The sinusoidal endothelium is interspersed with Kupffer cells and overlies the space of Disse, which contains extracellular matrix proteins and hepatic stellate cells. Dendritic cells from the parenchyma exit the liver through the space of Disse. (Adapted from Mescher AL. 2010 [15] and Adams DH et al. 2006 [18]).

2.3 Cellular pathways involved in stellate cell activation

HSCs have been recognized as human liver cells for over 100 years, yet HSC function was only clarified in recent times. HSCs, which constitute 5-8% of all liver cells, are resident perisinusoidal cells in the space of Disse [21,22]. During the last decades, the role of HSCs was thought to be restricted in storing vitamin A (approximately 80% of the total vitamin A in the body), and synthesizing ECM components in the normal and fibrotic liver [23,24]. However, HSCs also are important sources of paracrine, autocrine, juxtacrine and chemoattractant factors, all characteristics that make them critical cells in maintaining microenvironmental homeostasis of the hepatic sinusoid. It was reported that they have the capacity to interact with immune cells, and modulate their activity or promote their differentiation by releasing cytokines or directly acting as antigen presenting cells. Additionally, they can contribute to angiogenesis, hepatocyte regeneration and to the regulation of oxidant stress [22–24].

After liver injury, the HSCs undergo an activation process, which is referred to as the transition from a quiescent vitamin A-rich cell to a highly proliferative and fibrogenic cells. As a result of this transdifferentiation event, they acquire motility, contractile and proinflammatory properties [23,25]. Activated HSCs are smooth muscle α-actin (αSMA) positive myofibroblasts-like cells and are considered the major source of ECM in liver fibrosis [23]. The activation process is temporally divided into two different stages: initiation (also called preinflammatory stage) that renders the cells responsive to cytokines and other local stimuli, and perpetuation during which the cells maintain the activated phenotype and generate fibrosis [5,23].

During the initiation phase, the earliest changes in the HSC are due to paracrine stimulation by all neighbouring cell types, including hepatocytes, LSECs, KCs, platelets and leukocytes. After the injury, the hepatocytes undergo apoptosis and consequently release apoptotic fragments, which are potent fibrogenic elements [26]. Together with the hepatocytes, KCs and resident natural killer cells (Pit cells) are the first cells responsive to liver injury, releasing free radicals, intracellular constituent and signalling molecules [27]. In particular, KCs produce large amounts of reactive oxygen species (ROS) and tumour necrosis factor alpha (TNF-α), enhancing HSC activation and collagen production [5]. However, the initial stage of stimulation is the initiation of HSC proliferation, which has been mainly attributed to KC-derived transforming growth factor beta 1 (TGF-β1) and platelet-derived growth factor (PDGF) [23]. Moreover KCs and LSECs secrete MMPs that convert the latent TGF-β1 in to an activated pro-fibrogenic form that stimulates HSC collagen synthesis [28,29]. In addition, after the injury, leukocytes are recruited to the liver and join KCs in producing compounds that modulate HSC behaviour. Neutrophils produce ROS and nitric oxide, while lymphocytes Th1 and Th2 release cytokines including TNF-α, interleukin 2 and 6 [30].

Differently from the initiation phase, a massive deposition of ECM components characterizes the perpetuation phase. In particular, TGF-β1 leads to increased deposition of fibrillar collagens, fibronectin and release of MMPs by HSCs [23]. During the perpetuation phase, HSCs also produce TGF-β1 maintaining a positive autocrine loop [31]. TGF-β1 also induces the production of specific MMP inhibitor molecules, TIMP-1 and TIMP-2, leading to a net decrease in protease activity and therefore an increase in matrix accumulation resulting in complete remodelling of the liver ECM [32]. However, beside the matrix remodelling and fibrogenic properties, during the perpetuation phase HSCs undergo several other changes in cell behaviour, as proliferation, contractility, and chemotaxis [5]. As in the initiation phase, the most potent mitogen factor involved in the proliferation of HSCs is PDGF. The activation of its signalling pathway leads to stimulation of cell growth, but also to changes in cell shape and motility in HSCs [33,34]. In addition, PDGF has been identified as a chemoattractant molecule, combining its effect with that from the leukocyte chemoattractant MCP-1, inducing HSCs to migrate into the region of injury [35]. The contractility of HSC

shows a more complex regulation pathway, since it involves the interplay of many molecular components such as contractile regulatory proteins MLC kinase (MLCK), Rho kinase 2 (ROCK2) and endothelin-1. The cytological response to the acquisition of contractile properties is the expression of αSMA, while the physiological response is the impeded blood flow both by constricting individual sinusoids and by contracting the cirrhotic liver in Ca(2+)-dependent manner both *in vitro* and *in vivo* [36].

Concurrent with the perpetuation phase, the hepatocytes lose their microvilli and the endothelium loses its fenestrae, impairing the rapid bidirectional transport of solutes between sinusoidal blood and parenchymal cells [37].

2.4 Oxidative stress and liver fibrosis

Although TGF-β1 is the most potent stimulus of fibrogenesis, it acts together with other factors as interleukin-1β, TNF-α and oxidative stress [6,38]. In particular, oxidative stress, understood as an intracellular condition of biochemical imbalance between oxidative and reductive reactions towards oxidation, represents a very common link among different modes of persistent liver injury [39]. In aerobic life, the generation of ROS (including superoxide O_2^-, hydroxyl radical HO^- and non-radical hydrogen peroxide H_2O_2) is a natural mechanism involved in signal transduction pathways, defence against invading pathogens and gene expression to the promotion of growth or death [40]. Nevertheless, an excessive amount of ROS is highly toxic to cells, since they affect both structure and function of major cellular components: proteins, lipids and DNA [41]. Lipids are the main and consistent target of oxidative stress and lipid peroxidation in damaged hepatocytes is one of the first key events leading to liver fibrosis [42]. For instance, excessive oxidation of polyunsaturated membrane lipids is a key outcome in alcoholic liver diseases, due to the alcohol metabolism in the liver [39]. In the hepatocytes, ethanol is degraded through the microsomal system catalysed by cytochrome P450 2E1 (CYP2E1), which generates ROS leading to oxidative stress and cell death [41]. The conversion of ethanol into acetaldehyde by alcohol dehydrogenase in the hepatocytes represents the second metabolic pathway for alcohol. It has been shown that acetaldehyde stimulates H_2O_2 and collagen production by HSC, as well as the up-regulation of cytokines triggering an inflammatory response by KCs and LSECs during alcoholic liver diseases [43,44]. Acetaldehyde, and in particular its derivative malondialdehyde, was shown to be increased also in the serum of patients with chronic hepatitis [39]. Together with the generation of ROS by CYP2E1 activation, a significant increased amount of ROS has been shown to due to glutathione (GSH) depletion during cholestasis and drug-induced liver injury [45]. However, ROS do not damage the hepatocytes exclusively by these pathways; indeed, oxygen radicals may also sensitize hepatocytes to lipopolysaccharide and TNF-α toxicity [41]. The pathological response of the liver to severe oxidative stress is hepatocyte apoptosis. Moreover, increasing evidence has shown that oxidative stress may promote fibrosis and HSC activation in the human liver and in

rodents [46,47]. ROS have been identified as key mediators for the pro-fibrogenic actions on HSCs in several studies, by evaluating the role of conditioned medium from hepatocytes and LSECs in stimulating HSCs [46,48,49]. For these reasons, the liver constitutes a particularly susceptible organ to oxidative stress, and it is therefore equipped with special defence mechanisms to scavenge ROS [41].

2.5 Nrf2 pathway as key regulator of oxidative stress

In the liver, protective mechanisms against oxidative stress include several enzymes (e.g. superoxide dismutase and catalase and glutathione S-transferases GSTs) as well as no enzymatic compounds (e.g. tocopherol, vitamin E, beta-carotene, ascorbate and GSH) [50–52]. In many cell types, the response to oxidative stress is the induction of a series of antioxidant genes through the activation of the antioxidant response element (ARE) as a protective mechanism. Expression of genes containing ARE in the promotor region is largely regulated by nuclear factor E2-related factor 2 (Nrf2). Its activation affects the enzymes that are responsible for GSH homeostasis, NAD(P)H quinone oxidoreductase 1 and UDP-glucosyltransferase [53–55]. Under normal conditions, Nrf2 is an highly unstable protein with a half-life of around 15 minutes, since it is degraded in a Kelch-like ECH-associated protein 1 (Keap1)-dependent manner [53,54]. Nrf2 is constantly bound by Keap1, an adaptor molecule for the Cullin3-based E3 ubiquitin ligase complex, leading to the degradation of Nrf2 via the ubiquitin-proteasome pathway [54]. Elevated levels of ROS and electrophiles cause the inactivation of Keap1, resulting in Nrf2 release and stabilization. Nrf2 translocates into the nucleus and regulates the transcription of a network of genes involved in various cellular activities, including redox balance, metabolism, proliferation, and apoptosis (Figure 2) [56].

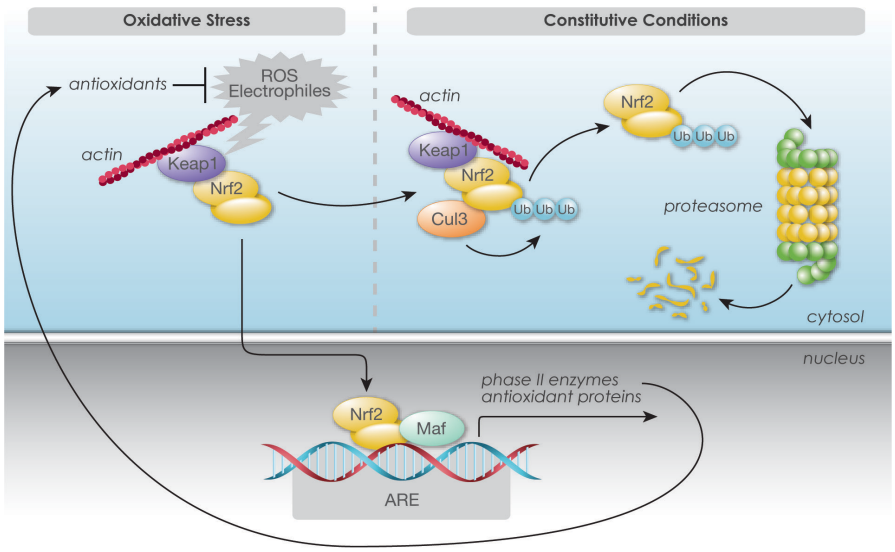

Figure 2. The Nrf2-Keap1 antioxidant pathway. Under constitutive conditions, Nrf2 continuously undergoes proteasomal degradation. Electrophiles, free radicals, or inducers of Nrf2, disrupt the Nrf2-Keap1 association leading to a diminished rate of proteolysis, and thereby enhancing nuclear accumulation. Nrf2 binds ARE elements in the promoter region of its target genes and induces a battery of cytoprotective genes and anti-oxidative enzymes resulting in an adaptive response (repair and removal of damaged protein, cell survival and reduction of oxidative damage). (Reprinted with permission from Olivia L. May, 2012 Cayman Chemical).

Thereby, Nrf2 has been identified as a multi-organ protector, since its involvement in protecting various cell types and is required for maintaining tissue homeostasis by increasing classic ARE-driven detoxification and antioxidant genes [57]. Nrf2 fulfils many different cellular activities, by regulating the expression of over 500 genes, which may be either activated or repressed through the ARE element or by transcription factors regulated by Nrf2 [55]. Once in the nucleus, Nrf2 may interact with the transcriptional regulators Jun and Fos, leading to the induction or suppression of gene transcription, respectively [63,64]. Nrf2 deregulation is a clear hallmark of many human cancers. Among other tumours, Nrf2 is elevated in some breast and lung cancer, while its expression is suppressed in ovarian serous adenocarcinoma as well as in hepatocellular carcinoma [60–64]. In cancers, Nrf2 plays an important role in cell migration, as reported for lung adenocarcinoma cells where it induces migration and metastasis via regulating the calcium binding protein S100P [65]. High susceptibility to carcinogenesis induced by several carcinogens or inflammation has been shown in multiple organ systems in Nrf2-knockout mice [66–68]. In the liver, loss of Nrf2 expression was associated with increased progression of human hepatocellular carcinomas as shown by experiments conducted in transgenic mice [69]. Other studies conducted on animal models suggest that the Nrf2 pathway counteracts alcoholic and non-alcoholic liver disease, viral hepatitis, fibrosis and cancer by activating gene expression [70]. In particular, an exacerbated liver cytotoxicity to acetaminophen (APAP) has been reported in Nrf2-knockout mice, while Keap1-knockout mice were significantly more resistant to APAP than control animals [71–73]. In a different study, *in vivo* analysis of murine liver showed an increase in nuclear translocation of Nrf2 after APAP administration, suggesting an active role of this pathway in the protection against APAP [74]. Nrf2-knockout also strongly aggravated liver damage after treatment with carbon tetrachloride or ethanol in a different set of studies in mice [75,76]. These protective effects are in part connected to the role that Nrf2 plays in the hepatocytes, where it is a key regulator of the constitutive and inducible expression of some phase II and III detoxification enzymes and antioxidant proteins, such as those involved in GSH synthesis [77]. In addition, Nrf2 participates in the regulation of hepatocyte proliferation as well as in the maintenance of a mature hepatocyte identity state during liver regeneration [78,79]. Nrf2 regulates the activity of the Cdk1/Cyclin B1 complex, determining the transition from the G2 to M cell cycle phase in the hepatocytes [80]. Nrf2 also displays an antifibrotic effect on the liver, lung and kidney, by promoting the dedifferentiation of fibroblasts [81–83]. It was also suggested that Nrf2 may interact with the TGF-β1/Smad pathways in regulating cellular motility and plasticity in many cancer cell types [84]. Thus, studying Nrf2 pathway in fibrotic disease, and in particular in relation to TGF-β1, may improve the understanding of the role of oxidative stress and enable the design of new antioxidants-based therapies against liver disorders. This point is further developed in Chapter 4 of this thesis, focusing more in details on the role of Nrf2 in liver fibrosis and HSC activation.

3. Project 1: 3D models for liver fibrosis

3.1 Introduction

Up to now, the most common methods to investigate liver fibrosis and cirrhosis are animal models or human liver biopsies [6]. The main two currently used animal models are rodents where fibrosis has been induced by carbon tetrachloride treatment or bile duct ligation [85]. However, animal systems might not be human-relevant, are costly and subject to ethical problems. In human, hepatic venous pressure gradient has been recently used clinically for fibrosis diagnosis, risk stratification, preoperative screening for liver resection, and assessing the prognosis of liver fibrosis [86]. However, this method does not allow direct analysis on liver tissues, and the most reliable method to assess liver fibrosis and cirrhosis remains the use of liver biopsies. Histological examinations as well as staining of ECM components are indeed useful to understand the stage of fibrosis as well as the causes which lead to the disease [6]. Nonetheless, human biopsies present many disadvantages, as sampling error or semi-quantitative measurement, as well as being an invasive procedure, which implies ethical considerations preventing multiple sampling from patients for research purposes. Hence, a cell-based model system would be a more convenient tool to induce, assess and study the molecular mechanisms during fibrosis development. Cell-based assays have been an important pillar for a wide range of basic and clinical *in vitro* research as well as for drug discovery, providing a simple, fast, and cost-effective system to minimize large-scale and expensive animal experiments [87]. To date, most of cell-based assays use traditional two-dimensional (2D) monolayer cells cultured on flat and rigid substrates. However, 2D cell culture does not adequately reflect the liver situation *in vivo*, mainly due to the loss of hepatocyte-specific phenotype and HSC activation in culture [88,89]. In particular, HSCs undergo activation, losing their quiescent, vitamin A-storing, phenotype and fully taking on their activated, proliferative, myofibroblasts-like phenotype within 7 days in culture [90]. For these reasons, there was a need of a more physiologically relevant cell culture model to study fibrotic diseases, which led to the development of new three-dimensional (3D) culture systems. Differently from 2D models, these 3D systems provide the correct cell polarization and cell-cell contacts [91–93]. For decades, it has been shown that 3D cultures of rat or human hepatocytes maintain liver-specific function for extended culture periods preserving also structural polarity and forming functional bile canaliculi [94–96]. Rat HSCs have also shown to partially revert their activated phenotype when cultured in a 3D microenvironment, such as on collagen, Matrigel or Engelbreth-Holm-Swarm tumour-extracted basement membrane gel [89,97]. However, due to the multicellular pathophysiology of fibrosis, biologically relevant models to study this disease require functional hepatocytes, as well as KC and HSC in a quiescent state and in close spatial interaction. For this reason multicellular models, including primary hepatocytes and primary NPCs, have been developed [88,91,98]. In particular, a collagen gel sandwich 3D model with human primary hepatocytes, HSC and macrophages has been reported to mimic the response to lipotoxic stress that occurs during

non-alcoholic steatohepatitis *in vivo* [98]. In another study, a fibrotic 3D-spheroid based on hepatocytes and HSC has been developed, but this system lacks macrophages that are involved in important steps during the chain of events leading to fibrosis [99]. A different study demonstrated that cultured liver cells on a 3D scaffold had a preserved composition of hepatocytes, HSC, KC and LSEC, and maintained liver function for up to 3 months [92]. However, the suitability of this model for the study of fibrosis cannot be assessed, due to the lack of data on fibrotic response as well as on changes in ECM after stimulation [92]. Therefore, although the benefit of these established models, most *in vitro* systems are of limited use to address fibrosis, due to short longevity in culture, inadequacy of cell composition but especially to high handling complexity [92,98,99].

This chapter of the thesis contains two studies on the development of new rat and human liver models. In particular, the first study aimed on the development of a 3D microtissue (MT) including rat primary hepatocytes, KC and HSC, as key essential cell types involved in hepatic fibrosis. The second and main part of this chapter focused on the development of an analogous model with human relevant cell lines representing hepatocyte (HepaRG), macrophages (THP-1) and HSCs (hTERT-HSC), in order to develop an alternative model to human primary-based systems. Both presented models were generated with the hanging drop method, allowing the production of scaffold-free and size-controlled MTs in a 96-well format. Such systems may be used to investigate the pathophysiology of fibrosis, as well as to the identification of new compounds with pro-fibrotic or anti-fibrotic potential.

3.2 Paper 1

Rat multicellular 3D liver microtissues to explore TGF-β1 induced hepatotoxicity and fibrosis in vitro

Vincenzo Prestigiacomo, Anna Weston, Laura Suter-Dick

Published Manuscript

Aims: Develop a novel 3D rat liver model containing hepatocytes, KC and HSC as key relevant cells in hepatic fibrosis.

Results: The generated model was able to respond to TGF-β1 and LPS, resulting in hepatocyte damage, HSC activation and release of cytokines.

Conclusion: This study showed that the new rat liver model is a powerful system to mimic fibrosis *in vitro* as well as to test potential fibrotic compounds.

Contents lists available at ScienceDirect

Journal of Pharmacological and Toxicological Methods

journal homepage: www.elsevier.com/locate/jpharmtox

Rat multicellular 3D liver microtissues to explore TGF-β1 induced effects

Vincenzo Prestigiacomo[a,b,*], Anna Weston[a], Laura Suter-Dick[a,c]

[a] University of Applied Sciences Northwestern Switzerland, School of Life Sciences, Muttenz, Switzerland
[b] University of Basel, Department of Biomedicine, 4058 Basel, Switzerland
[c] Swiss centre for applied human toxicology, 4055 Basel, Switzerland

ARTICLEINFO

Keywords:
Hepatic stellate cell
Kupffer cell
Microtissues
TGF-β1
Translational

ABSTRACT

Chronic liver damage can lead to fibrosis, encompassing hepatocellular injury, activation of Kupffer cells (KC), and activation of hepatic stellate cells (HSC). Inflammation and TGF-β1 are known mediators in the liver fibrosis adverse outcome pathway (AOP). The aim of this project was to develop a suitable rodent cell culture model for the investigation of key events involved in the development of liver fibrosis, specifically the responses to pathophysiological stimuli such as TGF-β1 and LPS-triggered inflammation.

We optimized a single step protocol to purify rat primary hepatocytes (Hep), HSC and KC cells to generate 3D co-cultures based on the hanging drop method.

This primary multicellular model responded to the profibrotic cytokine TGF-β1 (1 ng/mL) with signs of hepatocellular damage, inflammation and ultimately HSC activation (increase in αSMA expression). LPS elicited an inflammatory response characterized by increased expression of cytokines.

3D-monocultures comprising only Hep displayed different responses, underlying that parenchymal and non-parenchymal cells need to be present in the system to recapitulate fibrosis. The data also suggest that pre-activated HSC may reverse to a quiescent phenotype in 3D, probably due to the more physiological conditions.

1. Introduction

Liver cirrhosis is the end-stage of several liver diseases, in which acute liver damage leads to chronic inflammation and fibrosis (Iredale, 2007). Fibrosis also plays an important role in toxicology, and represents a distinct adverse outcome pathway (AOP). This AOP directly involves three hepatic cell types: The suggested sequence of events involves hepatocyte (Hep) injury and death, followed by the activation of Kupffer cells (KC) and hepatic stellate cells (HSC), leading to chronic inflammation and increased deposition of extracellular matrix (ECM) (Ankley et al., 2010; Horvat et al., 2016). Stimuli such as reactive oxygen species (ROS) and cytokines such as TNF-α and TGF-β1, lead to HSC activation and subsequently to increased deposition of fibrillar components of the ECM (Gäbele, Brenner, & Rippe, 2003) (Friedman, 2000). Activated HSC, in turn, produce more TGF-β1 and potentiate and perpetuate their activation in an autocrine loop (Arias, Lahme, Leur, Gressner, & Weiskirchen, 2002). At this stage several changes in cell behaviour occur, such as increases in proliferation, contractility, fibrogenesis, chemotaxis and release of matrix components.

Currently, studies of cellular and molecular mediators of liver fibrosis are conducted mainly on experimental animal models (Constandinou, Henderson, & Iredale, 2005) (Marques et al., 2012). The rodent *in vivo* models of chemically or surgically induced fibrosis have several disadvantages, as they are time-consuming and lead to considerable animal suffering. Cell culture techniques have recently moved from two-dimensional (2D) cultures to more complex three-dimensional (3D)-cell cultures, that allow long-term culture of multicellular systems. It has been shown that a 3D environment supports the maintenance of human Hep functions and partially restores a quiescent phenotype in rat HSC (Kyffin et al., 2019; Messner, Agarkova, Moritz, & Kelm, 2013). In 2016, Feaver et al. published a 3D model with human primary Hep, HSC and macrophages in a collagen gel sandwich (Feaver et al., 2016). In our laboratory, we have established a human 3D co-culture model with human cell lines (HepaRG, THP1 and hTERT-HSC) able to recapitulate in vitro the key events of a fibrosis AOP and the effect of TGF-β1 on the activation of HSC (Prestigiacomo, Weston,

Abbreviations: 2D, two-dimensional; 3D, three-dimensional; α-SMA, α-smooth muscle actin; AOP, Adverse outcome pathway; ECM, extracellular matrix; FBS, fetal bovine serum; GBSS, Gey's balanced salt solution; Hep, hepatocyte; HSC, hepatic stellate cell; HSC*, pre-activated HSC by culturing for 2 weeks on plastic; IL6, Interleukin 6; KC, Kupffer cell; KC*, pre-activated KC by exposure to 2 μg/mL LPS for 48 h prior the experiment; MT, 3D-microtissue; NPC, non-parenchymal cell; PFA, paraformaldehyde; ROS, reactive oxygen species; SD, standard deviation

* Corresponding author at: University of Basel, Department of Biomedicine, Mattensstrasse 28, 4058 Basel, Switzerland.
E-mail addresses: vincenzo.prestigiacomo@unibas.ch (V. Prestigiacomo), anna.weston@fhnw.ch (A. Weston), laura.suterdick@fhnw.ch (L. Suter-Dick).
https://doi.org/10.1016/j.vascn.2019.106650
Received 18 May 2019; Received in revised form 14 October 2019; Accepted 5 November 2019; Available online 13 November 2019

Table 1
Cell numbers after purification from rat liver. Fractions containing Hep, HSC or KC obtained from rat livers. Cell viability was determined using Trypan Blue exclusion staining. The values are expressed as mean ± SD ($N = 10$ for Hep; $N = 5$ for NPCs).

	Number of harvested cells	Viability (%)
Hepatocytes	$32 \times 10^6 \pm 1.6 \times 10^6$	93.4 ± 1.65
Stellate cells	$26 \times 10^6 \pm 1.38 \times 10^6$	85.6 ± 2.8
Kupffer cells	$34 \times 10^6 \pm 1.26 \times 10^6$	89.2 ± 2.4

Messner, Lampart, & Suter-Dick, 2017). Several other researchers de- veloped co-culture models aiming to reproduce the hepatic micro- environment, but often these models underrepresent non-parenchymal cells (NPCs), and/or required the use of growth factors (Kostadinova et al., 2013; Lauschke, Hendriks, Bell, Andersson, & Ingelman- Sundberg, 2016; Leite et al., 2016; van Grunsven, 2017). However, a more physiological rat co-culture model to facilitate *in vivo-in vitro* comparisons within the same species is still lacking, despite of rat being a common model for the study of liver fibrosis. In this work, we set off to establish a primary co-culture system with primary rat hepatic cells. We included parenchymal (Hep), as well as non-parenchymal (KC and HSC) co-cultured as multicellular, 3D-microtissues (MTs). We chal- lenged the *in vitro* system with pathophysiological stimuli that are key in the development of inflammation and liver fibrosis (LPS and TGF-β1), and were able to mimic *in vitro* characteristic responses to these stimuli.

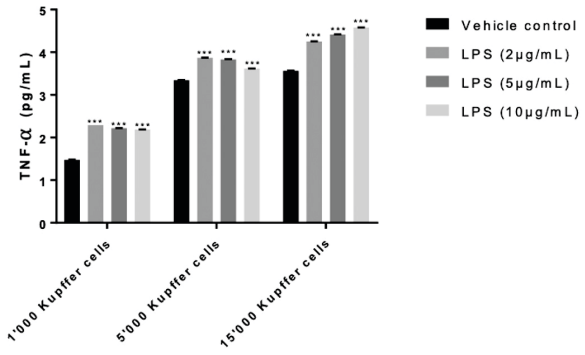

Fig. 2. TNF-α release after LPS-treatment of 2D cultures of rat primary Kupffer cells. At 48 h, LPS induced TNF-α release by KC; produced TNF-α was pro- portional to the number of KC/well. Mean ± SD of 6 replicates.

2. Material and methods

2.1. Isolation and enrichment of primary rat hepatic cells

Fresh rat primary liver cells were kindly provided by Dr. Franziska Boess (F. Hoffmann-La Roche, Basel). Cells were obtained from 200 to 300 g adult male Wistar rats by a two steps collagenase perfusion (Berry & Friend, 1969; Göldlin & Boelsterli, 1991). Total liver cells were fractioned in a Hep-rich fraction (sediment) and a NPC fraction (sus- pension). Further enrichment of HSC cells and KC from the NPC fraction was achieved by means of a discontinuous Nycodenz (Axon lab; Cat. 1,002,424) gradient in Gey's Balanced Salt Solution (GBSS) (Maschmeyer, Flach, & Winau, 2011).

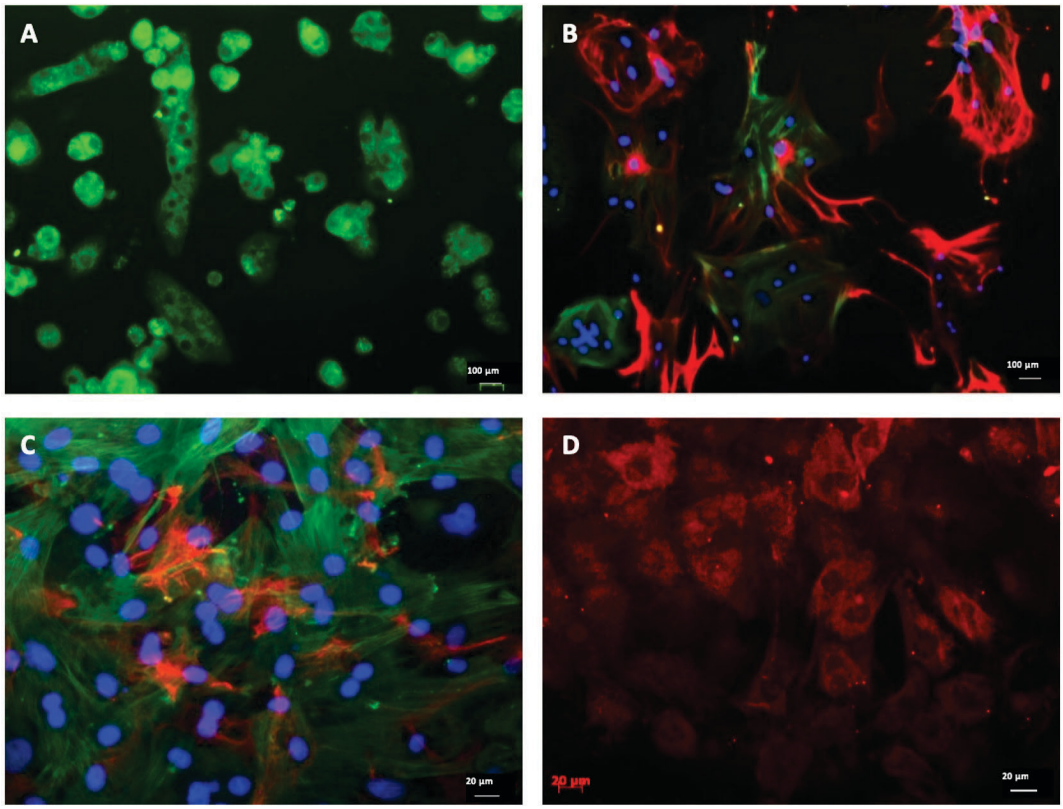

Fig. 1. Immunostaining of 2D culture of rat primary liver cells. (A) Hep show a multinucleate phenotype as well as positive staining for albumin after fixation at day 4. (B) Immunostaining of rat primary HSC after 7 days and (C) 14 days in culture. Red: desmin; Green: smooth muscle actin (αSMA); Blue: nuclei. The pictures show the typical HSC morphology with dendritic structures. After 7 days in culture, cells were positive for desmin with some expression of αSMA. After 14 days in culture activated HSC produced large amounts of αSMA and started losing desmin expression. (D) Immunostaining of F4/80 in rat primary Kupffer cells after 7 days in culture. Representative images from 4 different experiments. (For interpretation of the references to colour in this figure legend, the reader is referred to the web version of this article.)

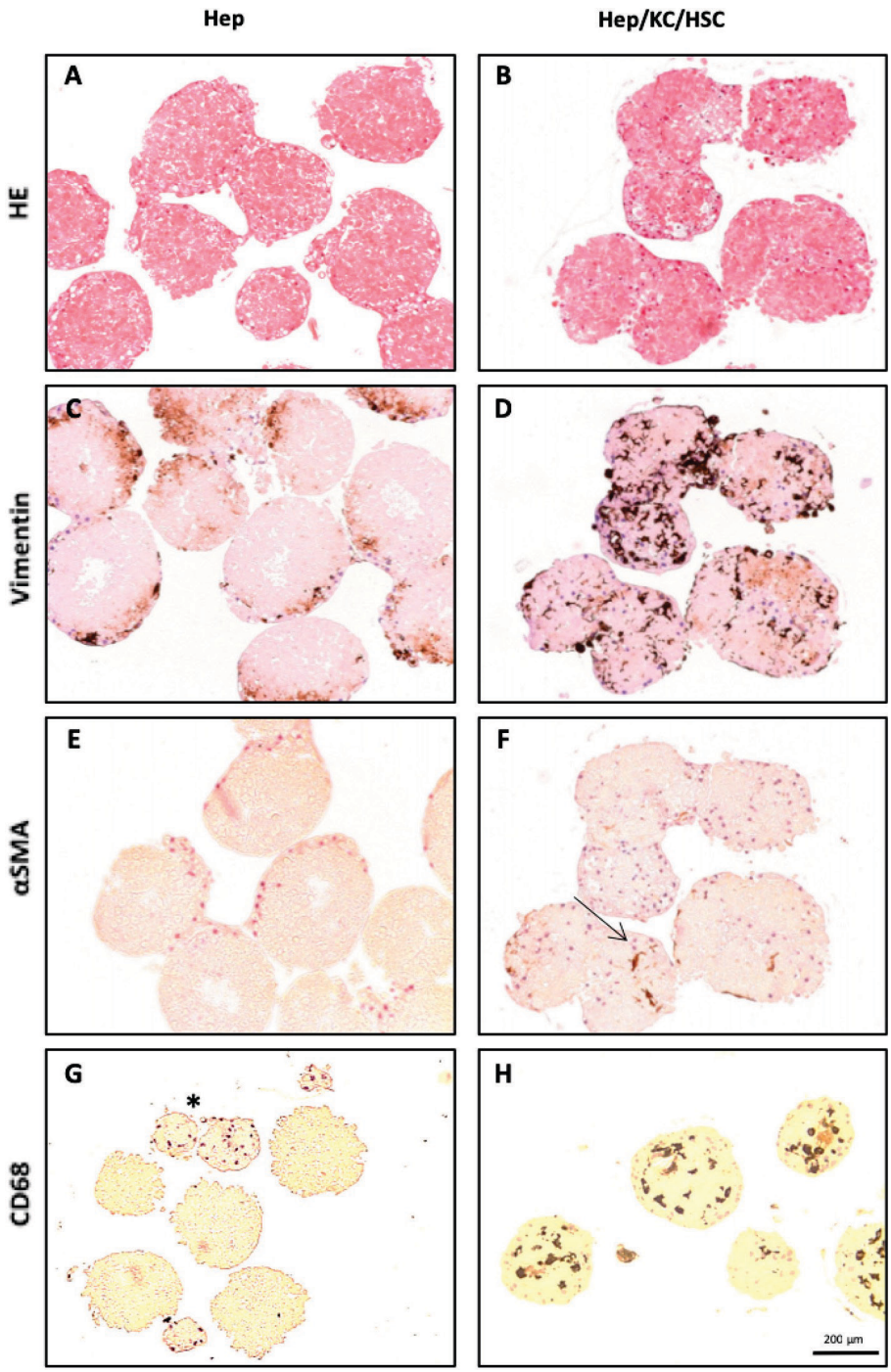

Fig. 3. Immunohistochemical detection of cell-type specific markers. MTs consisting of Hep-monocultures (A, C, E and G) or co-cultures (B, D, F and H) were kept in culture during 14 days before performing histological staining. Positive staining for vimentin, αSMA and CD68 was detected in co-culture tissues (D, F and H). Hep- monoculture did not express these NPC-markers, with exception of two potentially misplaced MTs in panel G (* smaller size and CD68-positive cells). The αSMA-stain was not very prominent (arrow, panel F) as activation of HSC had not been induced. Representative images from several MTs from two cell isolations.

The gradient consisted of three Nycodenz layers: 16.10% Nycodenz (density 1.09 g/mL); 12.27% Ny- codenz (density 1.07 g/mL) and 8.43% Nycodenz (density 1.05 g/mL) layered underneath 8 mL of the NPC fraction. After centrifugation at 1′500 ×*g* for 17 min at 4 °C, HSC were harvested from the 1.05 g/mL Nycodenz phase and the interface just above. KC were harvested from the interface between 1.07 g/mL and 1.09 g/mL. After washing, cell vitality was determined using Trypan Blue (Sigma; Cat. T8154) exclu- sion stain, and lipids in the HSC were visualized with UV light. Unless stated otherwise, cells were cultured in complete medium: DMEM High Glucose (Cat. 41,965) and Fetal Bovine Serum (FBS) (Cat. 10,270), purchased from Invitrogen, containing penicillin-streptomycin (Applichem Cat. A8943). For some experiments, HSC were pre-activated by culturing for 2 weeks on plastic (identified as HSC*); KC were pre- activated by exposure to 2 µg/mL LPS for 48 h prior the experiment (identified as KC*).

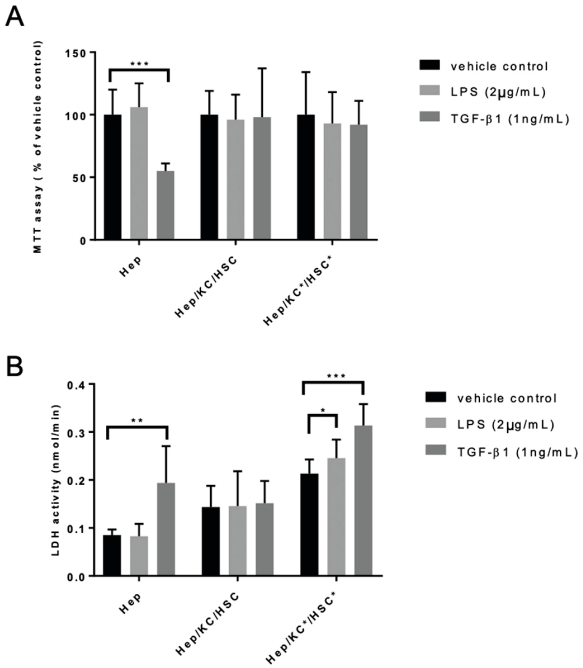

Fig. 4. Cell viability after exposure to LPS and TGF-β1. Effect of 14 days ex- posure to LPS and TGF-β1 on the viability of rat liver of MT consisting of Hep-monocultures (Hep), co-cultures (Hep/KC/HSC) and co-cultures generated with pre-activated NPCs (Hep/KC*/HSC*). (A) MTT-viability assay and (B) LDH activity in the medium collected over 14 days and analysed as a pool. Values are expressed as mean ± SD of 2 (Hep) or 3 (Hep/KC/HSC) cell isolations with 4 technical replicates each.

2.2. Generation and treatment of microtissues

All MTs were generated using the GravityPLUS™ Hanging Drop kit from InSphero (Schlieren, Switzerland; Cat. ISP-06-001), following provider's instructions. Each rat MT was generated with 2′000 Hep alone or 1′000 Hep + 500 KC +500 HSC. After four days, all MTs were transferred to GravityTRAP™ plates.

Exposures of MT to LPS (Sigma; Cat. L3129; 2 µg/mL) or TGF-β1 (Sigma; Cat. T5050; 1 ng/mL) were conducted for 14 days on 4 MTs pooled into one well; medium was refreshed every other day.

2.3. Viability assays

Cell viability was assessed either by MTT-assay or by measuring LDH-leakage into the medium. Briefly, 0.5 mg/mL MTT (3-(4,5-di- methylthiazol-2-yl)-2,5-diphenyltetrazolium bromide) was added to 4MTs pooled into one well and incubated at 37 °C for 4 h. After addition of DMSO and Sörensen buffer, the absorbance was measured at 550 nm with the FlexStation 3 Reader. LDH activity in the medium was mea- sured with Cytotoxicity Detection KitPlus (Sigma; Cat. MAK066) ac- cording to manufacturer's instructions. Cell supernatant was collected periodically over 14 days and combined before analysis. Absorbance at 450 nm was measured on a FlexStation 3 Reader.

2.4. Immunostaining

Monolayer cultures and MTs were fixed in 4% paraformaldehyde (PFA) for 15 min and 60 min, respectively. 2D and 3D-cultuers were permeabilized with 0.1% Triton-X-100 for 20 min and 60 min, respec- tively. MTs were immobilized in 2% agarose before embedding in paraffin. Staining of fixed monolayer and 3D cultures was performed following standard protocols using the following primary antibodies: Albumin (Abcam Ab53435), α-smooth muscle actin (αSMA) (Sigma, A5228), Desmin (Thermo Fisher, Cat. RB-9014-P), F4–80 (Abcam, Ab74383), Vimentin (Abcam, Ab92547). Alexa Fluor® 488 F(ab′)2 Fragment of Goat Anti-Mouse IgG (H + L) (Invitrogen, Cat. A11017) and Alexa Fluor® 546 F(ab′)2 Fragment of Goat Anti-Rabbit IgG (H + L) (Invitrogen, Cat. A11071). For histological slides of the MT, following primary antibodies were used: Vimentin (Epitomics, Cat. 2707–1), αSMA (Sigma, Cat. F3777), CD68 (Novacastra Laboratories, cat. NCL-L- CD68).

2.5. Gene expression analysis

RNA was isolated from 4 MTs pooled into one well following a TRIzol standard extraction procedure. Real time, Taqman qPCR was performed following standard protocols and using commercially available primers/probes: Albumin (Invitrogen, Cat. Rn00592480_m1), αSMA (Invitrogen, Cat. Rn01759928_g1), TGF-β1 (Invitrogen, Cat. Rn00572010_m1), Interleukin 6 (IL6) (Invitrogen, Cat. Rn01410330_m1) and TNF-α (Invitrogen, Cat. Rn01525859_g1). The cycle threshold values were assessed using the Corbett Rotorgene Analysis Software 6000 and 18SRNA (Invitrogen, Cat. Rn01428913_gH) was used as an internal standard for the calculation of the fold changes of each gene of interest.

2.6. Elisa

The presence of TNF-α in the supernatants of treated samples was determined using a commercial ELISA kit (Invitrogen, Cat. KRC3012).

2.7. Statistical analysis

Data were analysed using GraphPad Prism 7 (GraphPad Software, inc.) and expressed as mean values±standard deviation (SD). The Student's *t*-test was used for comparison between two groups. Data from three or more groups were analysed by one-way analysis of variance with Tukey's multiple comparisons test. $P \leq .05$ was considered sig- nificant and depicted as follows: *, $P \leq .05$; **, $P \leq .01$; ***, $P \leq .001$.

3. Results

3.1. Rat primary liver cell characterization and microtissue generation

Cells freshly collected from rat livers were partially purified using a Nycodenz gradient into three main populations in a reproducible manner (Table 1). Primary Hep showed a multinucleated phenotype and positive staining for albumin (Fig. 1A). HSC appeared as round cells containing lipid droplets, spread during 2–4 days in culture. At day 7 in culture they displayed the typical HSC morphology, expressing desmin and low levels of αSMA (Fig. 1B). With prolonged culture times, HSC became activated, were larger, expressed less desmin and stained po- sitive for αSMA. After 14 days in culture, the activated HSC appeared as a homogeneous population of highly proliferating cells expressing αSMA arranged in stress fibres (Fig. 1C). Enriched KC displayed the morphology of adherent, dendritic-type cells that expressed F4–80 glycoprotein (Fig. 1D), and produced TNF-α upon stimulation with LPS (Fig. 2).

Liver MT preparation with rat primary cells yielded 100% size-controlled MTs with an average diameter of 350 µm for co-cultures and 250 µm for Hep-monoculture MTs. Assessment of MT composition confirmed that co-culture MTs contained both Hep and NPCs, as determined by pre-staining with CellTracker dyes (data not shown) and immunohistochemistry of the NPC markers Vimentin, αSMA and CD68 (Fig. 3). Necrotic cores were observed in the Hep-monoculture MTs but not in the co-culture system (Fig. 3).

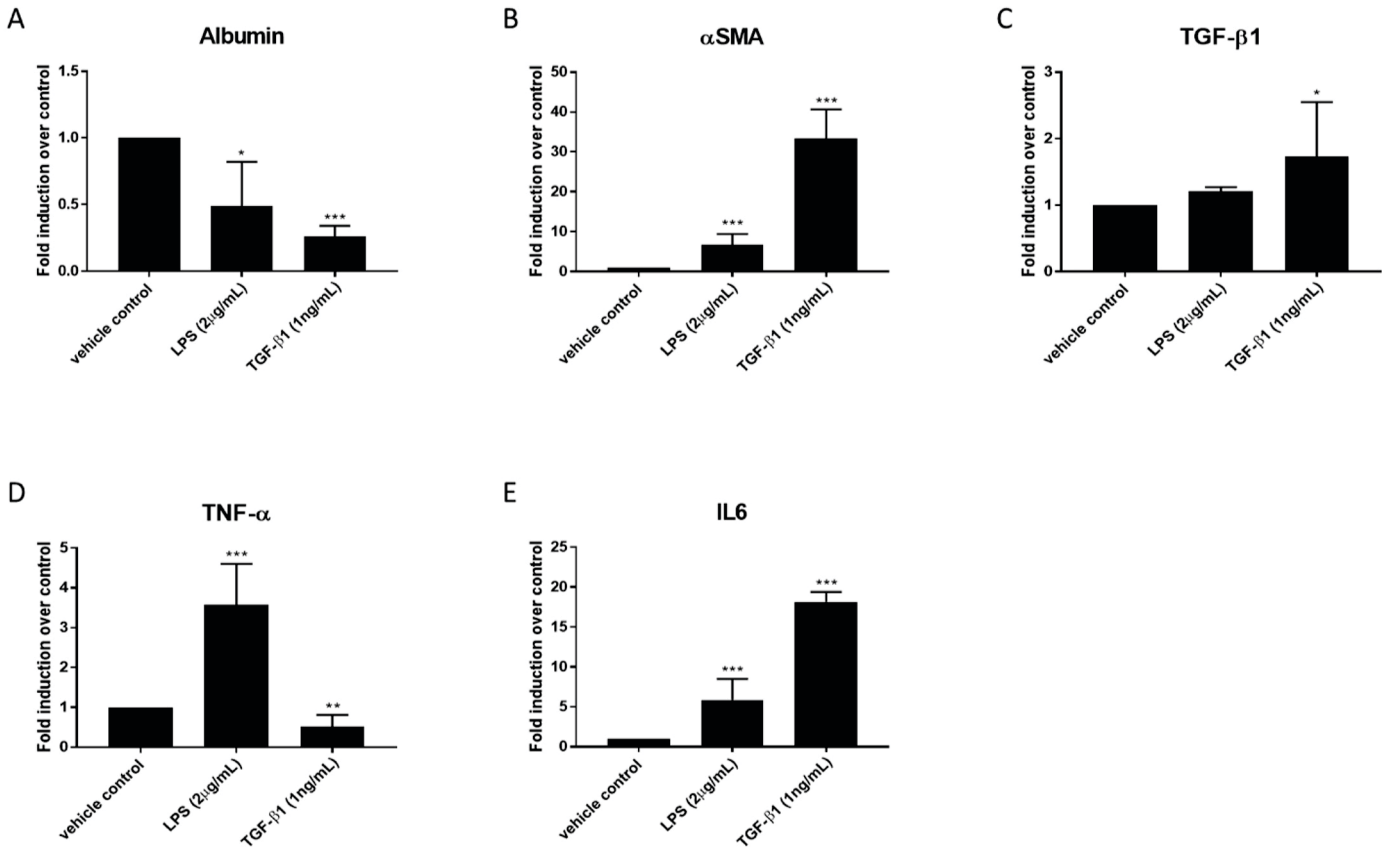

Fig. 5. Transcriptional responses of co-culture MT (Hep/KC/HSC) to pro-inflammatory (LPS) and pro-fibrotic (TGF-β1) stimuli. The following genes were analysed: Albumin (A), αSMA (B), TGF-β1 (C), TNF-α (D) and IL6 (E). Results are expressed as mean fold induction ± SD; $N = 4$.

3.1. *Response of rat liver microtissues to treatment with LPS and TGF-β1*

Rat liver MTs were stimulated with LPS and TGF-β1 to assess the cellular responses of Hep-monoculture and co-culture systems. In Hep- monoculture MTs TGF-β1 (1 ng/mL) induced a decrease in viability that was not observed when NPCs were present. This was determined by a reduction of formazan formation in the MTT assay and an increase in LDH-leakage into the medium (Fig. 4). In co-cultures exposed to LPS and TGF-β1, gene expression of specific HSC-activation and inflammatory markers (*i.e.* αSMA, TGF-β1, TNF-α, and IL-6) was increased while albumin expression was strongly reduced (Fig. 5).

Immunostaining further demonstrated the activation of NPC, as assessed by increase in vimentin- and αSMA-positive cells in co-cultures treated with TGF-β1 (Fig. 6B). This was not observed in Hep-mono- culture (Fig. 6A), which showed the expected low levels of both vi- mentin and αSMA-positive cells. In co-cultures containing pre-activated NPCs, vimentin was highly expressed before stimulation and its ex- pression was further enhanced by TGF-β1. Interestingly, pre-activated NPCs in MTs showed low basal expression of αSMA but were still able to respond to TGF-β1 with overexpression of this marker (Fig. 6C).

3. Discussion

In this study, we have established a rat 3D-liver culture system based on parenchymal (Hep) and non-parenchymal (KC and HSC) rat primary cells. We utilized this system for studying the cellular responses to pro-inflammatory and pro-fibrotic stimuli *in vitro*.

As a first step, we optimized the isolation of hepatic cell types from fresh rat livers. The enriched cell fractions expressed cell-type specific markers: albumin for Hep, desmin and vimentin for NPCs, F4–80 for KC and αSMA for activated HSC. NPCs also responded to pro-inflammatory and pro-fibrotic stimuli (LPS and TGF-β1, respectively).

As depicted in Fig. 1C and in agreement with previous reports, the HSC underwent activation upon culture for 14 days on plastic (Maschmeyer et al., 2011). This activation was characterized by high expression of αSMA, a decrease in lipid content and desmin expression accompanied by mor- phological changes (Olsen et al., 2011). After 7 days in culture, en- riched KC were positive for vimentin (NPC marker) and macrophage glycoprotein F4–80, a known KC marker (Kinoshita et al., 2010). These cells also showed the ability to produce and release TNF-α after chal- lenge with LPS.

As expected, MTs consisting of monocultures (Hep-monoculture) or co-cultures (Hep/KC/HSC) behaved differently. Monocultures showed a necrotic core that was not noted in the co-culture MTs. They also appeared to be more sensitive to TGF-β1-induced cytotoxicity (Figs. 4 and 6). There results suggest that a monoculture model, consisting of only Hep, can not be used as model system to access drug toxic effects in a physiological way. Moreover, our results show that multicellular MTs may be more stable, probably due to improved physiological cell-cell interactions. NPCs are known to produce several cytokines that protect the Hep against the TGF-β1-induced apoptosis (Cosgrove et al., 2008; Ikeda et al., 1996; Kim et al., 2000; Rolfe, James, & Roberts, 1997), but our data do not allow to identify specific factors. We could however demonstrate that NPCs in our system were able to produce cytokines that changed cell phenotypes in the 3D-co-cultures: The expression of TNF-α, IL6 and TGF-β1 were upregulated in KC upon stimulation with LPS. Both LPS and TGF-β1 were able to elicit an inflammatory

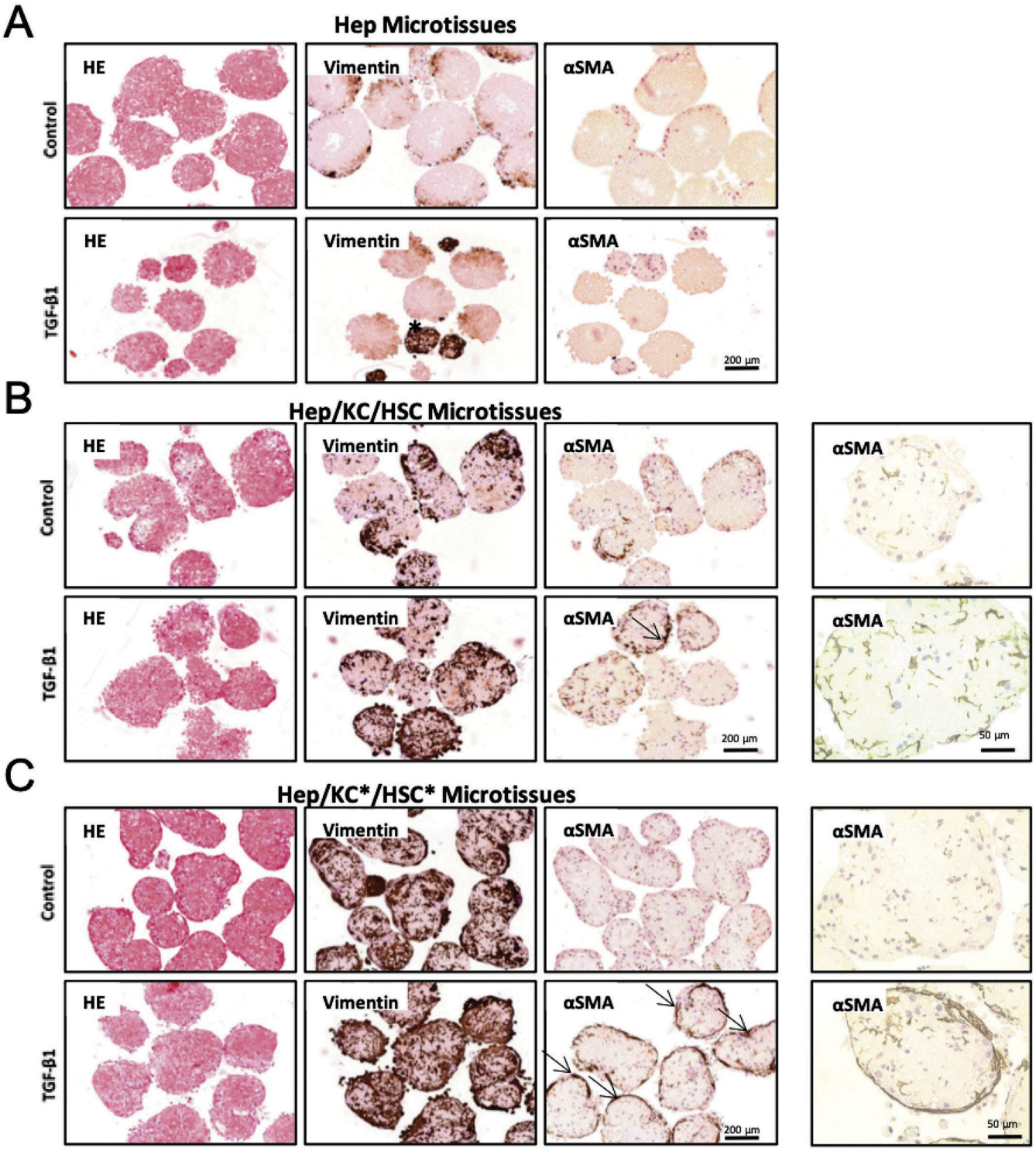

Fig. 6. Immunohistochemical detection of HSC-activation after treatment of co-cultures with TGF-β1 for 14 days. Co-culture MTs showed an increase in the vimentin and αSMA-positive cells after TGF-β1 exposure (see arrows). Panel A: Hep; Panel B: Hep/KC/HSC; Panel C: Hep/KC*/HSC*. Naïve (B) and pre-activated (C) HSC show low basal αSMA-expression but can both be activated by TGF-β1. Activated HSC seem to locate to the periphery of the MTs. Positive staining is shown in brown, while nuclei staining (Haematoxylin) in blue. Pictures taken with 10× and 40× magnification. (For interpretation of the references to colour in this figure legend, the reader is referred to the web version of this article.)

response (increase of IL6 synthesis), concomitant with a detrimental effect on Hep (decrease in albumin expression). Moreover, the levels of αSMA mRNA were strongly increased after LPS and TGF-β1 exposure in- dicating activation of the HSC cells. TGF-β1-treatment induced its own gene expression indicating the onset of its autocrine and positive loop in the system (Arias et al., 2002).

TGF-β1 also led to the proliferation of NPCs in the MTs, as established by an increase of vimentin-positive cells.In the context of hepatic fibrosis, our results using primary rat MTs also recapitulate some of the key events described as part of the AOP (Horvat et al., 2016). We could detect a decrease in albuminexpression, indicating primary hepatocellular damage. We were also able to elicit the activation of KC by treatment with the known TLR4-ligand LPS, as assessed by the increased expression of TNF-α, TGF-β1 and IL6.

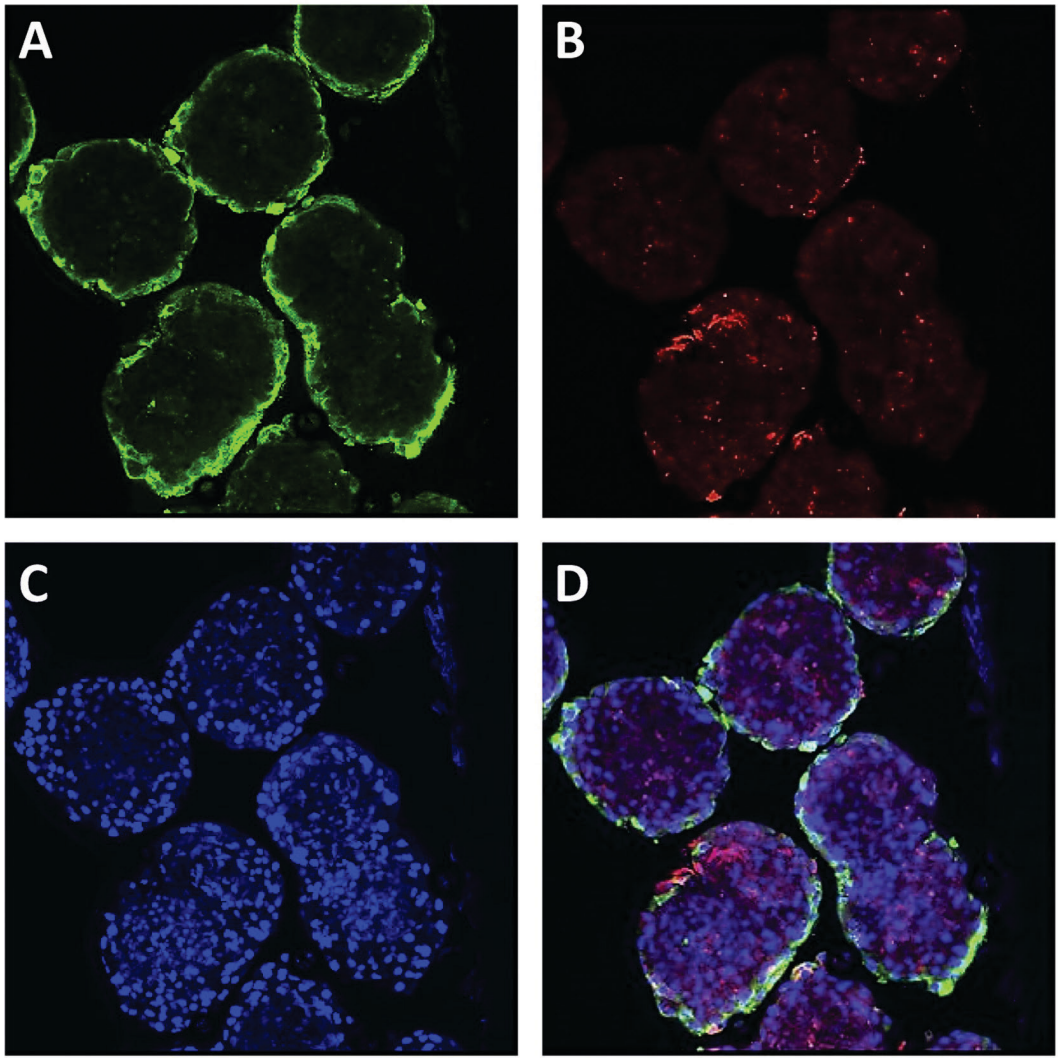

Supplementary Fig. 1. Immunostaining for αSMA and desmin in rat liver microtissues. MTs were generate with fresh isolated Hep and pre-activated NPCs, and stained one week after seeding. Desmin staining shows the presence of HSC in the MTs. However, not all the HSC were positive for αSMA staining, which is observed only at the surface of the MTs. Green: smooth muscle actin; Red: desmin; Blue: nuclei. Pictures were taken using confocal microscopy with 20× magnification. Representative images from 2 different cell isolations.

Finally, we could reproduce the TGF-β1-induced activation of HSCs determined as enhanced expression αSMA. As expected, Hep-monoculture MT failed to display such responses, further supporting the need of the intercellular interplay of Hep and NPCs in order to have a biological relevant fibrotic model.The influence of a more organotypical culture system on the cell phenotype is further supported by the behaviour of pre-activated HSC (HSC*).

Our preliminary results suggest that HSC* may revert to a more quiescent phenotype in the MT; the levels of αSMA change from high, widespread expression after pre-activation in 2D (Fig. 1) to low, scarce expression after incorporation of these HSC* into the 3D-MTs (Fig. 6C). We can exclude that this was an artefact due to a lack of HSC* in- corporation into the 3D MTs, since the presence of HSC in these MT was demonstrated by co-staining with desmin (Supplementary Fig. 1) and by the "re-activation" to αSMA-positive cells after 14 days of exposure to TGF-β1 (Fig. 6C). Based on the presented results and additional unpublished data, the self-assembly of the MT follows a rather con- sistent pattern, with the αSMA-positive, activated HSC in the periphery. The reason for the localization of αSMA-positive HSC cells cells predominately to the surface of the MT is unclear and would warrant further investigation. Further studies would be also necessary to elucidate the molecular and cellular processes, which may be involved in the observed "de-activation" of HSC. Despite these cells being con- sistently activated upon culture on 2D-plastic dishes as depicted in Fig. 1C and consistent with published results (Maschmeyer et al., 2011), we did not observe activated HSC under basal conditions in MT (Fig. 6C), which leads us to speculate that the 3D-, co-cultures drive the HCS towards a more quiescent phenotype.

3. Conclusion

In conclusion, MTs containing three primary hepatic cells (Hep, KC and HSC) are able to recapitulate key events in the liver fibrosis AOP, in particular hepatocellular damage, inflammatory responses and HSC- activation. Hep-monoculture MTs did not show this phenotype, in- dicating that the interplay of parenchymal and NPC plays indeed a key role. In addition, our data suggest that different cell types in co-culture influence the responses of other cell types. On the one hand, the pre- sence of NPC made the MTs more resistant to toxicity caused by LPS and TGF-β1. On the other hand, pre-activated HSC may reverse to a quiescent phenotype in 3D co-cultures.

The following are the supplementary data related to this article.

Funding

This work was supported by the Swiss Commission for Technology and Innovation (CTI) in collaboration with InSphero AG, and the School of Life Sciences (University of Applied Sciences Northwestern Switzerland).

Declaration of Competing Interest

The authors declare that they have no conflict of interest that may have influenced the data generation or interpretation. This work was supported by the Swiss Commission for Technology and Innovation (CTI) in collaboration with InSphero AG, and the School of Life Sciences (University of Applied Sciences Northwestern Switzerland). The funder had no role in study design, data collection and analysis, decision to publish, or preparation of the manuscript. This does not alter our ad- herence to Toxicology letters policies on sharing data and materials.

Ackowledgments

We would like to acknowledge the Swiss Commission for Technology and Innovation (CTI) in collaboration with InSphero AG, and the School of Life Sciences (University of Applied Sciences Northwestern Switzerland) for granted this research. We would like to acknowledge Dr. Jens Kelm, Dr. Simon Messner and Dr. Patrick Guye for their scientific support. We are very thankful to Dr. Franziska Boess for kindly providing the rat liver cell suspension used for this research.

References

Ankley, G. T., Bennett, R. S., Erickson, R. J., Hoff, D. J., Hornung, M. W., Johnson, R. D., & Villeneuve, D. L. (2010). Adverse outcome pathways: A conceptual framework to support ecotoxicology research and risk assessment. *Environmental Toxicology and Chemistry, 29*, 730–741. https://doi.org/10.1002/etc.34.

Arias, M., Lahme, B., Van de Leur, E., Gressner, A. M., & Weiskirchen, R. (2002). Adenoviral delivery of an antisense RNA complementary to the 3′ coding sequence of transforming growth factor-beta1 inhibits fibrogenic activities of hepatic stellate cells. *Cell Growth & Differentiation: The Molecular Biology Journal of the American Association Cell growth, 13*, 265–273.

Berry, M. N., & Friend, D. S. (1969). High-yield preparation of isolated rat liver par- enchymal cells: A biochemical and fine structural study. *The Journal of Cell Biology, 43*, 506–520.

Constandinou, C., Henderson, N., & Iredale, J. P. (2005). Modeling liver fibrosis in ro- dents. *Methods in Molecular Medicine, 117*, 237–250. https://doi.org/10.1385/1- 59259-940-0:237.

Cosgrove, B. D., Cheng, C., Pritchard, J. R., Stolz, D. B., Lauffenburger, D. A., & Griffith, L. G. (2008). An inducible autocrine cascade regulates rat hepatocyte proliferation and apoptosis responses to tumor necrosis factor-alpha. *Hepatology Baltimore Md, 48*, 276–288. https://doi.org/10.1002/hep.22335.

Feaver, R. E., Cole, B. K., Lawson, M. J., Hoang, S. A., Marukian, S., Blackman, B. R., ... Dash, A. (2016). Development of an in vitro human liver system for interrogating nonalcoholic steatohepatitis. *JCI Insight, 1*, e90954. https://doi.org/10.1172/jci. insight.90954.

Friedman, S. L. (2000). Molecular regulation of hepatic fibrosis, an integrated cellular response to tissue injury. *The Journal of Biological Chemistry, 275*, 2247–2250.

Gäbele, E., Brenner, D. A., & Rippe, R. A. (2003). Liver fibrosis: Signals leading to the amplification of the fibrogenic hepatic stellate cell. *Frontiers Bioscience Journal Virtual Library, 8*, d69–d77.

Göldlin, C. R., & Boelsterli, U. A. (1991). Reactive oxygen species and non-peroxidative mechanisms of cocaine-induced cytotoxicity in rat hepatocyte cultures. *Toxicology, 69*, 79–91.

van Grunsven, L. A. (2017). 3D in vitro models of liver fibrosis. *Advanced Drug Delivery Reviews, 121*, 133–146. https://doi.org/10.1016/j.addr.2017.07.004.

Horvat, T., Landesmann, B., Lostia, A., Vinken, M., Munn, S., & Whelan, M. (2016). Adverse outcome pathway development from protein alkylation to liver fibrosis. *Archives of Toxicology*. https://doi.org/10.1007/s00204-016-1814-8.

Ikeda, K., Kubo, S., Hirohashi, K., Kinoshita, H., Kaneda, K., Kawada, N., & Inoue, M. (1996). Mechanism that regulates nitric oxide production by lipopolysaccharide-sti- mulated rat Kupffer cells. *Physiological Chemistry and Physics and Medical NMR, 28*, 239–253.

Iredale, J. P. (2007). Models of liver fibrosis: Exploring the dynamic nature of in- flammation and repair in a solid organ. *The Journal of Clinical Investigation, 117*, 539–548. https://doi.org/10.1172/JCI30542.

Kim, Y. M., Kim, T. H., Chung, H. T., Talanian, R. V., Yin, X. M., & Billiar, T. R. (2000). Nitric oxide prevents tumor necrosis factor alpha-induced rat hepatocyte apoptosis by the interruption of mitochondrial apoptotic signaling through S-nitrosylation of caspase-8. *Hepatol. Baltim. Md, 32*, 770–778. https://doi.org/10.1053/jhep.2000.18291.

Kinoshita, M., Uchida, T., Sato, A., Nakashima, M., Nakashima, H., Shono, S., & Seki, S. (2010). Characterization of two F4/80-positive Kupffer cell subsets by their function and phenotype in mice. *Journal of Hepatology, 53*, 903–910. https://doi.org/10.1016/j.jhep.2010.04.037.

Kostadinova, R., Boess, F., Applegate, D., Suter, L., Weiser, T., Singer, T., & Roth, A. (2013). A long-term three dimensional liver co-culture system for improved predic- tion of clinically relevant drug-induced hepatotoxicity. *Toxicology and Applied Pharmacology, 268*, 1–16. https://doi.org/10.1016/j.taap.2013.01.012.

Kyffin, J. A., Sharma, P., Leedale, J., Colley, H. E., Murdoch, C., Harding, A. L., ... Webb, S. D. (2019). Characterisation of a functional rat hepatocyte spheroid model. *Toxicology In Vitro: An International Journal Published in Association BIBRA, 55*, 160–172. https://doi.org/10.1016/j.tiv.2018.12.014.

Lauschke, V. M., Hendriks, D. F. G., Bell, C. C., Andersson, T. B., & Ingelman-Sundberg, M. (2016). Novel 3D culture Systems for Studies of human liver function and assess- ments of the hepatotoxicity of drugs and drug candidates. *Chemical Research in Toxicology, 29*, 1936–1955. https://doi.org/10.1021/acs.chemrestox.6b00150.

Leite, S. B., Roosens, T., El Taghdouini, A., Mannaerts, I., Smout, A. J., Najimi, M., ... van Grunsven, L. A. (2016). Novel human hepatic organoid model enables testing of drug- induced liver fibrosis in vitro. *Biomaterials, 78*, 1–10. https://doi.org/10.1016/j. biomaterials.2015.11.026.

Marques, T. G., Chaib, E., da Fonseca, J. H., Lourenço, A. C. R., Silva, F. D., Ribeiro, M. A. F., & D'Albuquerque, L. A. C. (2012). Review of experimental models for inducing hepatic cirrhosis by bile duct ligation and carbon tetrachloride injection. *Acta Cirúrgica Brasileira, 27*, 589–594.

Maschmeyer, P., Flach, M., & Winau, F. (2011). Seven steps to stellate cells. *Journal of Visualized Experiments*. https://doi.org/10.3791/2710.

Messner, S., Agarkova, I., Moritz, W., & Kelm, J. M. (2013). Multi-cell type human liver microtissues for hepatotoxicity testing. *Archives of Toxicology, 87*, 209–213. https:// doi.org/10.1007/s00204-012-0968-2.

Olsen, A. L., Bloomer, S. A., Chan, E. P., Gaça, M. D. A., Georges, P. C., Sackey, B., & Wells, R. G. (2011). Hepatic stellate cells require a stiff environment for myofibro- blastic differentiation. *American Journal of Physiology. Gastrointestinal and Liver Physiology, 301*, G110–G118. https://doi.org/10.1152/ajpgi.00412.2010.

Prestigiacomo, V., Weston, A., Messner, S., Lampart, F., & Suter-Dick, L. (2017). Pro- fibrotic compounds induce stellate cell activation, ECM-remodelling and Nrf2 acti- vation in a human 3D-multicellular model of liver fibrosis. *PLoS ONE, 12*, e0179995. https://doi.org/10.1371/journal.pone.0179995.

Rolfe, M., James, N. H., & Roberts, R. A. (1997). Tumour necrosis factor alpha (TNF alpha) suppresses apoptosis and induces DNA synthesis in rodent hepatocytes: A mediator of the hepatocarcinogenicity of peroxisome proliferators? *Carcinogenesis, 18*, 2277–2280.

3.3 Paper 2

Pro-fibrotic compounds induce stellate cell activation, ECM-remodelling and Nrf2 activation in a human 3D-multicellular model of liver fibrosis

Vincenzo Prestigiacomo, Anna Weston, Simon Messner, Franziska Lampart, Laura Suter-Dick

Published manuscript

Aims: Develop a novel 3D liver cell line based model containing hepatocytes, KC and HSC as key relevant cells in hepatic fibrosis.

Results: The generated model was able to respond to proinflammatory cytokines (LPS, TNF-α, TGFβ1) as well as pro-fibrotic cytokines (MTX, TAA) resulting in hepatocytes damage, HSC activation and collagen deposition.

Conclusion: This study showed the ability of this new human liver model to recapitulate all the key events leading to fibrosis after drug injury.

PLOS ONE

RESEARCH ARTICLE

Pro-fibrotic compounds induce stellate cell activation, ECM-remodelling and Nrf2 activationin ahuman3D-multicellularmodel of liverfibrosis

Vincenzo Prestigiacomo[1,2*], Anna Weston[1], Simon Messner[3], Franziska Lampart[1], Laura Suter-Dick[1]

1 University of Applied Sciences Northwestern Switzerland, School of Life Sciences, Muttenz, Switzerland, **2** University of Basel, Department of Pharmaceutical Sciences, Basel, Switzerland, **3** InSphero AG, Schlieren, Canton of Zürich, Switzerland

* vincenzo.prestigiacomo@fhnw.ch

Citation: Prestigiacomo V, Weston A, Messner S, Lampart F, Suter-Dick L (2017) Pro-fibrotic compounds induce stellate cell activation, ECM- remodelling and Nrf2 activation in a human 3D- multicellular model of liver fibrosis. PLoS ONE 12 (6): e0179995. https://doi.org/10.1371/journal.pone.0179995

Editor: Partha Mukhopadhyay, National Institutes of Health, UNITED STATES

Received: January 9, 2017

Accepted: June 7, 2017

Published: June 30, 2017

Data Availability Statement: All relevant data are within the paper.

Funding: The work performed at FHNW was partly funded by the CTI (Commission for Technology and Innovation) and partly by SCAHT (Swiss Center for Applied Human Toxicology), both Swiss federal organisations. The studies performed at InSphero AG were funded internally. The funders had no role in study design, data collection and analysis, decision to publish, or preparation of the

Abstract

Background & Aims

Currently most liver fibrosis research is performed *in vivo*, since suitable alternative *in vitro* systems which are able to recapitulate the cellular events leading to liver fibrosis are lacking. Here we aimed at generating a system containing cells representing the three key players of liver fibrosis (hepatocyte, Kupffer cells and stellate cells) and assess their response to pro- fibrotic compounds such as TGF-β1, methotrexate (MTX) and thioacetamide (TAA).

Methods

Human cell lines representing hepatocytes (HepaRG), Kupffer cell (THP-1 macrophages) and stellate cells (hTERT-HSC) were co-cultured using the InSphero hanging drop technol- ogy to generate scaffold-free 3D microtissues, that were treated with pro-fibrotic compounds (TGF-β1, MTX, TAA) for up to 14 days. The response of the microtissues was evaluated by determining the expression of cytokines (TNF-α, TGF-β1 and IL6), the deposition and secre- tion of ECM proteins and induction of gene expression of fibrosis biomarkers (e.g. αSMA). Induction of Nrf2 and Keap1, as key player of defence mechanism, was also evaluated.

Results

We could demonstrate that the multicellular 3D microtissue cultures could be maintained in a non-activated status, based on the low expression levels of activation markers. Macro- phages were activated by stimulation with LPS and hTERT-HSC showed activation by TGF- β1. In addition, MTX and TAA elicited a fibrotic phenotype, as assessed by gene-expression and protein-deposition of ECM proteins such as collagens and fibronectin. An involvement of the antioxidant pathway upon stimulation with pro-fibrotic compounds was also observed.

manuscript. This does not alter our adherence to PLOS ONE policies on sharing data and materials.

Competing interests: The authors declare that they have no conflict of interest that may have influenced the data generation or interpretation.

Abbreviations: AOP, Adverse outcome pathway; ATP, Adenosine triphosphate; BSA, Bovine serum albumin; CD44, Cluster of Differentiation 44; CD68, Cluster of Differentiation 68; Col1α1, Collagen 1 alpha 1; Col1α2, Collagen 1 alpha 2; Col4α1, Collagen 4 alpha 1; DMSO, Dimethyl sulfoxide; ECM, Extracellular matrix; FBS, Fetal bovine serum; GOI, Gene of interest; H&E, Haematoxylin and eosin stain; HBV, Hepatitis B virus; HCV, Hepatitis C virus; HSC, Hepatic stellate cells; IL1β, Interleukin 1 beta; IL6, Interleukin 6; KC, Kupffer cells; Keap1, Kelch-like ECH-associated protein 1; LPS, Lipopolysaccharide; MMP2, Metalloproteinase 2; mRNA, messenger RNA; MT, Microtissue; MTX, Methotrexate; Nrf2, Nuclear factor E2-related factor 2; PBS, Phosphate buffer saline; PCR, Polymerase chain reaction; PDGF, Platelet-derived growth factor; PFA, Paraformaldehyde; ROS, Reactive oxygen species; SD, Standard deviation; S.E.M., Standard error of the mean; TAA, Thioacetamide; TGF-β1, Trans-

Conclusion

Here, for the first time, we demonstrate the *in vitro* recapitulation of key molecular and cellu- lar events leading to liver fibrosis: hepatocellular injury, antioxidant defence response, acti- vation of Kupffer cells and activation of HSC leading to deposition of ECM.

Introduction

Liver fibrosis and cirrhosis are canonical endpoint of many chronic liver diseases, including virus infections (HBV, HCV), non-alcoholic steatohepatitis or damage due to alcohol con- sumption [1]. In addition, liver fibrosis is also a relevant toxicological outcome and has been identified as an Adverse Outcome Pathway (AOP), a novel tool in human risk assessment designed to provide mechanistic representation of critical toxicological effects [2,3]. Liver fibrosis is characterized by an accumulation of fibrillar extracellular matrix (ECM), leading to liver failure, portal hypertension, and increased risk of cancer. The pathophysiology of fibrosis requires chronic liver damage (including chronic alcohol consumption, chemically-induced hepatocyte damage, and viral infections) and involves the interplay of several hepatic cell types; it requires hepatocyte injury and cell death, activation of Kupffer cells (KC), activation of hepatic stellate cells (HSC), and chronic inflammation [4,5].

Hepatic stellate cells, activated by fibrogenic cytokines (e.g. TGF-β1 and TNF-α), have been identified as the major collagen-producing cells in the injured liver. Stimuli initiating stellate cell activation derive from injured hepatocytes and neighbouring KC. Upon hepatocyte injury, activated KC produce large amounts of reactive oxygen species (ROS) and release cytokines such as TNF-α, TGF-β1, PDGF and IL1β, leading ultimately to stellate cell activation and increased deposition of fibrillar components of the ECM [4–6]. Activated stellate cells, in turn, produce more TGF-β1 and potentiate and perpetuate their activation in an autocrine loop [7].

It is well documented that liver diseases including hepatitis, fibrosis, cirrhosis, and hepato- cellular carcinoma induce antioxidant stress response [8]. Oxidative stress also contributes to the release of pro-fibrogenic growth factors, cytokines and prostaglandins that may lead to liver fibrosis and/or cirrhosis [8]. Nrf2 (NF-E2-related factor-2) is an essential transcription factor that regulates an array of detoxifying and antioxidant defence and is finely regulated also by its interaction with Keap1 [9]. Yang et al. showed up-regulation of Keap1 and Nrf2 mRNA and protein in liver tissues of CCl4-induced fibrosis of rat compared with tissues of wild type animals [10].

Emerging anti-fibrotic therapies aim at inhibiting the accumulation of fibrogenic cells and/or preventing the deposition of ECM proteins [4]. The advances in the research of anti- fibrotic therapies are however hampered by the lack of appropriate *in vitro* systems for the study of liver fibrosis. Until now, the majority of the investigations on liver fibrosis are still per- formed in rodents that underwent chemically-induced fibrosis [11]. These animal models have the advantages of providing the physiological relevance, but with the strong disadvantages of being time consuming, expensive as well as non-human. The efficient development of anti- fibrotic drugs will therefore strongly depend on the availability of a suitable *in vitro* system that more faithfully replicates the pro-fibrogenic microenvironment of human liver [5].

Biological relevant models to study liver fibrosis require functional hepatocytes, as well as KC and HSC in a quiescent (non-activated) status and in close spatial interaction. Three- dimensional (3D) cell culture systems appear to outperform conventional cell cultures with regards to their metabolic activity and responses to toxicants [12,13]. Several methods have

been published for the generation of scaffold-free liver MT; however, these systems are gener- ally based on primary cells and often underrepresent non-parenchymal cells [14,15]. Also, most *in vitro* liver models are of limited use due to short longevity in culture, inadequacy of cell composition and/or high handling complexity [13,14,16–18]. Recently, work on a fibrotic 3D-model based on hepatocytes and HSC has been published, but this system lacks macro- phages as a key component in the chain of events leading to fibrosis [18]. A suitable *in vitro* model for the study of liver fibrosis should mimic processes that involve the relevant cell types (hepatocytes, KC and HSC) leading to the development of the fibrotic phenotype. Such a sys- tem would be a major asset for the understanding of the pathophysiology of fibrosis, as well as for the experimental evaluation of substances with regards to the pro-fibrotic and anti-fibrotic potential.

Here, we aimed at investigating liver fibrosis mechanisms in a novel human hepatic micro- tissue (MT) model that responds to pro-fibrotic stimuli in a similar way to what is known to occur in the human liver. To this end, we utilized human relevant cell lines representing the hepatocyte, the KC and the HSC. With this system, we could not only recapitulate HSC- and KC activation and other key molecular events implicated in fibrosis, but also the deposition of ECM *in vitro*. Our results show that methotrexate (MTX) and thioacetamide (TAA), two well characterized compounds that cause hepatic fibrosis in animals and man [19, 20] elicited the fibrotic phenotype *in vitro*. This system can thus be used for the investigation of cellular and molecular events involved in the development of fibrosis as well as an *in vitro* test system for the evaluation of anti-fibrotic therapies.

Material and methods

Reagents and chemicals

Cell culture media for HepaRG cells were purchased from Biopredic. DMEM High Glucose (Cat. 41965) and Fetal Bovine Serum (FBS) (Cat. 10270) were purchased from Invitrogen. Pen- icillin-Streptomycin (Cat. A8943) used for cell culture was purchased by AppliChem). LPS (Cat. L3129), TNF-α (Cat. SRP3177), TGF-β1 (Cat. T5050), Thioacetamide (TAA) (Cat.163678) and Methotrexate (MTX) (Cat. M8407) were purchased from Sigma.

Human cell lines

HepaRG cells were obtained from Biopredic International (Rennes, France). The cells were seeded at 1 x 10^5 undifferentiated cells/cm^2 in ADD710 Growth Medium Supplement (Biopre- dic). The cells were cultured at 37˚C under 5% CO_2 for 14 days before differentiation. After 14 days of culture, cell differentiation was induced with ADD720 Differentiation Medium Supple- ment (Biopredic) for 14 days. Then the cells were maintained for up to 4 weeks.

hTERT-HSC were kindly provided by Dr. Bernd Schnabl (UC San Diego, USA) [21] and were cultured in DMEM High Glucose supplemented with 10% FBS and 1% Penicillin-Strep- tomycin. The cells were kept in the humidified incubator at 37˚C with 5% CO_2.

THP-1 monocytic cells (Cell Line Service) were cultured at 2–10 x 10^5 cells/mL in RPMI 1640 containing 10% FBS, 1% Penicillin/Streptomycin and maintained at 37˚C under 5% CO_2. THP-1 cells were differentiated into macrophages over 48 hours in RPMI 1640 medium containing 5–25 ng/mL PMA, according to a previously published method [22]. The supernatants were then removed and the wells were washed with fresh medium. Successful differentiation was assessed by the ability of the cells to secrete cytokines upon exposure to 1 μg/mL LPS for 48h.

Immunocytochemistry analysis

Monolayer cultures of hTERT-HSC were fixed in 4% paraformaldehyde (PFA) for 15 minutes, followed by permeabilization with 0.1% Triton-X-100 for 20 minutes. Blocking was performed with 1% BSA in PBS for 60 minutes and washing with PBS; all steps were performed at RT. Pri- mary antibody against αSMA (Sigma, A5228, dilution 1:200) and secondary antibody Alexa Fluor[1] 488 F(ab')2 Fragment of Goat Anti-Mouse IgG (H+L) (Invitrogen, A11017, dilution 1:400) were used for thestaining.

Generation of microtissues

All microtissues (MTs) were generated using the GravityPLUS™ Hanging Drop System from InSphero (Cat. ISP-06-001). Briefly, 40 μL cell suspension/well were pipetted in a 96-well-for- mat GravityPLUS™ plate that has been designed specifically to generate reproducible hanging drops. In this system, cells are allowed to assemble themselves in a scaffold-free manner form- ing spherical MTs. After 2–3 days incubation, MTs are transferred to 96-well GravityTRAP™ plates, were they can be maintained in culture over several weeks. Human liver MTs were gen- erated using 2'000 cells per MT, with either HepaRG-cells (hepatocyte monoculture), or HepaRG in combination with THP-1 and hTERT-HSC. Cell-ratios were empirically chosen to give the best resemblance of the native cellular distribution in liver, approximately 80% hepa- tocytes and 20% NPCs (including inflammatory cells and stellate cells), as assessed by immunohistochemistry.

Pharmacological stimulation of microtissues

For functional characterization, the generated MT were exposed to LPS (2 μg/mL), TGF-β1 (1 ng/mL), or TNF-α (50 ng/mL). Further, MTs were exposed to the pro-fibrotic compounds MTX (30–250 μM) and TAA (10–80 mM). The supernatants were collected for protein analy- sis and the MTs were used for viability assay (MTT and ATP), mRNA extraction or immuno- histological analysis.

Immunohistochemistry

MTs were fixed with 4% PFA 1h in PBS containing calcium and magnesium. Fixed microtis- sues were embedded in 2% agarose in PBS. The samples were subjected to paraffin embed- ding, cut and analysed with standard procedures. Microtissues were stained with standard hematoxylin & eosin (H&E) and for immunohistochemistry with the following antibodies: albumin (BETHYL Laboratories INC, Cat. A80-229A), Ki67 (Novocastra Laboratories, Cat. NCL-L-Ki67-MM1), vimentin (Epitomics, Cat. 2707–1), αSMA (Sigma, Cat. F3777), Colla- gen I (Abcam, Cat. ab88147) and CD68 (Novacastra Laboratories, Cat. NCL-L-CD68).

Quantification of immunohistochemistry staining

Five random areas from each immunohistochemistry (IHC) specimen were selected. Staining intensity on each image file was assessed by using the IHC Toolbox on the image analysing software NIH ImageJ (version 2.0.0-rc-56/1.51h). Two different colour segmentations were used: one recognized brown-positive cells and the other blue-positive area (nuclei). Integrated optical density was obtained as total number of brown pixels multiplied by the brown intensity of those pixels, and quantitative IHC staining value (QISV) was calculated as integrated optical density divided by total area occupied by the brown (positive cells to the staining) and blue cells (total cell number) [23].

Cell viability assay

The viability of the microtissues was assessed by using the Cell-Titer Glo[1] Luminescent Cell Viability Assay 2.0 (Promega), following standard laboratory procedures.

For some MTs the viability was also determined by 3-(4,5-dimethylthiazol-2-yl)-2,5-diphe- nyltetrazolium bromide (MTT) assay. Briefly, 0.5 mg/mL MTT solution in medium was added to each well and incubated at 37˚C for 4 hours. The medium was then replaced by 89 μL DMSO, incubated on a shaker for a few minutes; 11 μL Sörensen buffer was added to each well and the absorbance was measured at 550 nm.

Gene expression analysis

mRNA was isolated following TRIzol extraction procedure. RNA was reverse transcribed using a reverse transcriptase (Promega) and oligo dT (Qiagen) and real time PCR was per- formed using FastStart TaqMan Mix (Roche) and TaqMan probes from Invitrogen. Real time, TaqMan PCR was performed on selected genes (Col1α1, Col4α1, fibronectin1, CD44, IL6, TGF-β1, αSMA, Nrf2 and Keap1) (see Table 1). The following qRT-PCR Program was used: 10 minutes denaturation at 95˚C, followed by 40 cycles of 15 seconds at 95˚C and 1 minute at 60˚C. The Ct values were assessed using the Corbett Rotorgene Analysis Software 6000 and actin was used as an internal standard for the normalization of the fold changes of each gene of interest (GOI).

ELISA

The presence of cytokines (TNF-α) and extracellular matrix components (COL1α2 and MMP2) in the supernatants was determined using commercial ELISA kits: human TNFα (Thermo Fisher, KHC3014), COL1α2 and MMP2 (Cloud Clone Corp., SEA215Hu and SEA100Hu).

Statistical analysis

Data were analysed using GraphPad Prism 7 (GraphPad Software, inc.) and expressed as mean values ± SD or mean values ± S.E.M. The Student *t* test was used for comparison between two groups. Data from three or more groups were analysed by one-way analysis of variance with Tukey's multiple comparisons test. IHC analysis was performed in 5 independent areas/stain- ing, significance was calculated using Student *t* test. $P < 0.05$ was considered to be significant.

Table 1. TaqMan probes used for the research.

Gene of interest	Abbreviation	Invitrogen Ref.nr.
Actin Beta (Housekeeping gene)	ACTB	Hs99999903_m1
Collagen 1 alpha 1	COL1α1	Hs00164004_m1
Collagen 4 alpha 1	COL4α1	Hs00266237_m1
Fibronectin 1	FN1	Hs00415006_m1
CD44 (hyaluronic acid receptor)	CD44	Hs01075861_m1
Interleukin 6	IL6	Hs00985639_m1
Transcription growth factor Beta 1	TGF-β1	Hs00998133_m1
Actin, alpha 2, smooth muscle	ACTA2 (αSMA)	Hs00909449_m1
Nuclear factor (erythroid-derived 2)-like 2	NFE2L2 (Nrf2)	Hs00975961_g1
Kelch-like ECH-associated protein	Keap1	Hs00202227_m1

https://doi.org/10.1371/journal.pone.0179995.t00

Results

Characterization of hTERT-HSC

The hTERT-HSC cell lines showed typical stellate cell morphology with dendritic structure. The cells were highly proliferative and showed low expression of αSMA, a marker for activated stellate cells. Upon treatment with TGF-β1 or TNF-α, activation of hTERT-HSC cells was observed, indicated by enhanced staining for αSMA (Fig 1). TGF-β1 elicited stellate cell activation after 2 days (with an increase of αSMA-positive cells from 10% to 90%), whereas 10-day stimulation was required with TNF-α to elicit a similar phenotype (Fig 1).

Characterization of macrophages

After differentiation of THP-1 monocytes to macrophages with PMA for 48 h about 90% of THP-1 cells attached and spread showing the expected phenotype. Differentiated macrophages exposed to LPS (1 μg/mL) for 48 h showed the expected increase of TNF-α secretion. The level of secreted TNF-α was increased 5-fold by LPS in all the tested samples (Fig 2). 10ng/mL PMA was chosen as minimal concentration for a stable differentiation, since the cells easily detached after PBS washing in the 5 ng/mL PMA samples.

Morphological characterization ofmicrotissues

Microtissues (MTs) showed a regular spherical shape and a diameter of approximately 200– 350 μm. The presence of the three cell types in the co-cultures was demonstrated by the expres- sion of vimentin, marker of mesenchymal non-parenchymal cells, and CD68, marker for macrophages (Fig 3). In addition, we observed dendritic-shaped cells expressing vimentin, likely to be quiescent hTERT-HSC. The vimentin-positive cells are always located in the inner part of the microtissues, indicating a preferential spatial organization of the three cell types, with hTERT-HSC and macrophages located in the centre and surrounded by the hepatocytes.

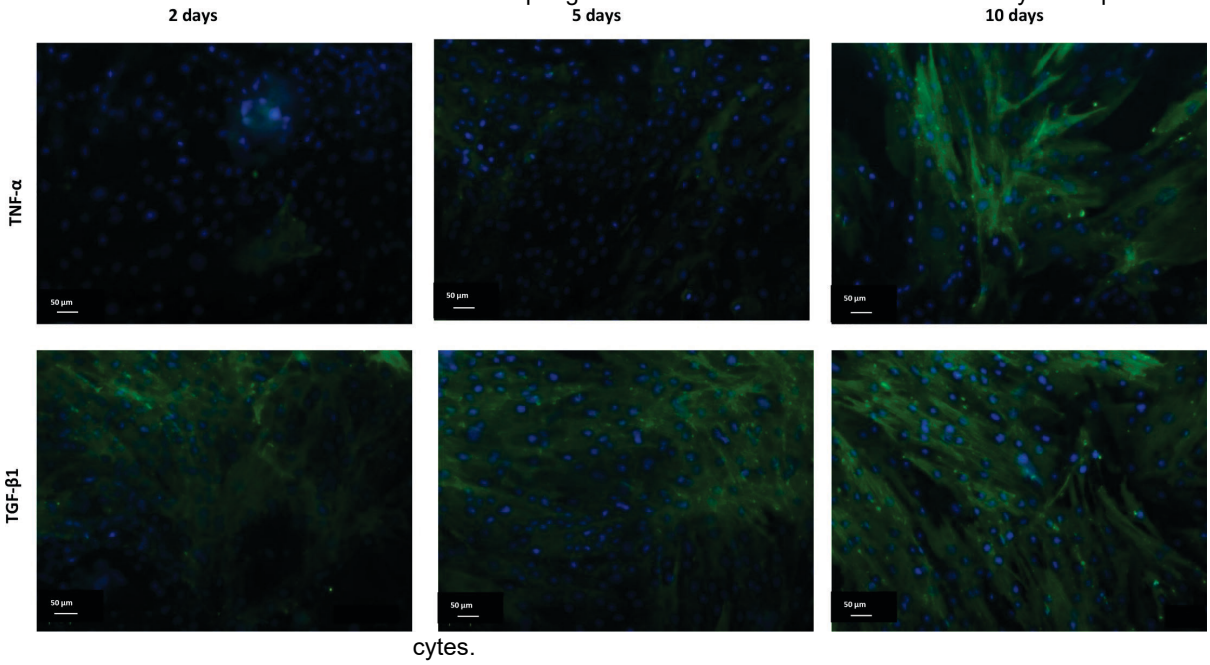

Fig 1. TNF-α and TGF-β1 promote αSMA production in monolayer culture of hTERT-HSC. hTERT-HSC cells were treated for 2, 5 or 10 days with TNF-α (50ng/mL) or TGF-β1 (1ng/mL). After treatment, the cells were fixed and stained against αSMA (green) and nuclei (DAPI, blue). Pictures taken using fluorescence microscopy. Scale bar: 50μm.

https://doi.org/10.1371/journal.pone.0179995.g001

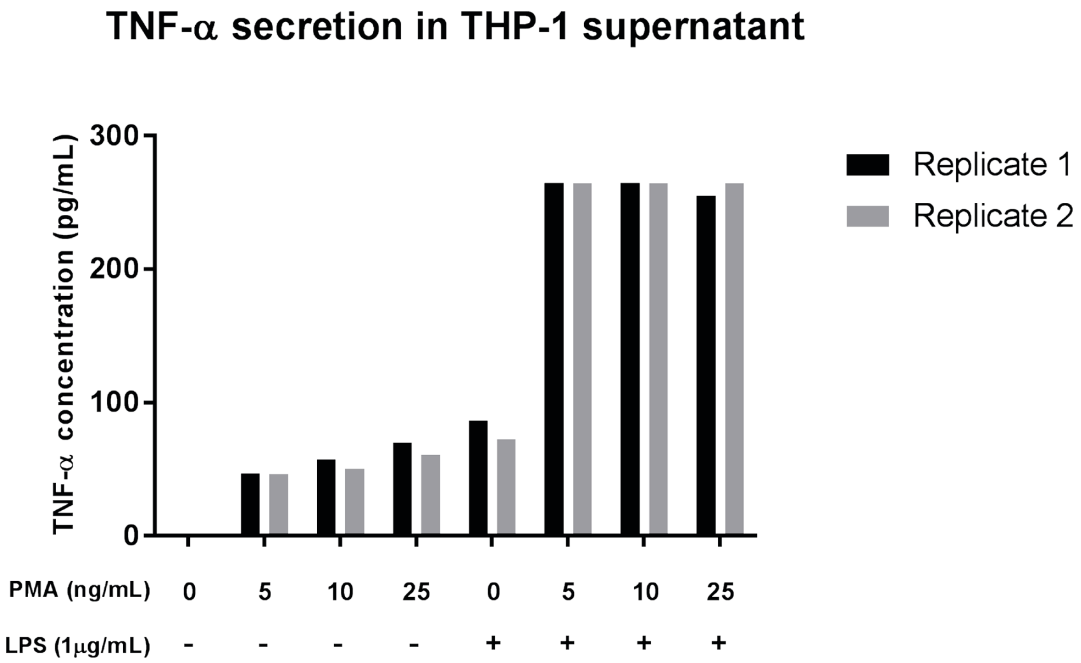

Fig 2. LPS induces TNF-α production in PMA-treated THP-1 cells. THP-1 were treated with 0, 5, 10 and 25 ng/mL PMA for 48h prior exposure to 1 μg/mL LPS. The concentration of TNF-α was measured from the 48h culture supernatants by ELISA. These findings indicate that PMA differentiated THP-1 cells are well differentiated and yet respond adequately to a subsequent low-concentration of LPS. Values are presented as duplicates.

https://doi.org/10.1371/journal.pone.0179995.g002

Responses to LPS, TNF-α and TGF-β1

The treatment with LPS and TNF-α resulted in increased cellular viability of co-cultured microtissues, whereas TGF-β1 decreased their viability after 14 days of treatment (Fig 4A). Sig- nificant decrease in cell viability was also showed after treatment with LPS and TNF-α in HepaRG-only microtissues, in contrast with the cell proliferation showed in the co-culture model with the same compounds.

HepaRG showed a strong induction of IL-6 expression after stimulation with LPS and TNF-α (Fig 5F). On the other hand and as expected, HepaRG monocultures, exhibited only moderate or no increase in expression of extracellular matrix proteins after stimulation with TGF-β1 (Fig 5).

In the co-cultures containing the three cell types, analysis of gene expression changes after treatment with LPS, TNF-α, and TGF-β1 showed a strong transcriptional induction of the extracellular matrix proteins collagen I and IV, fibronectin, CD44, as well as the cytokines IL-6 and TGF-β1 (Fig 5).

Responses of multicellular MTs to the pro-fibrotic substances MTX and TAA

In order to test whether the newly established *in vitro* model is capable of recapitulating induction of liver fibrosis, we tested the pro-fibrotic chemicals methotrexate (MTX) and

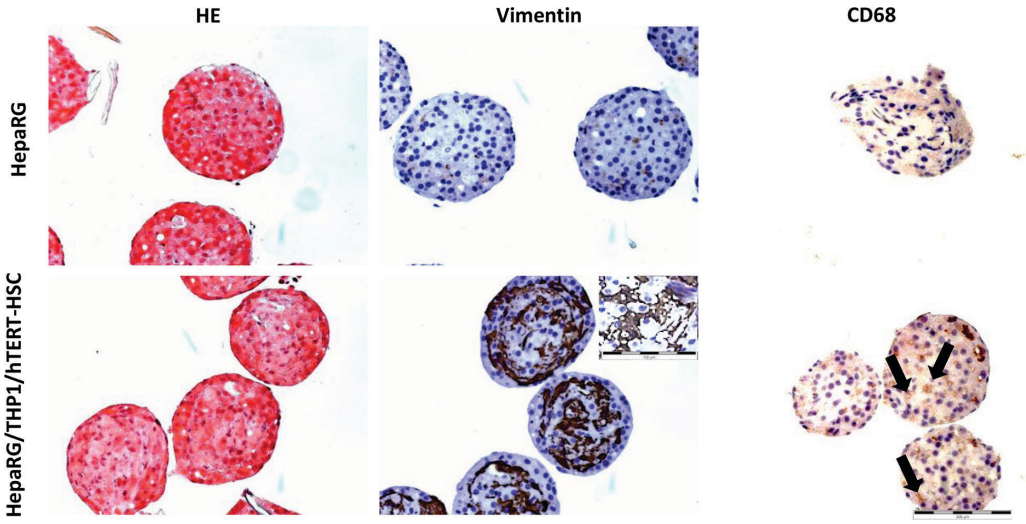

Fig 3. Staining of formalin fixed paraffin embedded human microtissues generated with HepaRG-cells or HepaRGs/THP-1/ hTERT-HSC. Microtissues were stained with Hematoxylin & Eosin (H&E), mesenchymal NPC-marker vimentin and macrophages marker CD68. Microtissues were kept in culture during 14 days before performing histological staining. Co-culture systems showed positive staining for vimentin and CD68 indicating the presence of the three different cell types. Arrows indicate CD68-positive cells. Dendritic stellate cells are shown in the zoom of vimentin staining picture. Scale bar: 200μm (20X magnification) and 100μm (40X magnification).

https://doi.org/10.1371/journal.pone.0179995.g003

thioacetamide (TAA). Non-treated MTs were rather quiescent and maintained a relatively constant cell composition with minimal proliferation over at least 2 weeks (Fig 6). Exposure of co-culture MTs to MTX and TAA over 14 days showed a dose-dependent decrease in viability (Fig 4B), mainly due to an effect on HepaRG cells. This is consistent with the decrease in albu- min staining detected by IHC (Fig 6). After TGF-β1 stimulation, NPCs proliferated, as indi- cated by an increase of Ki67 and vimentin positive cells; the number of vimentin positive cells showed a 4-fold increase as assessed by QISV (Fig 7). The increase in the CD68-, αSMA- and vimentin-positive cells, clearly show that a change in the cellular composition of the microtis- sues is occurring after treatment with TGF-β1, MTX and TAA; in particular hTERT-HSC and THP-1 macrophages are proliferating at the expense of the HepaRG, which are decreasing. In addition, the increase in αSMA-positive cells demonstrated the activation of HSC. Thus, the MTs show a strong change in the cellular composition after stimulation with TGF-β1 and, to a lesser extent, with the profibrotic compunds MTX and TAA (Fig 7). The cellular defence mechanism was also activated upon treatment of the MT with TAA and MTX, as the mRNA levels of both Nrf2 and Keap1 were increased (Fig 8).

Extracellular matrix remodelling expected during the progression of fibrosis was observed in the MTs treated with the model compounds. Gene expression of MTs treated with MTX and TAA showed significant, dose-dependent transcriptional induction of collagen I, collagen IV, fibronectin I and CD44 (Fig 8). The observed increase in gene expression resulted in increased secretion of collagen 1 and MMP2 in the supernatants at 14 days (Fig 9). These find- ings were further confirmed by the increased protein deposition of collagen I and αSMA observed by histological examination (Fig7).

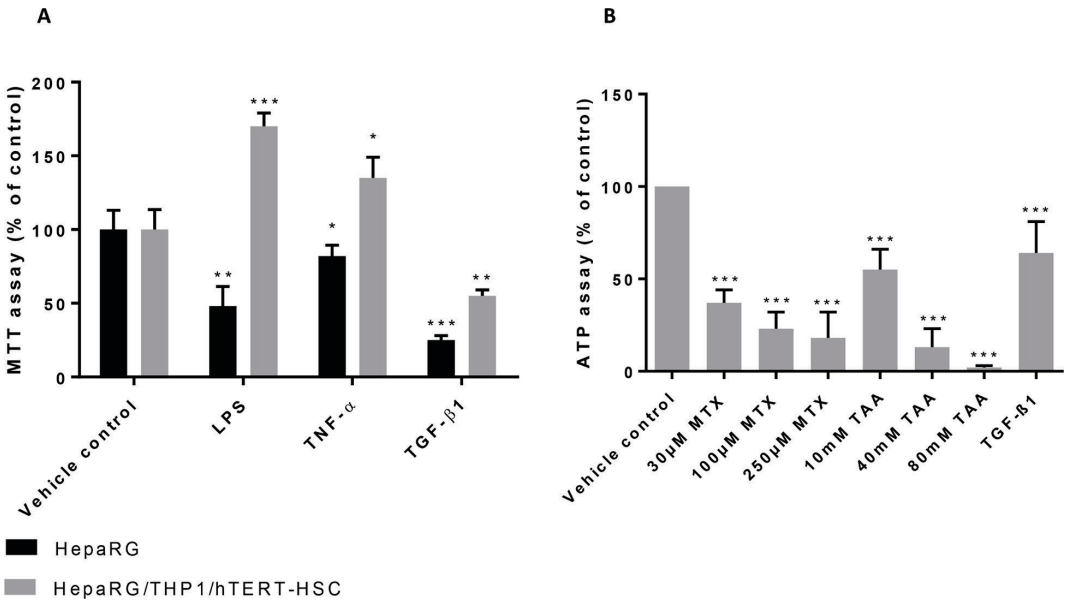

Fig 4. Viability response of human liver microtissues treated with pro-fibrotic compounds. (A) Effect of LPS, TNF-α and TGF-β1 on viability of human liver microtissues was assessed by MTT assay. Microtissues were incubated with 0.5mg/mL MTT solution for 4h after 14 days of exposure to the tested compounds. DMSO and Sörensen buffer were then added into the wells and absorbance was read at 550nm using FlexStation 3. Values are expressed as percentage of negative control. *; P 0.05, **; P 0.01, ***; P 0.001 vs vehicle control. (n = 6, mean ± SD). (B) Effect of MTX, TAA and TGF-β1 on the ATP production. ATP content was measured using CellTiter-Glo® Luminescent Cell Viability Assay 2.0 after 14 days of exposure to MTX, TAA and TGF-β1. Values are expressed as percentage of negative control. ***; P ≤ 0.001 vs vehicle control (n = 6, mean ± SD).

https://doi.org/10.1371/journal.pone.0179995.g004

Discussion

In this work, we provide experimental evidence demonstrating that multi-cellular MTs gener- ated with well characterized human cell lines can recapitulate the key cellular and molecular events leading to hepatic fibrosis. We reproducibly generated human liver MT using HepaRG, hTERT-HSC and THP-1, three human cell lines representing hepatocytes, macrophages and stellate cells. The use of stellate cells in culture has been attempted previously but often not considered a good option for the study of fibrosis *in vitro* due to the fact that stellate cells often undergo spontaneous activation when grown on plastic dishes [24]. This is mainly due to the physical properties of cell culture dishes, which have a tissue tension greater than that of the fibrotic/cirrhotic liver (20 KPa) and much larger than that of normal liver tissue (5 KPa) [5]. hTERT-HSC have been reported to revert to a more quiescent status when cultured on extra- cellular matrix components [25]. In our hands, however, hTERT-HSC showed low levels of expression of the stellate cell activation marker αSMA before induction with TGF-β1. In both 2D culture and in the scaffold-free 3D MT, hTERT-HSC responded to pro-fibrotic stimuli such as LPS, TNF-α, TGF-β1 and pro-fibrotic compounds (MTX and TAA) by attaining an activated status. In the scaffold-free 3D liver MTs that we generated, the hTERT-HSC are kept in a more physiological environment, surrounded by other relevant cell types (HepaRG and THP1) as shown by IHC staining for αSMA and vimentin. In addition, the co-culture of
HSC with hepatocytes and Kupffer cells is a model that incorporates all three cell types involved in the AOP leading to fibrosis, and is therefore very well suited to recapitulate cell-

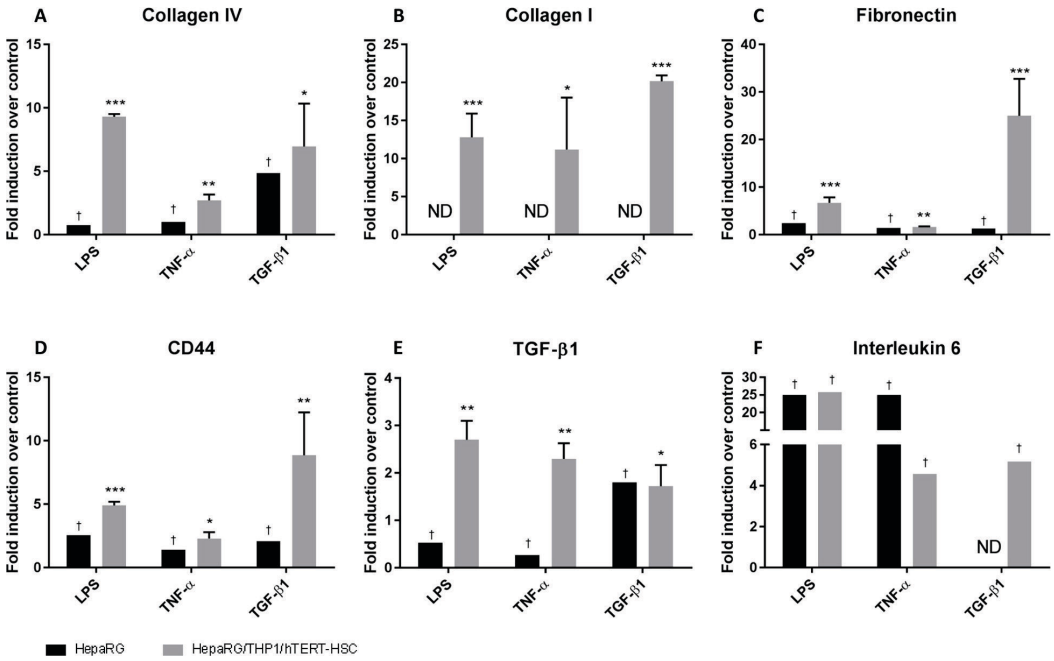

Fig 5. Gene expression of fibrotic markers and cytokines in human liver microtissues exposed to LPS, TNF-α and TGF-β1. mRNA was extracted using TRIzol conventional procedure and fold induction were calculated as 2^(-ΔΔCT) for each sample and vehicle control and expressed as mean fold induction ± S.E.M of three replicates with six MTs each. Actin was used as reference gene for each sample. † pool of 16 microtissues analysed as duplicate; no statistical analysis were performed on these samples. ND: no-detected values. *; P ≤ 0.05, **; P ≤ 0.01, ***; P ≤ 0.001 vs vehicle control.

https://doi.org/10.1371/journal.pone.0179995.g005

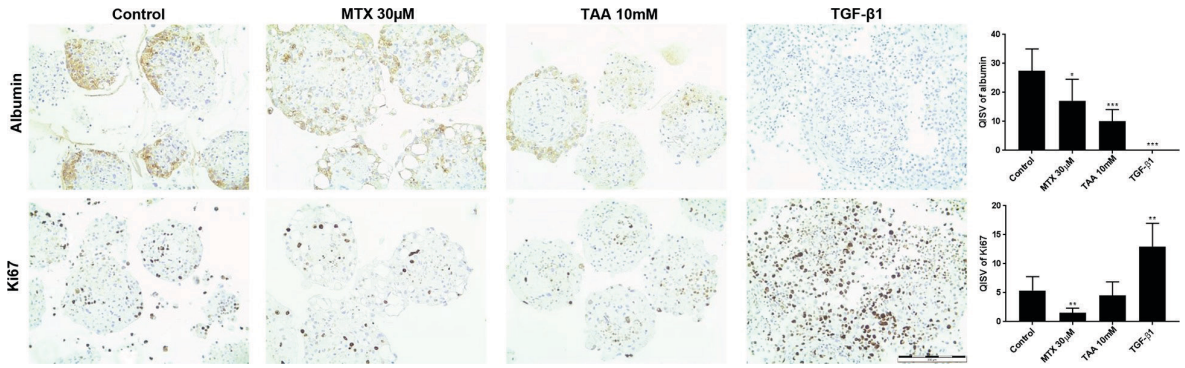

Fig 6. Albumin production and cell proliferation in liver microtissues. Formalin fixed paraffin embedded slides of HepaRG/THP-1 macrophages/hTERT-HSC microtissues were stained with Albumin and Ki67 antibodies after 14 days of treatment with MTX, TAA and TGF-β1. Microtissues were fixed in 4% PFA and embedded in 2% agarose prior paraffinization. Microtissues showed decrease in albumin production after MTX, TAA and especially TGF-β1 exposure. Ki67 shows strong induction of cell proliferation in the microtissues after TGF-β1 exposure. Scale bar: 200μm. Graphics show Quantitative IHC Staining Value (QISV) as mean ± S.D. (N = 5). *; P ≤ 0.05,
; P ≤ 0.01, *; P ≤ 0.001 vs vehicle control.

https://doi.org/10.1371/journal.pone.0179995.g006

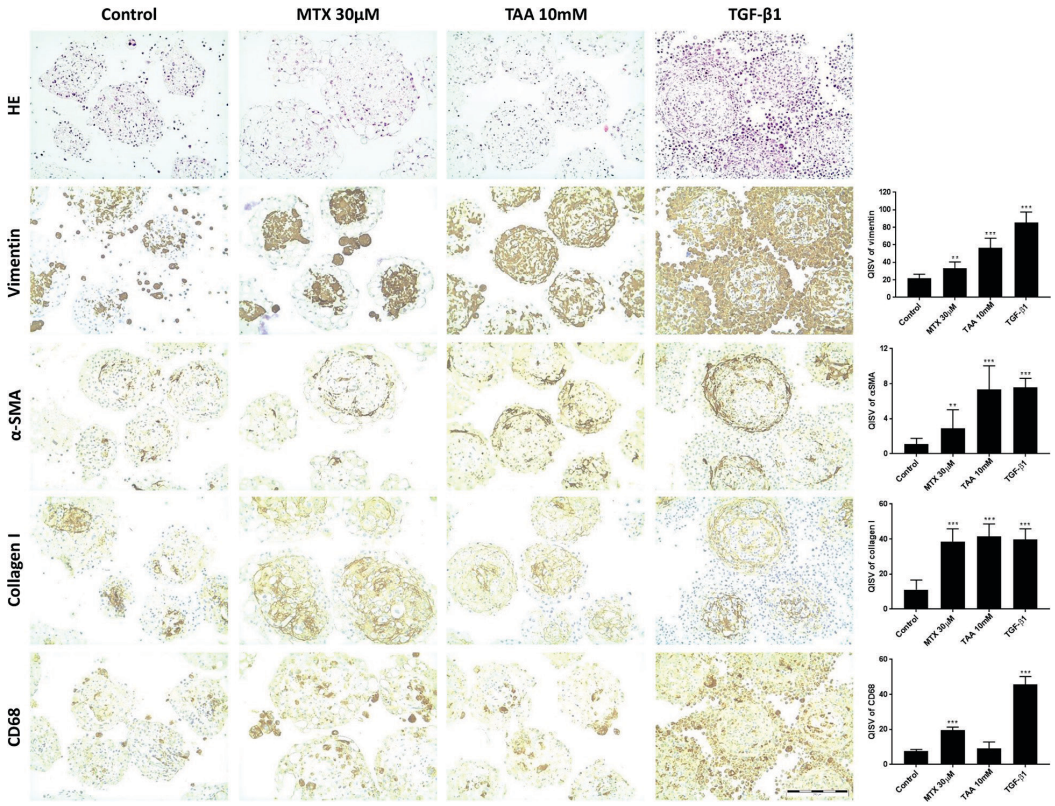

Fig 7. Immunostaining of formalin fixed paraffin embedded human microtissues after exposure to MTX, TAA and TGF-β1. Formalin fixed paraffin embedded slides of HepaRG/THP-1 macrophages/hTERT-HSC microtissues were stained with Hematoxylin & Eosin (H&E), vimentin, α-smooth muscle actin (αSMA), collagen I and CD68 after 14 days of treatment with MTX, TAA and TGF-β1. Microtissues were fixed in 4% PFA and embedded in 2% agarose prior paraffinization. Microtissues showed increase in the vimentin, αSMA, collagen I and CD68 positive cells after MTX, TAA and TGF-β1 exposure. Vimentin and CD68 stainings show proliferation of stellate cells and THP-1 macrophages in the microtissues, suggesting the onset of inflammation process, while αSMA and collagen I indicate activation of stellate cells and deposition of collagen. Scale bar: 200μm. Graphics show Quantitative IHC Staining Value (QISV) as mean ± S.D. (N = 5). *: P ≤ 0.05, **: P ≤ 0.01, ***: P ≤ 0.001 vs vehicle control.

https://doi.org/10.1371/journal.pone.0179995.g007

cell interactions leading to fibrosis *in vitro*. The results we obtained after stimulation with TGF-β1 clearly demonstrate that the hTERT-HSC cell line is able to respond to well established pro-fibrotic stimuli by increasing the expression of the key factors: the activation marker αSMA and ECM proteins (collagen I and IV, fibronectin, and CD44). Similarly, in our hands differentiated THP-1 macrophages served as an excellent surrogate for KC, as they were able to produce cytokines (in particular TNF-α) upon stimulation with LPS in both 2D and 3D cul- tures. In our system, we used HepaRG cells as equivalent of hepatocytes. These cells are known to display many characteristics of human hepatocytes [26] including retention of metabolic activity [27]. Similarly to reported data with primary murine hepatocytes [28], HepaRG MTs responded to LPS and TNF-α by increasing transcription of IL6, showing for the first time that also HepaRG cells are able to produce IL6 following injuring stimuli. HepaRG were also able to produce albumin in the 3D culture, indicating a functional phenotype up to three weeks in culture. However, albumin was significantly decreased after treatments with MTX and TGF-

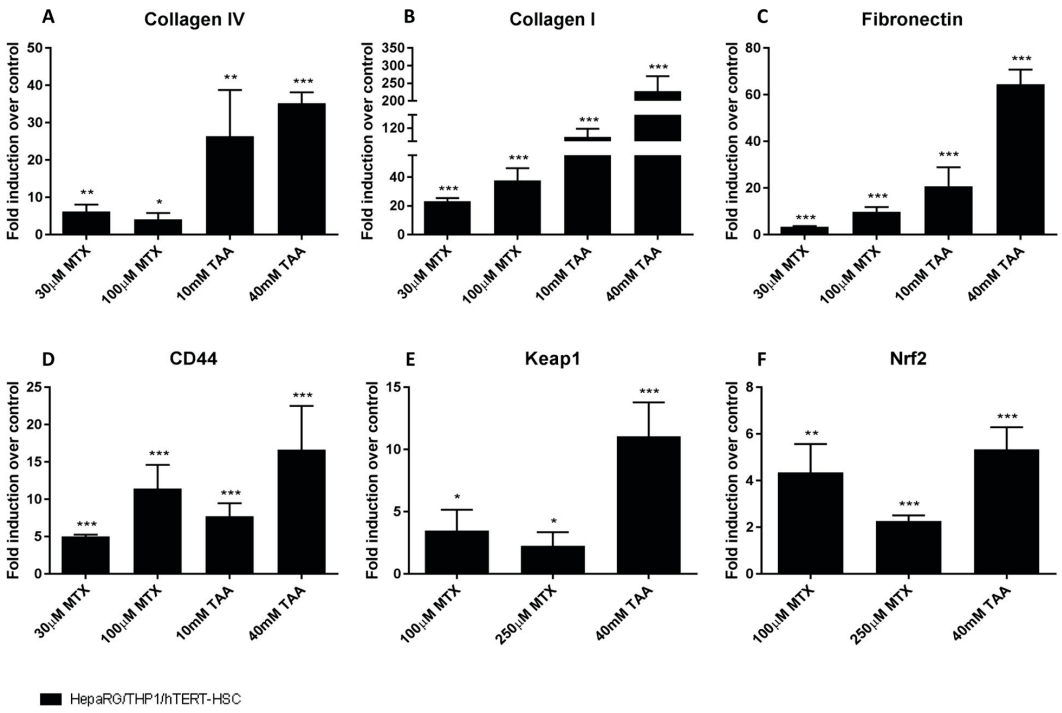

Fig 8. Effect of MTX and TAA on gene expression of fibrotic markers in human liver microtissues. mRNA was extracted using TRIzol conventional procedure and fold induction were calculated as 2^(-ΔΔCT) for each sample and negative control and expressed as mean fold induction ± S.E.M. of three replicates with six MTs each. Actin was used as reference gene for each sample. *; P ≤ 0.05,
; P ≤ 0.01, *; P ≤ 0.001 vs vehicle control.

https://doi.org/10.1371/journal.pone.0179995.g008

β1 suggesting hepatocytes damage and onset of fibrosis in the microtissues. The higher biologi- cal relevance of this model system allows studying responses in an integrated biological system with intricate crosstalks between the main contributing cell types to fibrosis. For example, bio- logical response to LPS stimulation is only possible in presence of inflammation responsive cells (THP-1) and resulted in high activation of HSCs. This would not be possible in conven- tional monocultures. IHC staining for vimentin (as marker for NPCs) shows a physiological liver cell ratio of Hep/NPCs with approximately 80% hepatocytes, 20% NPCs including inflam- matory cells and stellate cells prior treatments. Thus, we were able to generate a complex cellu- lar model system with cell types and ratios which mimic *in vivo* liver organization. Moreover, with such model systems, it is for the first time possible to study in detail the contribution of the different cell types on induction and progression of fibrosis in an *in vitro* model system.

Human liver MT recapitulate the sequence of events leading to fibrosis

The recently published sequence of key events leading to liver fibrosis involve hepatocellular injury/death, KC-activation and macrophage recruitment, TGF-β1 expression and release of cytokines (TNF-α and IL6), HSC activation, and collagen accumulation [29]. In Fig 10, we depicted our results in the context of the published AOP and of literature on known pathways related to liver fibrosis. Our results strongly indicate that the events leading to fibrosis in vivo can be reproduced by the herein described liver MT model system.

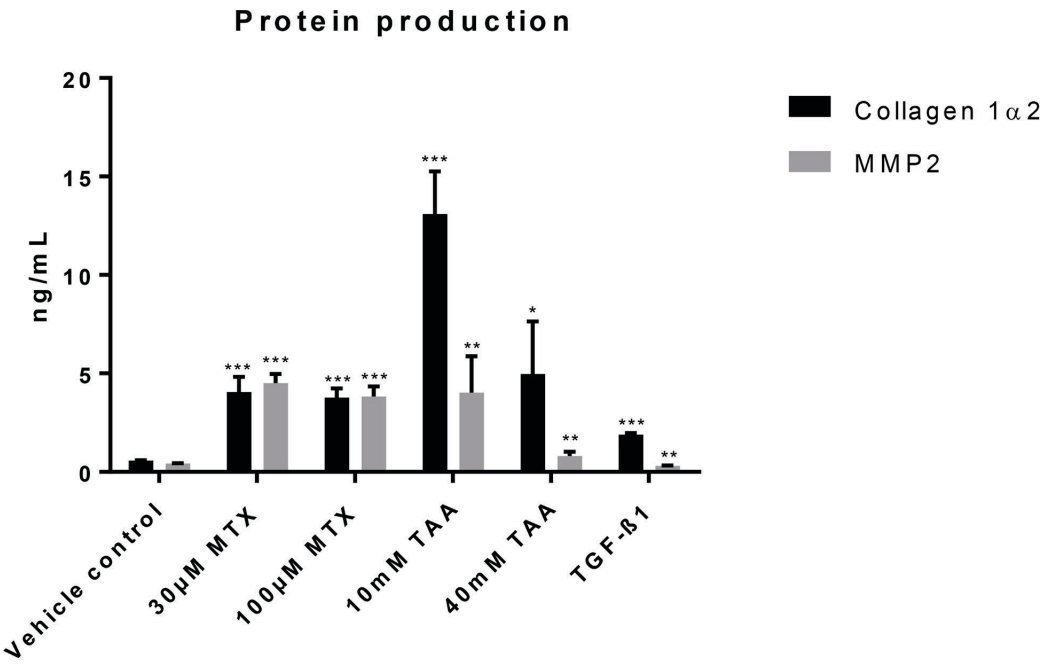

Fig 9. Secretion of Collagen I and MMP2 in supernatant medium after exposure of microtissues to pro-fibrotic compounds.
Protein amount was assessed by ELISA in supernatant medium after 14 days of exposure to MTX, TAA and TGF-β1. *; P ≤ 0.05, **; P ≤ 0.01, ***; P ≤ 0.001 vs vehicle control (n = 4, mean ± SD).

https://doi.org/10.1371/journal.pone.0179995.g009

First: Hepatocellular injury/cell death was detected after exposure of MTs to TGF-β1, MTX and TAA by cell viability assays where the treatments caused a dose-dependent decrease in via- bility. Hepatocyte damage was also highlighted by albumin staining with a complete loss of albumin after exposure to TGF-β1. With LPS, TNF-α, TGF-β1 we could demonstrate that the major target of the cytotoxicity in the co-culture system were the HepaRG cells. MTs consist- ing of HepaRG alone showed a decrease in cell viability, while in co-culture systems there seemed to be an increase in the number of living cells. This suggests compensation due to the proliferation of hTERT-HSC and/or THP-1 macrophages. Immunostaining results (Ki67 and vimentin), confirm the proliferation of vimentin-positive non-parenchymal cells and macro- phages (expressing CD68) after TGF-β1 stimulation. HepaRG injury could also be confirmed by upregulation of mRNA level of IL6 after exposure to LPS and TNF-α, suggesting the onset of an inflammatory response.

Second: Hepatic KC and macrophages are usually responsive to the TLR4-ligand LPS by increased cytokine release [30]. After exposure of liver microtissues to LPS, we detected an increase of expression of TNF-α, IL6 and TGF-β1, indicating the onset of an inflammatory response. Moreover, treatment of microtissues with TNF-α, also led to increased expression and secretion of TGF-β1, produced either by the THP-1 cells or by the hTERT-HSC in agree- ment with a described autocrine loop [31].

Third: The last cellular events in the cascade leading to liver fibrosis involve activation of stellate cells and ECM-remodelling [29]. This was also observed in our system as exposure of MTs to TGF-β1 led to an increase in the number of αSMA-positive cells and the induction of

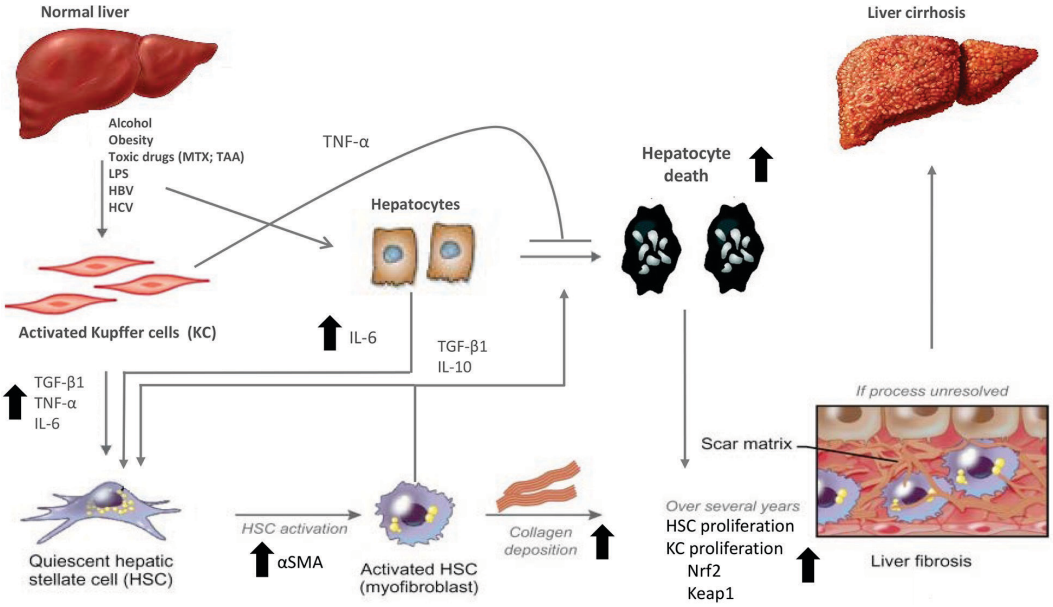

Fig 10. Molecular signalling between hepatic stellate cells, Kupffer cells and hepatocytes after liver injuries. The picture shows the potential complex interactions between matrix-producing hepatic stellate cells and liver-resident macrophages and hepatocytes after liver injuries such as pro-fibrotic compounds (MTX and TAA). Some of these interactions have been previously published, some are supported by our data and some are still speculative. In our liver microtissues THP1 macrophages (as surrogate of Kupffer cells) produced large amount of TNF-α, IL6 and TGF-β1 detected by increase in gene expression. HepaRG (hepatocyte-like cells) also produced cytokines (IL-6) after specific stimulation such as LPS and TNF-α and showed hepatocyte damage after exposure to TGF-β1 as demonstrated by decreased albumin staining. The cytokines were able to enhance stellate cell activation (increase in αSMA production) and collagen deposition. Furthermore increase in expression of oxidative related genes, such as Nrf2 and Keap1, was measured at high concentrations of MTX and TAA suggesting the involvement of this cellular defence. Arrows indicate measured parameters.

https://doi.org/10.1371/journal.pone.0179995.g010

ECM components (collagen I, IV, fibronectin, CD44, and MMP2). CD44 (hyaluronic acid receptor) is usually upregulated in stellate cells of injured liver and it is also correlated to their activated and migratory phenotype [32]. Also MMP2 upregulation in the supernatant con- firms the remodelling of the ECM, as previously published [33]. Thus, the co-cultured MTs were able to recapitulate the described cellular key events that lead to liver fibrosis.

Response of liver microtissues to pharmacologically induced fibrosis

Similar to the results obtained with the positive control TGF-β1, both MTX and TAA induced strong expression of ECM-components and a rearrangement of the cellular composition of the MTs: increased numbers of vimentin-positive NPC cells appeared surrounded by big and round apoptotic cells that could be the injured HepaRG, as also supported by the decrease in albumin. These NPCs contributed to changes in the ECM, demonstrated by the increased secretion and deposition of collagen I, the strong transcriptional induction of hyaluronic acid receptor (CD44) and fibronectin, as well as a 10-fold increase in secretion of MMP2 into the medium. Taken together, the results suggest an increase in the propensity of the stellate cells to become invasive and highly proliferative and demonstrate the remodelling of the ECM upon challenge of liver MT with fibrotic compounds. All these effects were more pronounced in TAA-treated samples than in MTX-treated samples.

In addition to the effects on viability and ECM, the involvement of oxidative stress and the activation of the Nrf2 pathway in liver fibrosis have previously been reported [10]. The induc- tion of Nrf2 and Keap-1 after exposure to MTX and TAA clearly indicates that this cellular defence mechanism is active in our culture system. In the early stages of fibrosis, ROS pro- duced directly by injured hepatocytes and/or recruited neutrophils could directly induce acti- vation of Kupffer cells and macrophages [34]. The Nrf2 and Keap-1 gene upregulation we measured in our system could be related to similar protective mechanisms, but due to the mul- ticellular nature of the co-cultured MT, we cannot pinpoint if this pathway has been activated in the HepaRG cells or in the THP-1 or hTERT-HSC.

Conclusion

Summarizing, in this study, we have demonstrated that a 3D-liver MT co-culture containing HepaRG, THP-1 and hTERT-HSC is able to recapitulate the known cellular events leading to the fibrotic phenotype [29].

Treatment with pro-fibrotic substances demonstrates that this system reproduces the key cellular and molecular events including hepatocellular injury, activation of the cellular defence pathway, macrophage activation, stellate cell activation and deposition of ECM (Fig 10). Phar- macological interventions (pro-fibrotic compounds, LPS, TNF-α and TGF-β1) at several levels of the fibrosis AOP [29] provided convincing evidence supporting that the described sequence of cellular events could be reproduced *in vitro*.

The application of such a system would be a great contribution for the further understanding of the mechanism through which clinically relevant compounds lead to liver fibrosis. The implementation of this system for the detection of potential pro-fibrotic compounds may replace currently used animal studies. In addition, the model system allows testing of anti- fibrotic compounds in a physiological relevant *in vitro* system, providing researchers a novel tool to study inhibition of fibrosis progression.

Acknowledgments

We would like to acknowledge the financial support of the Swiss Commission for Innovation and Technology (CTI), the Swiss Centre for Applied Human Toxicology (SCAHT) and the scientific support of Dr. Jens Kelm. We are very thankful to Dr. B. Schnabl for making the hTERT-HSC available for our research.

Author Contributions

Conceptualization: LSD VP.

Data curation: VP AW FL.

Formal analysis: VP AW.

Funding acquisition: LSD SM.

Investigation: VP AW FL.

Methodology: VP SM.

Project administration: LSD.

Resources: VP AW FL SM LSD.

Supervision: LSD.

Validation: VP SM LSD.

Visualization: VP LSD.

Writing – original draft: VP LSD.

Writing – review & editing: VP LSD FL SM.

References

1. Iredale JP. Models of liver fibrosis: exploring the dynamic nature of inflammation and repair in a solid organ. J Clin Invest 2007; 117:539–48. https://doi.org/10.1172/JCI30542 PMID: 17332881
2. Ankley GT, Bennett RS, Erickson RJ, Hoff DJ, Hornung MW, Johnson RD et al. Adverse outcome path- ways: a conceptual framework to support ecotoxicology research and risk assessment. Environ Toxicol Chem 2010; 29:730–41. https://doi.org/10.1002/etc.34 PMID:20821501
3. Vinken M. The adverse outcome pathway concept: a pragmatic tool in toxicology. Toxicology 2013; 312:158–65. https://doi.org/10.1016/j.tox.2013.08.011 PMID: 23978457
4. Bataller R and Brenner DA. Liver fibrosis. J Clin Invest 2005 115:209–18. https://doi.org/10.1172/ JCI24282 PMID:15690074
5. Trautwein C, Friedman SL,Schuppan D and Pinzani M. Hepatic fibrosis: Concept to treatment. J Hepa- tol 2015; 62:S15–24. https://doi.org/10.1016/j.jhep.2015.02.039 PMID: 25920084
6. Friedman SL. Molecular regulation of hepatic fibrosis, an integrated cellular response to tissue injury. J Biol Chem 2000; 275:2247–50. PMID: 10644669
7. Arias M, Lahme B, Van de Leur E, Gressner AM and Weiskirchen R. Adenoviral delivery of an antisense RNA complementary to the 3' coding sequence of transforming growth factor-beta1 inhibits fibrogenic activities of hepatic stellate cells. Cell Growth Differ 2002; 13:265–73. PMID: 12114216
8. Cichoz-Lach H and Michalak A. Oxidative stress as a crucial factor in liver diseases. World J Gastroen- terol 2014; 20:8082–91. https://doi.org/10.3748/wjg.v20.i25.8082 PMID:25009380
9. Bryan HK, Olayanju A, Goldring CE and Park BK. The Nrf2 cell defence pathway: Keap1-dependent and -independent mechanisms of regulation. Biochem Pharmacol 2013; 85:705–17. https://doi.org/10. 1016/j.bcp.2012.11.016 PMID: 23219527
10. Yang JJ, Tao H, Hu W, Liu LP, Shi KH, Deng ZY, et al. MicroRNA-200a controls Nrf2 activation by target Keap1 in hepatic stellate cell proliferation and fibrosis. Cell Signal. 2014; 26(11):2381–9 https://doi.org/ 10.1016/j.cellsig.2014.07.016 PMID: 25049078
11. Marques TG, Chaib E, da Fonseca JH, Lourenço AC, Silva FD, Ribeiro MA Jr. et al. Review of experi- mental models for inducing hepatic cirrhosis by bile duct ligation and carbontetrachloride injection. Acta Cirúrgica Brasileira 2012; 27:589–594. PMID: 22850713
12. Tostoes RM, Leite SB, Serra M, Jensen J, Bjorquist P, Carrondo MJ et al. Human liver cell spheroids in extended perfusion bioreactor culture for repeated-dose drug testing. Hepatology 2012; 55:1227–36. https://doi.org/10.1002/hep.24760 PMID: 22031499
13. Kostadinova R,Boess F,Applegate D,Suter L, Weiser T, Singer T et al. A long-term three dimensional liver co-culture system for improved prediction of clinically relevant drug-induced hepatotoxicity. Toxi- cology and applied pharmacology 2013; 268:1–16. https://doi.org/10.1016/j.taap.2013.01.012 PMID: 23352505
14. Messner S, Agarkova I, Moritz W and Kelm JM. Multi-cell type human liver microtissues for hepatotoxicity testing. Arch Toxicol 2013; 87:209–13. https://doi.org/10.1007/s00204-012-0968-2 PMID: 23143619
15. Brophy CM, Luebke-Wheeler JL, Amiot BP, Khan H, Remmel RP, Rinaldo P et al. Rat hepatocyte spheroids formed by rocked technique maintain differentiated hepatocyte gene expression and func- tion. Hepatology 2009; 49:578–86. https://doi.org/10.1002/hep.22674 PMID: 19085959
16. Godoy P, Hewitt NJ, Albrecht U, Andersen ME, Ansari N, Bhattacharya S et al. Recent advances in 2D and 3D in vitro systems using primary hepatocytes, alternative hepatocyte sources and non-parenchy- mal liver cells and their use in investigating mechanisms of hepatotoxicity, cell signaling and ADME. Arch Toxicol 2013; 87:1315–530. https://doi.org/10.1007/s00204-013-1078-5 PMID: 23974980
17. Kasuya J, Sudo R, Masuda G, Mitaka T, Ikeda M and Tanishita K. Reconstruction of hepatic stellate cell-incorporated liver capillary structures in small hepatocyte tri-culture using microporous membranes. J Tissue Eng Regen Med. 2012; 9(3):247–56. https://doi.org/10.1002/term.1630 PMID: 23086892
18. Leite SB, Roosens T, El Taghdouini A, Mannaerts I, Smout AJ, Najimi M et al. Novel human hepatic organoid model enables testing of drug-induced liver fibrosis in vitro. Biomaterials 2015; 78:1–10. https://doi.org/10.1016/j.biomaterials.2015.11.026 PMID: 26618472

19. Ding Z and Zhuo L. Attenuation of hepatic fibrosis by an imidazolium salt in thioacetamide-induced mouse model. J Gastroenterol Hepatol 2013; 28:188–201. https://doi.org/10.1111/j.1440-1746.2012. 07265.x PMID: 22989190

20. Barker J, Horn EJ, Lebwohl M, Warren RB, Nast A, Rosenberg W et al. Assessment and management of methotrexate hepatotoxicity in psoriasis patients: report from a consensus conference to evaluate current practice and identify key questions toward optimizing methotrexate use in the clinic. J Eur Acad Dermatol Venereol 2011; 25:758–64. https://doi.org/10.1111/j.1468-3083.2010.03932.x PMID: 21198946

21. Schnabl B, Purbeck CA, Choi YH, Hagedorn CH and Brenner D. Replicative senescence of activated human hepatic stellate cells is accompanied by a pronounced inflammatory but less fibrogenic pheno- type. Hepatology 2003; 37:653–64. https://doi.org/10.1053/jhep.2003.50097 PMID: 12601363

22. Park EK, Jung HS, Yang HI, Yoo MC, Kim C and Kim KS. Optimized THP-1 differentiation is required for the detection of responses to weak stimuli. Inflamm Res 2007; 56:45–50. https://doi.org/10.1007/ s00011-007-6115-5 PMID: 17334670

23. Hsu YH, Lin WL, Hou YT, Pu YS, Shun CT, Chen CL et al. Podocalyxin EBP50 Ezrin Molecular Com- plex Enhances the Metastatic Potential of Renal Cell Carcinoma Through Recruiting Rac1 Guanine Nucleotide Exchange Factor ARHGEF7. Am J Pathol. 2010; 176(6): 3050–3061. https://doi.org/10. 2353/ajpath.2010.090539 PMID: 20395446

24. Gaça MD, Zhou X, Issa R, Kiriella K, Iredale JP, Benyon RC. Basement membrane-like matrix inhibits proliferation and collagen synthesis by activated rat hepatic stellate cells: evidence for matrix-depen- dent deactivation of stellate cells. Matrix Biol. 2003; 22(3):229–39. PMID: 12853033

25. Schnabl B, Choi YH, Olsen JC, Hagedorn CH and Brenner DA. Immortal activated human hepatic stel- late cells generated by ectopic telomerase expression. Lab Invest 2002; 82:323–33. PMID: 11896211

26. Gerets HH, Tilmant K, Gerin B, Chanteux H, Depelchin BO, Dhalluin S et al. Characterization of primary human hepatocytes, HepG2 cells, and HepaRG cells at the mRNA level and CYP activity in response to inducers and their predictivity for the detection of human hepatotoxins. Cell Biol Toxicol. 2012; 28(2):69– 87. https://doi.org/10.1007/s10565-011-9208-4 PMID: 22258563

27. Takahashi Y, Hori Y, Yamamoto T, Urashima T, Ohara Y and Tanaka H. Three-dimensional (3D) spher- oid cultures improve the metabolic gene expression profiles of HepaRG cells. Biosci Rep. 2015.

28. Panesar N, Tolman K and Mazuski JE. Endotoxin stimulates hepatocyte interleukin-6 production. J Surg Res 1999; 85:251–8. https://doi.org/10.1006/jsre.1999.5648 PMID: 10423326

29. Horvat T, Landesmann B, Lostia A, Vinken M, Munn S and Whelan M. Adverse outcome pathway development from protein alkylation to liver fibrosis. Arch Toxicol. 2016

30. Rossol M, Heine H, Meusch U, Quandt D, Klein C, Sweet MJ et al. LPS-induced cytokine production in human monocytes and macrophages. Crit Rev Immunol 2011; 31:379–446. PMID: 22142165

31. Dooley S and ten Dijke P. TGF-beta in progression of liver disease. Cell Tissue Res 2012; 347:245–56. https://doi.org/10.1007/s00441-011-1246-y PMID: 22006249

32. Kikuchi S, Griffin CT, Wang SS, Bissell DM. Role of CD44 in epithelial wound repair: migration of rat hepatic stellate cells utilizes hyaluronic acid and CD44v6. J Biol Chem. 2005; 280(15):15398–404 https://doi.org/10.1074/jbc.M414048200 PMID: 15691832

33. Préaux AM, Mallat A, Nhieu JT, D'Ortho MP, Hembry RM and Mavier P. Matrix metalloproteinase-2 activation in human hepatic fibrosis regulation by cell-matrix interactions. Hepatology. 1999; 30(4):944– 50. https://doi.org/10.1002/hep.510300432 PMID: 10498646

34. Poli G. Pathogenesis of liver fibrosis: role of oxidative stress. Mol Aspects Med 2000; 21:49–98. PMID: 10978499

3.4. Conclusion

The research goal addressed in Project 1 was to develop new liver models able to recapitulate all the key events leading to fibrosis. In the first paper (Prestigiacomo V et al., Journal of Toxicological and Pharmacological Methods 2019), the isolation of KC and HSC from a single liver homogenate was optimized to a single step process allowing a quick and inexpensive purification of the required cells. However, the main achievement of this paper was the establishment of a primary cell culture system with rat hepatocytes, KC and HSC to investigate liver fibrosis using the hanging drop technology in a 96-well format. In these 3D MTs the key phenotypical characteristics of functional cells were maintained, such as albumin production for the hepatocytes, release of TNF-α from KC and production of desmin and αSMA for HSCs. In addition, this model responded to LPS and TGF-β1, which induced αSMA expression, affected cell viability and induced release of cytokines. In addition, it is noteworthy that pre-activated HSC partly reverted to the inactive phenotype when cultured in 3D MTs, as shown by the loss of αSMA production. This last evidence suggests that HSC may have a transmutable phenotype that comes to play in the established 3D-co-culture system. The investigation of the molecular mechanism behind this plasticity could be of great significance in investigating potential pharmacological interventions to treat liver fibrosis. This model represents the first system with both rat primary parenchymal, KC and HSC generated with a simple and reproducible method with the ability to recapitulate fibrotic events *in vitro*.

In the second paper of this chapter (Prestigiacomo V et al., PLoS ONE 2017), a human 3D-liver co-culture model containing HepaRG, THP-1 macrophages and hTERT-HSC was successfully established and characterized. This model responded to pro-inflammatory stimuli (LPS, TNF-α and TGF-β1) as well as to pro-fibrotic stimuli (MTX and TAA), resulting in a fibrotic phenotype *in vitro*. HepaRG showed hepatocyte damage after exposure to MTX, TAA and TGF-β1 as demonstrated by decreased albumin staining. In this model THP-1 macrophages (as surrogate of Kupffer cells) produced large amount of TNF-α, interleukin 6 and TGF-β1 detected by increase in gene expression. In addition, the tested compounds were able to enhance HSC activation (increase in αSMA production) and collagen deposition. Furthermore increase in expression of oxidative related genes, such as Nrf2 and Keap1, was measured at high concentrations of MTX and TAA suggesting the involvement of this cellular defence pathway. This system showed all the key events of fibrosis, such as hepatocyte damage, oxidative stress, HSC activation, ECM remodelling and chronic inflammation. Remarkably, all these events were elicited after exposure to liver cytokines or toxicants administration. This system can thus be used for the investigation of cellular and molecular events involved in the development of fibrosis as well as an *in vitro* test system for the evaluation of anti-fibrotic therapies.

4. Project 2: PDGF, TGF-β1 and Nrf2 in the regulation of hepatic stellate cell activation

4.1 Introduction

As described in chapter 2.2, the initiation and perpetuation of HSC activation require specific signalling pathways. In particular, the mitogenic growth factor PDGF, as well as the fibrogenic TGF-β1, plays a crucial role during HSC activation. PDGF has been identified as the most potent mitogen for HSCs for more than 20 years [100]. PDGFs are members of the cysteine-knot-type growth factors, and consist of five known dimer configurations (AA, AB, BB, CC, DD), formed by four different disulfide-bonded polypeptide chains (A, B, C, D) [101]. All the different chains share a common growth factor domain of around 100 amino acid residues in length, and the accessory amino acid sequences found in the N- or C-terminal extensions of all PDGF chains are involved in the regulation of the biological properties of these factors [102]. PDGFs are synthesized and assembled into disulphide-linked dimers in the endoplasmic reticulum as inactive precursors and proteolytic processing is necessary for activation and biological function. PDGF-AA, PDGF-AB and PDGF-BB are cleaved and activated in the exocytic pathway, whereas PDGF-CC and PDGF-DD are cleaved and activated extracellularly [103–105]. PDGF dimers transduce their signals by binding to α- and β- class III tyrosine kinase receptors (PDGFRα and PDGFRβ), which consist of five extracellular immunoglobulin-like domains and an intracellular tyrosine kinase domain [106]. The five dimeric isoforms of PDGF display distinct abilities to bind and activate the two PDGFRs. PDGF-AA, PDGFAB, PDGF-BB and PDGF-CC can bind to and activate PDGFRα, while PDGF-BB and PDGF-DD can specifically bind to and activate PDGFRβ. PDGF-AB, PDGF-BB and PDGF-CC can also stimulate heterodimeric PDGFRα/β complexes [102]. Following PDGF binding, receptor dimerization occurs. This process brings the intracellular domains of the receptor close to each other, promoting autophosphorylation *in trans*, leading to the activation of the kinase domain and to the several downstream cascades, such as phosphatidylinositol 3-kinase, phospholipase C-γ, the Src family of tyrosine kinases, the tyrosine phosphatase SHP-2, and mitogen-activated protein kinase (MAPK) [106]. The activation of these signalling pathways leads to stimulation of cell growth, but also to changes in cell shape and motility. Although platelets are a major storage site, PDGFs are widely expressed in many cell types. In particular, HSCs express only the A- chain of PDGF, while both receptor isoforms are present on their membrane [23,100]. During fibrosis an increase of PDGFRβ has been shown during early phase of HSC activation [107], and depletion of PDGFRβ in HSCs led to the decrease of injury and fibrosis [108].

TGF-β1 has been identified as the most potent fibrogenic cytokine in the liver, since it directly induces HSC activation [23]. TGF-β1 is a secreted polypeptide member of the transforming growth factor beta superfamily of cytokines, and it performs many cellular functions, including the control of cell growth, proliferation, differentiation and apoptosis [109]. Only three (TGF-β1, TGF-

β2, and TGF-β3) of the five existing isoforms of TGF-β are expressed in mammals. These factors are synthesized as inactive precursors, which do not bind to their receptors and have no biological effect [110]. Prior secretion, the factor is cleaved in the N-terminal pro-region, known as latency-associated peptide (LAP); despite the cleavage, the LAP domain remains associated with the rest of the protein, facilitating the transit of TGF-β out from the cell [110]. This latent complex may associate with latent-TGF-β-binding protein, necessary for the TGF-β targeting to the extracellular matrix [110]. Serine protease, plasmin, neuraminidase, cathepsins B and D, and thrombospondin-1, as well as other proteases and changes in the pH can convert LAP-TFG-β to biologically active TGF-β [110]. Once activated, the TGF-β homodimers transduce their signal by bringing hetero-tetrameric complexes of type II (TβRII) and type I (TβRII or ALK5) serine/threonine kinase receptors. The constitutively active TβRII then leads to phosphorylation-dependent activation of TβRI [109]. To transduce its signal, the activated TβRI recruits many molecular mediators, which is possible to categorize in Smad and Non-Smad pathways [111]. Among the Non-Smad pathways, the MAPK family, Rho-like GTPases and phosphatidylinositol 3-kinase/Akt play a crucial role in the TGF-β mediated signal transduction [111]. Components of the MAPK pathway, as Ras, ERK1/2, p38, and JNK play a key role in the cellular response to pro-inflammatory cytokines, environmental stress signalling and apoptotic agents after TGF-β stimulation [112]. It has been shown that p38 MAPK activity influences cell activation in quiescent hepatic and pancreatic stellate cells [113,114]. TGF-β-induced activation of Rho-like GTPases induces the exchange of GDP for GTP, leading to the stimulation of ROCK kinases, which in turn phosphorylate numerous substrates including the LIM kinases [115]. ROCK activation increases actin–myosin contractile force generation, with a contribution from LIMK-induced actin filament stabilisation in epithelial cells, as well as differentiation of lung fibroblast into αSMA-expressing myofibroblasts [115,116]. However, despite the relevant role of Non-Smad pathways in the TGF-β cascade, the canonical Smad pathway remains the main molecular mechanism for TGF-β-induced signals. The activated TβRI induces the phosphorylation of the cytoplasmic signalling molecules receptor-regulated Smads (R-Smads); in particular the phosphorylation of Smad2 and Smad3 induces their partnering with the signalling transducer Smad4, and their translocation to the nucleus [117]. In the nucleus the R-Smad complex interact interacting with transcriptional co-activators like p300 and Creb-binding-protein, or repressors like SkiL or TGIF, to regulate the expression of target genes [118]. It has been shown that Smad3 is required for HSC matrix production and matrix interaction, by promoting collagen and fibronectin expression [119]. Furthermore, TGF-β1 signalling is required for αSMA production and its organization in stress fibres [120]. A TGF-β1 control element (TCE) as well as two potential Smad3-binding elements have been identified in the αSMA promoter of rat lung smooth muscle cells and fibroblasts, respectively [121,122]. Beside the R-Smad, also inhibitory Smads are involved in the pathway regulation. Particularly, Smad7 is a general antagonist of TGF-β family, acting as a competitor with R-Smads for the TβRI receptor and preventing their

phosphorylation [109]. Furthermore, Smad7 can recruit the E3 ubiquitin ligases, such as Smurf1 and Smurf2, which are involved in the degradation of ALK5 receptor via proteasomal pathway [109].

Oxidative stress has been recently identified as a modulator of HSC activation and fibrosis [46,47]. It was reported that oxidative stress may directly affect PDGF and TGF-β1 pathways [123,124]. Lipid peroxidation products (e.g. 4-hydroxy-2-nonenal) have been shown to induce the expression of PDGF in rat aortic smooth muscle cells with consequent stimulation of cell growth [124], while TGF-β1 has been shown to modulate and be modulated by oxidative stress in many different ways. TGF-β1, in fact, does not only induce ROS production in mitochondria and microsomes in hepatocytes, but also downregulates the expression of antioxidant enzymes such as glutaredoxin, catalase, superoxide dismutase, and glutathione peroxidase during fibrogenic diseases [125–127]. TGF-β1 also increases the expression of the transcription factor ATF3 which decreases the cellular amount of GSH by inhibiting the expression of the GSH catalytic subunit gamma-glutamyl-cysteine synthetase [128,129]. On the other hand, ROS directly modulate the TGF-β1 by acting on the LAP fragment of the latent complex [123]. ROS can also modulate the activity of phosphatases (such as PTP1B, PP2A, MKP-1 and PPM1A) that can indirectly modulate the TGF-β pathway by acting on the activation state of Smad protein and MAPKs [123,130,131]. Oxidative stress, mediated partly by lipid peroxidation products, induces collagen synthesis in rat HSCs [132]. As the other liver cells, quiescent HSCs present protective mechanisms against oxidative stress such as enzymes from the GST family, which form GSH conjugates with lipid peroxidation products (e.g. 4-hydroxy-2-nonenal) [132]. Upon activation, HSCs lose most forms of GST and associated enzymatic activities, becoming then more susceptible to oxidative stress [132]. Nrf2 was found to be active in HSCs, and in particular it was shown that rat activated HSCs express significantly lower level of Nrf2 compared to quiescent cells [47]. Consistently, Keap1 increases significantly in activated HSC, suggesting a possible regulative mechanism of Nrf2 pathway in HSC activation. In the same study, TGF-β1 was reported to reduce the presence of Nrf2 in a rat HSC cell line, by acting through the epigenetic regulation operated by the microRNA-200a [47]. Nrf2 also inhibits TGF-β1-induced expression of fibrosis markers in a human HSC cell line [47]. In human renal tubular epithelial cells, Nrf2 reduces the transition to fibroblast as well as collagen and fibronectin production [83]. Smad7 has been identified as the molecular effector of this pathway; in Keap1 knockdown cells, Smad7 was indeed elevated, promoting a strong inhibition of the TGF-β1 pathway. In HepG2 cells, Nrf2 suppresses phosphorylation, nuclear translocation, and DNA binding of Smad3 [81]. A deeper characterization of Nrf2 pathway in human HSCs may reveal a suitable pathway to which act in order to protect from or revert HSCs activation.

This chapter is divided into two main parts based on the different pathways studied in relation to HSC activation. Both studies were carried out on primary HSCs as well as hTERT-HSCs, focusing on cellular events such as proliferation, migration and differentiation. The first study describes the

two key cytokines involved in HSC activation, PDGF and TGF-β1, focusing on the understanding of how they interact with each other in regulating HSC activation *in vitro*. Indeed, despite their well-known involvement in HSC activation, the specific role of those two key factors remains unclear, mostly due to the lack of recent studies on human primary HSC. The second study focuses on the role of Nrf2 pathway in HSC and on its potential intervention during activation and fibrogenesis in relation to TGF-β1/Smad pathway. Although the Nrf2 role in hepatocytes and liver disease has been widely reported, neither its function in HSC nor its role during activation is known.

4.2 Paper 3

TGF-β1 and PDGF control different aspects of stellate cell activation during liver fibrosis

Vincenzo Prestigiacomo, Chiara Bongiovanni, Laura Suter-Dick

Submitted manuscript

Aims: Elucidate the role of TGF-β1 and PDGF on the main cellular process that characterize HSC activation, such as proliferation, migration and differentiation.

Results: TGF-β1 treatments elicited HSC activation, characterised by production of αSMA and collagens, while PDGF-AB treatment induced proliferation and cell migration in both primary and hTERT-HSCs.

Conclusion: These data suggest that both independent pathways represent key events leading to HSC activation *in vitro*. However, to achieve full cell activation, simultaneous exposure of HSCs to both factors is necessary *in vitro*.

TGF-β1 and PDGF control different aspects of stellate cell activation during liver fibrosis

Vincenzo Prestigiacomo[1,2],Chiara Bongiovanni[1], Laura Suter-Dick[1].

[1]University of Applied Sciences Northwestern Switzerland, School of Life Sciences, Muttenz, Switzerland.
[2]University of Basel, Department of Pharmaceutical Sciences, 4056-Basel, Switzerland.

Corresponding author: Vincenzo Prestigiacomo
Email: vincenzo.prestigiacomo@fhnw.ch T +41 61 647 48 26 F +41 61 647 47 01

Abstract

Liver fibrosis is a reversible wound-healing response to acute or chronic cellular injury. The primary effector cell of liver fibrosis is the hepatic stellate cell (HSC), which orchestrates the deposition of extracellular matrix in normal and fibrotic liver. The aim of this work was to elucidate cellular processes involved in HSC trans-differentiation, such as proliferation, migration and differentiation, to better understand the role of key signalling pathways in the development of fibrosis.

Following stimulation of human primary and immortalised (hTERT) HSCs with TGF-β1 and/or PDGF-AB we evaluated cell viability, activation state trough smooth muscle α-actin (αSMA) expression, proliferation, migration, as well as gene expression for of activation and fibrosis markers.

Upon exposure to TGF-β1, HSCs transdifferentiated into myofibroblasts-like cells, which produce αSMA and collagens. Contrarily, PDGF-AB-treatment did not affect the cellular activation and fibrogenic capacities, but induced proliferation and cell migration in a concentration-dependent manner. Simultaneous exposure of HSCs to both factors showed a synergistic effect leading to full cell activation. These data suggest that both independent pathways converge and represent key events leading to HSC activation *in vitro*. Moreover, primary and hTERT-HSCs behave similarly, identifying this HSC cell line as a suitable model to study HSC activation *in vitro*.

Key words: hepatic stellate cell, TGF-β1, PDGF, activation, fibrosis

Introduction

Hepatic fibrosis is a complex fibrogenic and inflammatory process that results from perpetuation of the normal wound healing response, triggered by chronic liver injury (including chronic viral hepatitis infection, non-alcoholic fatty liver disease, alcoholic liver disease, cholestasis and auto-immune liver disease) [1, 2] . Chronic hepatocyte death leads to the release of cellular contents (e.g. DNA and damage-associated molecular patterns known as DAMPs) that activate resident macrophages (Kupffer cells) that produce large amounts of reactive oxygen species and release pro-inflammatory cytokines such as TNFα, TGF-β1, PDGF and IL-1β, leading ultimately to stellate cell (HSC) activation [2, 3] .

HSCs constitute 5-8% of all liver cells and are found in the sub-endothelial space of Disse, between the anti-luminal side of sinusoidal endothelial cells and the basolateral surface of hepatocytes [4, 5] . During the last decades, HSCs, were mainly viewed as “storing cell”, with the main role of storying approximately 80% of the body's vitamin A (retinol, retinoic acid), and synthesizing extracellular matrix (ECM) components in the normal and fibrotic liver [5, 6] . Nevertheless, it has been reported that HSCs can activate the immune response by releasing cytokines and directly acting as antigen presenting cells; they can also contribute to angiogenesis, hepatocyte regeneration and the regulation of oxidant stress [5–7] .

After liver injury, HSCs undergo an activation process, losing their content of lipid droplets and transdifferentiating from quiescent vitamin A storing cells into smooth muscle α-actin (αSMA) positive myofibroblasts-like cells. Activated HSCs produce a network of fibrillar collagen and fibronectin, replacing the low-density, basement membrane-like matrix of the liver [2, 8] . The activation process is temporally divided into an initiation phase, that renders the cells responsive to cytokines and other local stimuli, and a perpetuation phase, where the cells maintain the activated phenotype and generate fibrosis [6] .

HSC initiation and perpetuation requires specific signalling pathways; thus, understanding how they interact with each other can contribute to the identification of possible therapeutic interventions to revert HSC activation and hepatic fibrosis. Of particular importance for the HSC are growth factor and fibrogenic signalling pathways. More that 20 years ago, platelet-derived growth factor (PDGF) was identified as the most potent mitogen for HSCs [9] . The PDGF family consists of disulphide-bonded homodimers of A-, B-, C- and D-polypeptide chains, and the heterodimer PDGF-AB [10] . PDGF dimers transduce their signals by binding to α- and β- class III tyrosine kinase receptors (PDGFRA and PDGFRB), which consist of five extracellular immunoglobulin-like domains and an intracellular tyrosine kinase domain [10] . While the production of only the A-chain of PDGF has been shown in HSC, both receptors can be detected on their membrane; in particular an increase of PDGFRB has been shown during early phase of HSC activation [6, 9, 11] . The activation of these signalling pathways leads to stimulation of cell growth, but also to

changes in cell shape and motility in HSC [12, 13] . However, HSCs lead to fibrosis not only by increasing the cell number, but also increasing the ECM production per cell [6] . In particular, TGF-β1 has been identified as the most potent fibrotic cytokine in the liver [6, 14] . After liver injury, TGF-β1 is released from the activated Kupffer cells leading to HSC activation with the consequent release of ECM [15] . During the perpetuation phase, HSCs produce TGF-β1 maintaining an positive autocrine loop [14, 16] . Hallmarks of TGF-β1-induced HSCs are αSMA production, as well as the remodelling of ECM, with deposition of fibrillar collagens and fibronectin and release of metalloproteinases (MMPs) [2] .

Although the involvement of several signalling pathways in the activation of HSC has been recognized, the specific role of some key factors remains unclear. Recently, Kikuchi et al. showed the effect of PDGFs on proliferation and migration of human HSCs, but no date are yet available about the effect of TGF-β1 on those cellular processes [17] . The aim of our work was to elucidate the dynamic range of human hepatic HSC transdifferentiation. Using human primary HSC and immortalised HSC (hTERT-HSC), we evaluated changes of several cellular processes, such as proliferation, migration and activation in presence of TGF-β1 and/or PDGF-AB. Here, we report that simultaneous exposure of hTERT-HSC to both factors showed a synergistic effect leading to full HSC activation.

Material and methods

Reagent and chemicals

DMEM High Glucose (41965; Invitrogen), Fetal Bovine Serum (10270; Invitrogen), Penicillin-Streptomycin (A8943; Applichem), TGF-β1 (T5050; Sigma), PDGF-AB (P8147; Sigma), SB-431542 hydrate (SB43) (S4317; Sigma), SB-525334 (SB52) (S8822; Sigma). Triton X-100 (T8787; Sigma), Bovine serum albumin (05473; Fluka), formaldehyde (18814; Polysciences), αSMA antibody (A5228; Sigma), secondary antibody Alexa Fluor® 488 F(ab')2 Fragment of Goat Anti-Mouse IgG (H+L) (A11017; Invitrogen), DAPI (D9542; Sigma) and Propidium Iodide (7109; Sigma).

Cell culture

Human primary HSCs were purchased from iXCells Biotechnologies, USA, (Cat. 10HU-210) or Innoprot, Spain (Cat. P10653). They were cultured in DMEM High Glucose supplemented with 10% Fetal Bovine Serum and 1% Penicillin-Streptomycin and used up to 5 passages. hTERT-HSC were kindly provided by Dr. Bernd Schnabl (UC San Diego, USA) [8] and were cultured in DMEM High Glucose supplemented with 10% Fetal Bovine Serum and 1% Penicillin-Streptomycin up to 12 passages. The cells were kept in the humidified incubator at 37˚C with 5% CO_2.

Cell viability assay

A cell density of 3 x 10^4 cells/cm^2 was seeded in a 96-well plate and incubated with chemicals at 37°C, after overnight cell attachment. The cells were treated with 0-20 ng/mL TGF-β1 or 0-30 ng/mL PDGF-AB in serum-free medium. The treatments were refreshed every day for all the duration of the experiment. The assay was performed after 24 hours, 48 hours and 7 days of exposure by incubation of the samples with 100 µL Cell Counting Kit-8 (96992; Sigma), diluted 1:10 with DMEM medium for 2 hours. Following, the volume was transferred in a 96-well microplate and the absorbance was measured at 450 nm by using the FlexStation™ 3 Microplate Reader. Wells without cells were used as blank. CyQUANT® NF Kit (C35006; Thermo Fisher) was used to normalize the viability data with the number of cells.

Immunocytochemistry analysis

To assess the activation state of the cells, immunostaining for αSMA was performed for both TGF-β1- and/or PDGF-AB-treated and untreated cells. The two Smad inhibitors SB43 [18] (10 µM) and SB52 [19] (1 µM) were used as well. The cells were fixed in 4% formaldehyde for 15 minutes, followed by permeabilization with 0.1% Triton-X-100 for 20 minutes. Blocking was performed with 1% bovine serum albumin in PBS for 60 minutes, followed by incubation with primary antibody against αSMA (dilution 1:200 in blocking solution) for 90 minutes. Incubation with secondary antibody was performed for 60’ in blocking solution. All steps were conducted at room

temperature and washing steps with 1X PBS were conducted between each step and at the end. DAPI and Propidium Iodide were used to stain the nuclei.

Click-iT EdU Proliferation assay

The Click-iT® EdU Alexa Fluor® 488 Imaging Kit (C10637; Invitrogen) was used to measure the proliferation rate of the cells after treatments. 3 x 10^4 cells/cm^2 were seeded in 96-well plate format and immediately treated with 0.5-1 ng/mL TGF-β1, 1-5 ng/mL PDGF-AB and a mixture with 1 ng/mL TGF-β1 and 5 ng/mL PDGF-AB for 48 hours. EdU dye was added only during the last 30 hours of each experiment and detected following manufacture's instructions. The pictures were acquired with the Olympus Laser Confocal Scanning Microscope FV1000D spectral type (inverted microscope IX81) and analysed with ImageJ to determinate the proliferation rate.

Gene expression analysis

RNA from TGF-β1 and PDGF-AB-treated cells (with and without Smad inhibitors), was isolated following TRIzol extraction procedure. RNA was reverse transcribed using a reverse transcriptase (Promega) and oligo dT (Qiagen) and real time PCR was performed using FastStart TaqMan Mix (Roche) and TaqMan probes from Invitrogen. Real time, Taqman qPCR was performed on selected genes (αSMA, catenin β1, collagen I, collagen IV, fibronectin 1, CD44, Lox, Loxl2, MMP2, PDGFRA, PDGFRB, Snail1) (see Table 1). The following qRT-PCR Program was used: 10 minutes denaturation at 95˚C, followed by 40 cycles of 15 seconds at 95˚C and 1 minute at 60˚C. The Ct values were assessed using the Corbett Rotorgene Analysis Software 6000 and B2M was used as an internal standard for the normalization of the fold changes of each gene of interest.

Table 1. TaqMan probes used

Gene of interest	Abbreviation	Invitrogen Ref.nr.
Beta-2-microglobulin (Housekeeping gene)	B2M	Hs00187842_m1
Actin, alpha 2, smooth muscle	ACTA2 (αSMA)	Hs00426835_g1
Catenin beta 1	CTNNB1	Hs00355049_m1
Collagen 1 alpha 1	Col I	Hs00164004_m1
Collagen 4 alpha 1	Col IV	Hs00266237_m1
Fibronectin 1	FN1	Hs00415006_m1
Hyaluronic acid receptor	CD44	Hs01075861_m1
Lysyl oxidase	Lox	Hs00942480_m1
Lysyl oxidase like 2	Loxl2	Hs00158757_m1
Metalloproteinase 2	MMP2	Hs01548727_m1
PDGF receptor alpha	PDGFRA	Hs00998018_m1
PDGF receptor beta	PDGFRB	Hs01019589_m1
Snail family transcriptional repressor 1	Snail1	Hs00195591_m1

Migration assay

The migratory capacity of HSCs was investigated using the Culture-Insert 2 Well (80209; Ibidi) according to the manufacturer's instructions. Briefly, 70 µL of 3 x 10^5 cells/mL suspension were incubated in each chamber in serum-free medium overnight. After cell attachment, the culture insert was gently removed by using sterile tweezers, leaving a cell-free gap of approximatively 500 µm. Medium was slowly aspired and 1 mL/well of serum free DMEM medium was added. HSC migration was evaluated in presence of TGF-β1, PDGF-AB and SB52 inhibitor. The wound healing process was followed by time laps microscopy, using Olympus cellVivo incubation system with 4X magnification. Pictures were acquired every hour for a period of 48 hours. Pictures were analysed with ImageJ and migration area was calculated with MRI Wound Healing Tool (http://dev.mri.cnrs.fr/projects/imagej-macros/wiki/Wound_Healing_Tool) as previously published [20] .

Statistical analysis

Experiments with primary HSC were conducted with at least 3 batches of cells as indicated in the legend. Data were analysed using GraphPad Prism 7 (GraphPad Software, inc.) and expressed as mean values ± standard deviation (SD) as indicated in the legend. The Student’s t-test was used for comparison between two groups. Data from three or more groups were analysed by one-way analysis of variance with Tukey's multiple comparisons test. $P \leq 0.05$ was considered to be significant.

Results

TGF-β1, but not PDGF-AB, induces αSMA production

TGF-β1 and PDGF-AB did not show any cytotoxicity effect on hTERT-HSC over 7 and 6 days, respectively (Fig. 1 A-B). Viability assays values were normalized with the cell number by using the CyQuant assay, in order to eliminate the influence of cell proliferation on cell viability. Treated-cells displayed up to 2-fold and almost 1.5-fold higher activity of cellular dehydrogenase than untreated-cells for TGF-β1 and PDGF-AB respectively, suggesting an increase of metabolic activity. Based on these results, 0.5-1 ng/mL TGF-β1 and 1-5 ng/mL PDGF-AB were chosen for the subsequent experiments. Untreated hTERT-HSC and primary HSC showed low αSMA production (Fig. 1 C-D); TGF-β1 elicited HSC activation after 48 hours (with an increase of αSMA-positive cells from approximately 10% to 90%) in both immortalised and primary HSC. This induction was strictly correlated to TGF-β1/Smad pathway as it was inhibited by simultaneous incubation with the Smad inhibitors SB43 and SB52. Incubation of hTERT-HSC with PDGF-AB did not increase αSMA production.

Proliferation and migration of HSCs require PDGF-AB signalling

To explore the proliferative and migratory capacities of HSC, we performed an EdU proliferation assay and a wound healing assay after exposure to TGF-β1 and/or PDGF-AB. The proliferation rate was 70% for hTERT-HSC, and dependent on batch the primary HSC proliferated within a range of 30-70%. PDGF-AB induced cell proliferation already at the concentration of 1 ng/mL, with a concentration-dependent effect on primary HSC (Fig. 2 A-B). PDGF-AB also played a dominant role in leading the complete repair of the wound gap even when combined with TGF-β1. hTERT-HSC treated with 5 ng/mL PDGF-AB for 24 hours displayed 3.5-fold higher migration rate than the untreated controls; while primary HSC treated for 12 hours migrated 4 times faster than their untreated counterparts (Fig. 3 A-B). In particular, the proliferation rate raised from 70% to 87% for hTERT-HSC and from 50% to 67% for primary HSC after exposure to 5 ng/mL PDGF-AB. In contrast, TGF-β1 and SB inhibitors did not have any significant effects on migration of neither immortalized nor primary HSCs (Fig. 3 A-B). Moreover, TGF-β1 did not change the proliferation rate of primary HSC and led to a dose-dependent decrease in proliferation of hTERT-HSCs (Fig. 2 A-B). Immunohistochemical analysis during the wound-healing process (Fig. 4) clearly demonstrates the complementary effects of TGF-β1 and PDGF-AB. hTERT-HSC treated with TGF-β1 do not migrate but display a clear activated phenotype as demonstrated by the presences of αSMA stress fibres (Fig. 4 B). PDGF-AB, on the other hand, leads to widespread migration and no increase in αSMA-positive cells (Fig. 4 C). The combination of both factors elicit cell migration leading to gap closure and formation of αSMA stress fibres (Fig. 4 D).

TGF-β1 is essential for HSCs activation

To assess the pro-fibrogenic effect of both TGF-β1 and PDGF-AB, mRNA levels of several HSC activation markers as well as ECM components were analysed in both immortalized (Fig. 5) and primary (Fig. 6) HSC. TGF-β1 at 1 ng/mL, but not PDGF-AB, elicited a significant increase in gene expression of αSMA, Collagens I and IV (Col I and Col IV) as well as fibronectin (FN1), hyaluronic acid receptor (CD44) and Lox genes (Figs. 5 and 6), suggesting an effect on the ECM remodelling. Significant increases were also observed for αSMA, Snail1, CD44 and Lox, indicating activation of HSC by TGF-β1. Additional treatment with SB43 and SB52 blocked the effect of TGF-β1 for all measured genes, especially on the hTERT-HSC. In these cells, the inhibitors alone were able to decrease the basal expression level of all genes, suggesting the inhibition of endogenous TGF-β1 signalling (Fig. 5). This effect was not clear for the primary HSCs, where the gene expression values of the SB52-treated cells were comparable to the values of the control (Fig. 6). In primary HSC, SB52 led to an increase in expression of PDGF receptors A and B, indicating a possible interconnection between the TGF-β1 and PDGF pathways (Fig. 6 F).

Discussion

TGF-β1 guides HSCs towards a fibrogenic phenotype

Transforming growth factor-β1 (TGF-β1) is known to act as a key regulator in chronic liver diseases, and is considered the major pro-fibrotic cytokine in the liver [6] . In our study, TGF-β1 played a crucial role in the trans-differentiation of both primary and hTERT-HSC into a αSMA-positive myofibroblasts-like cell type (Fig. 1 C-D, Fig. 4). This effect is specifically dependent from the TGF-β1 pathway, since it involves the Smad proteins as demonstrated by the loss of αSMA production in presence of the Smad inhibitors SB43 or SB52. As expected, only in a small percentage of untreated-cells or SB-treated cells the antibody staining revealed the presence of stress fibres, while αSMA expression and its organization into stress fibres were highly represented in TGF-β1-treated cells. TGF-β1 also increased the mRNA levels for Lysyl Oxidase (Lox) family genes, which are markers for activated HSC (Fig. 5-6) [21] . TGF-β1 triggered the gene expression of pro-fibrotic proteins, which leads to the remodelling of the ECM and ultimately to liver fibrosis (Fig. 5-6). Upregulation of collagen types I and IV, fibronectin and CD44 was in fact detected following TGF-β1 treatment. TGF-β1 likewise enhanced the expression of Snail1, beta catenin (CTNNB1) and Metalloproteinase 2 (MMP2), which are involved in the epithelial to mesenchymal transition and in remodelling of ECM, respectively (Fig. 5-6) [22, 23] . Both hTERT and primary HSCs reacted similarly to TGF-β1 exposure in terms of cell activation, suggesting that this used HSC cell line may be a suitable model to study TGF-β1-induced HSC activation, as being characterized by a quiescent phenotype as shown by low presence of αSMA prior induction.

In addition, we showed for the first time the effect of TGF-β1 on proliferation and migration of primary HSCs. TGF-β1 had no significant effect on the proliferation of primary HSC (Fig. 2 B), as previously reported by Yang C et al. for rat primary HSC and LX2 cell line [24] . Interestingly, we showed a decrease of cell proliferation through TGF-β1 treatment, in a dose dependent manner on the hTERT-HSC after 48 hours (Fig. 2 A). Analogue observations were only found with rat HSC, for which thymidine incorporation assays showed a decrease of growth following TGF-β1 treatment [25] , and the anti-proliferative effect of TGF-β1 on smooth muscle cells and epithelial cells is well documented [26–29] . The antiproliferative effect on hTERT-HSC could be due to an alteration of non-Smad pathways, such as the upregulation of cyclin-dependent kinase inhibitors including p15, p21 and p27 showed for epithelial cells [29] . Additional experiments would be required to clarify this point.

HSC activation also leads to migration and TGF has been shown to either a positive or negative role in the migration of cancer cells [30] . It has been shown that TGF-β1 induces cell migration of rat primary HSC and LX2 through a polycarbonate membrane, but no data are available for hTERT-HSC or human primary HSC [24] . In our hands, TGF-β1 did not induce any significant changes in HSC migration (Fig. 3 A-B). Here, we hypothesize that the changes in the cytoskeleton

occurring during activation of the HSC, did not allow the cells to migrate in a significantly different way than the negative control.

PDGF-AB drives HSCs towards a mitogenic phenotype

PDGFs are key regulators of critical biological and pathological functions including tissue remodelling, scarring and fibrosis [31] . PDGF isoforms have been shown to act as potent activators of fibroblast proliferation, migration and survival [17, 32] . As expected, a significant increment of cell growth and migration was observed following PDGF-AB treatment for 48 hours in both primary and hTERT-HSCs (Fig. 2 and 3). As previously reported [17] , PDGF affected both proliferation and migration of HSCs, but no significant changes were seen in the activation markers (such as protein level of αSMA and mRNA levels of Lox genes) and ECM component genes in both HSCs (Fig. 1, 5 and 6).

Furthermore, while PDGF receptor expression is low in healthy liver, increased expression has been shown in HSCs during injury [11] . Depletion of PDGFRB in HSCs led to the decrease of injury and fibrosis, while its activation accelerated fibrosis [33] . Recent studies have also highlighted the involvement of PDGFRA in HSC activation [34] . Here, we have shown an increase in the gene expression of both PDGF receptors A and B through SB52 treatment (Fig. 6 F). These data suggest the interconnection between the TGF-β1 and PDGF pathways, as recently suggested from other studies [13] . The presence of SB52 could in fact inhibit the Smad signalling coming from autocrine TGF-β1, resulting into a more mitogenic phenotype (with increase expression of PDGF receptors) rather than an activated phenotype. This led us to the hypothesis that a combination of more cytokines is required to fully characterize HSC activation *in vitro,* in order to mimic the complex immunoresponce occurring during liver injuries *in vivo*.

TGF-β1 and PDGF-AB synergize to promote HSC migration and activation

TGF-β and PDGF signalling pathways transmit extracellular stimuli into gene transcription, promoting HSC activation under pathological conditions [12] . These two signalling pathways are functionally divergent; PDGF promotes proliferation and migration of HSCs, while TGF-β induces trans-differentiation of quiescent HSCs into myofibroblasts [6] . Recent data suggested a cross-talk between them [12, 13] . For instance, PDGFRA has been shown to be required for Smad-dependent TGF-β signalling, acting as a working partner of TGF-β receptor II [13] . The data obtained in our work confirm the presence of some interconnection of the two pathways. In particular, our data show that in order to achieve a fully activated phenotype, HSCs require both stimuli. Specifically, αSMA expression and mRNA levels of several activation markers (MMP2, Snail1 and Collagen IV), were increased after co-stimulation with TGF-β1 and PDGF-AB. PDGF-AB played a dominant role in the increase in proliferation and migration of the HSCs, while TGF-β1 strongly promoted stress fibre formation.

Taken together, our data demonstrate that PDGF-AB and TGF-β1 synergize leading to full HSC activation, characterised by increase in proliferation, migration and activation, suggesting that both independent pathways converge and represent key events leading to HSC activation *in vitro*. The data also suggest that a possible therapeutic strategy to promote liver regeneration/repair without inducing fibrosis may include the promotion of PDGF-dependent cell proliferation and migration together with a repression of TGF-β1-mediated fibrogenesis.

Acknowledgements

We would like to acknowledge the financial support of the Swiss Centre for Applied Human Toxicology (SCAHT). We are very thankful to Dr. B. Schnabl for making the hTERT-HSC available for our research.

Conflict of interest statement

The authors confirm that there are no conflicts of interest.

Author contributions

The study was designed by V.P. and L.S.D.; V.P and C.B. contributed to the experiments with the human cell line, while V.P. performed the experiments on primary cells; experimental data were analysed by V.P., C.B. and L.S.D.; V.P. and L.S.D. wrote the manuscript.

References

[1] **Zhang C-Y, Yuan W-G, He P, et al.** Liver fibrosis and hepatic stellate cells: Etiology, pathological hallmarks and therapeutic targets. *World J. Gastroenterol.* 2016; 22; 10512–22.

[2] **Prestigiacomo V, Weston A, Messner S, et al.** Pro-fibrotic compounds induce stellate cell activation, ECM-remodelling and Nrf2 activation in a human 3D-multicellular model of liver fibrosis. *PLOS ONE* 2017; 12; e0179995.

[3] **Trautwein C, Friedman SL, Schuppan D, et al.** Hepatic fibrosis: Concept to treatment. *J. Hepatol.* 2015; 62; S15-24.

[4] **Schnabl B, Choi YH, Olsen JC, et al.** Immortal activated human hepatic stellate cells generated by ectopic telomerase expression. *Lab. Investig. J. Tech. Methods Pathol.* 2002; 82; 323–33.

[5] **Weiskirchen R, Tacke F**. Cellular and molecular functions of hepatic stellate cells in inflammatory responses and liver immunology. *Hepatobiliary Surg. Nutr.* 2014; 3; 344–63.

[6] **Lee UE, Friedman SL**. Mechanisms of Hepatic Fibrogenesis. *Best Pract. Res. Clin. Gastroenterol.* 2011; 25; 195–206.

[7] **Friedman SL**. Hepatic stellate cells: protean, multifunctional, and enigmatic cells of the liver. *Physiol. Rev.* 2008; 88; 125–72.

[8] **Schnabl B, Purbeck CA, Choi YH, et al.** Replicative senescence of activated human hepatic stellate cells is accompanied by a pronounced inflammatory but less fibrogenic phenotype. *Hepatol. Baltim. Md* 2003; 37; 653–64.

[9] **Marra F, Choudhury GG, Pinzani M, et al.** Regulation of platelet-derived growth factor secretion and gene expression in human liver fat-storing cells. *Gastroenterology* 1994; 107; 1110–7.

[10] **Heldin C-H**. Targeting the PDGF signaling pathway in tumor treatment. *Cell Commun. Signal. CCS* 2013; 11; 97.

[11] **Wong L, Yamasaki G, Johnson RJ, et al.** Induction of beta-platelet-derived growth factor receptor in rat hepatic lipocytes during cellular activation in vivo and in culture. *J. Clin. Invest.* 1994; 94; 1563–9.

[12] **Liu Y, Wen XM, Lui ELH, et al.** Therapeutic targeting of the PDGF and TGF-beta-signaling pathways in hepatic stellate cells by PTK787/ZK22258. *Lab. Investig. J. Tech. Methods Pathol.* 2009; 89; 1152–60.

[13] **Liu C, Li J, Xiang X, et al.** PDGF receptor-α promotes TGF-β signaling in hepatic stellate cells via transcriptional and posttranscriptional regulation of TGF-β receptors. *Am. J. Physiol. - Gastrointest. Liver Physiol.* 2014; 307; G749–59.

[14] **Li H-Y, Ju D, Zhang D-W, et al.** Activation of TGF-β1-CD147 positive feedback loop in hepatic stellate cells promotes liver fibrosis. *Sci. Rep.* 2015; 5; 16552.

[15] **Friedman SL**. Molecular regulation of hepatic fibrosis, an integrated cellular response to tissue injury. *J. Biol. Chem.* 2000; 275; 2247–50.

[16] **Arias M, Lahme B, Van de Leur E, et al.** Adenoviral delivery of an antisense RNA complementary to the 3' coding sequence of transforming growth factor-beta1 inhibits fibrogenic activities of hepatic stellate cells. *Cell Growth Differ. Mol. Biol. J. Am. Assoc. Cancer Res.* 2002; 13; 265–73.

[17] **Kikuchi A, Pradhan-Sundd T, Singh S, et al.** Platelet-Derived Growth Factor Receptor α Contributes to Human Hepatic Stellate Cell Proliferation and Migration. *Am. J. Pathol.* 2017; 187; 2273–87.

[18] **Hjelmeland MD, Hjelmeland AB, Sathornsumetee S, et al.** SB-431542, a small molecule transforming growth factor-beta-receptor antagonist, inhibits human glioma cell line proliferation and motility. *Mol. Cancer Ther.* 2004; 3; 737–45.

[19] **Gerbaud P, Pidoux G, Guibourdenche J, et al.** Mesenchymal activin-A overcomes defective human trisomy 21 trophoblast fusion. *Endocrinology* 2011; 152; 5017–28.

[20] **Hauck PM, Wolf ER, Olivos DJ, et al.** Early-Stage Metastasis Requires Mdm2 and Not p53 Gain of Function. *Mol. Cancer Res.* 2017; DOI: 10.1158/1541-7786.MCR-17-0174.

[21] **Perepelyuk M, Terajima M, Wang AY, et al.** Hepatic stellate cells and portal fibroblasts are the major cellular sources of collagens and lysyl oxidases in normal liver and early after injury. *Am. J. Physiol. Gastrointest. Liver Physiol.* 2013; 304; G605-614.

[22] **Wang M, Zhao D, Spinetti G, et al.** Matrix metalloproteinase 2 activation of transforming growth factor-beta1 (TGF-beta1) and TGF-beta1-type II receptor signaling within the aged arterial wall. *Arterioscler. Thromb. Vasc. Biol.* 2006; 26; 1503–9.

[23] **Duarte S, Baber J, Fujii T, et al.** Matrix metalloproteinases in liver injury, repair and fibrosis. *Matrix Biol. J. Int. Soc. Matrix Biol.* 2015; 44–46; 147–56.

[24] **Yang C, Zeisberg M, Mosterman B, et al.** Liver fibrosis: insights into migration of hepatic stellate cells in response to extracellular matrix and growth factors. *Gastroenterology* 2003; 124; 147–59.

[25] **Shen H, Huang G-J, Gong Y-W**. Effect of transforming growth factor beta and bone morphogenetic proteins on rat hepatic stellate cell proliferation and trans-differentiation. *World J. Gastroenterol.* 2003; 9; 784–7.

[26] **Churchman AT, Anwar AA, Li FYL, et al.** Transforming growth factor-beta1 elicits Nrf2-mediated antioxidant responses in aortic smooth muscle cells. *J. Cell. Mol. Med.* 2009; 13; 2282–92.

[27] **Okita Y, Kamoshida A, Suzuki H, et al.** Transforming growth factor-β induces transcription factors MafK and Bach1 to suppress expression of the heme oxygenase-1 gene. *J. Biol. Chem.* 2013; 288; 20658–67.

[28] **Robson CN, Gnanapragasam V, Byrne RL, et al.** Transforming growth factor-beta1 up-regulates p15, p21 and p27 and blocks cell cycling in G1 in human prostate epithelium. *J. Endocrinol.* 1999; 160; 257–66.

[29] **Griswold-Prenner I, Kamibayashi C, Maruoka EM, et al.** Physical and Functional Interactions between Type I Transforming Growth Factor β Receptors and Bα, a WD-40 Repeat Subunit of Phosphatase 2A. *Mol. Cell. Biol.* 1998; 18; 6595–604.

[30] **Humbert L, Lebrun J-J**. TGF-beta inhibits human cutaneous melanoma cell migration and invasion through regulation of the plasminogen activator system. *Cell. Signal.* 2013; 25; 490–500.

[31] **Bonner JC**. Regulation of PDGF and its receptors in fibrotic diseases. *Cytokine Growth Factor Rev.* 2004; 15; 255–73.

[32] **Donovan J, Shiwen X, Norman J, et al.** Platelet-derived growth factor alpha and beta receptors have overlapping functional activities towards fibroblasts. *Fibrogenesis Tissue Repair* 2013; 6; 10.

[33] **Kocabayoglu P, Lade A, Lee YA, et al.** β-PDGF receptor expressed by hepatic stellate cells regulates fibrosis in murine liver injury, but not carcinogenesis. *J. Hepatol.* 2015; 63; 141–7.

[34] **Kikuchi A, Monga SP**. PDGFRα in liver pathophysiology: emerging roles in development, regeneration, fibrosis, and cancer. *Gene Expr.* 2015; 16; 109–27.

Figure legend

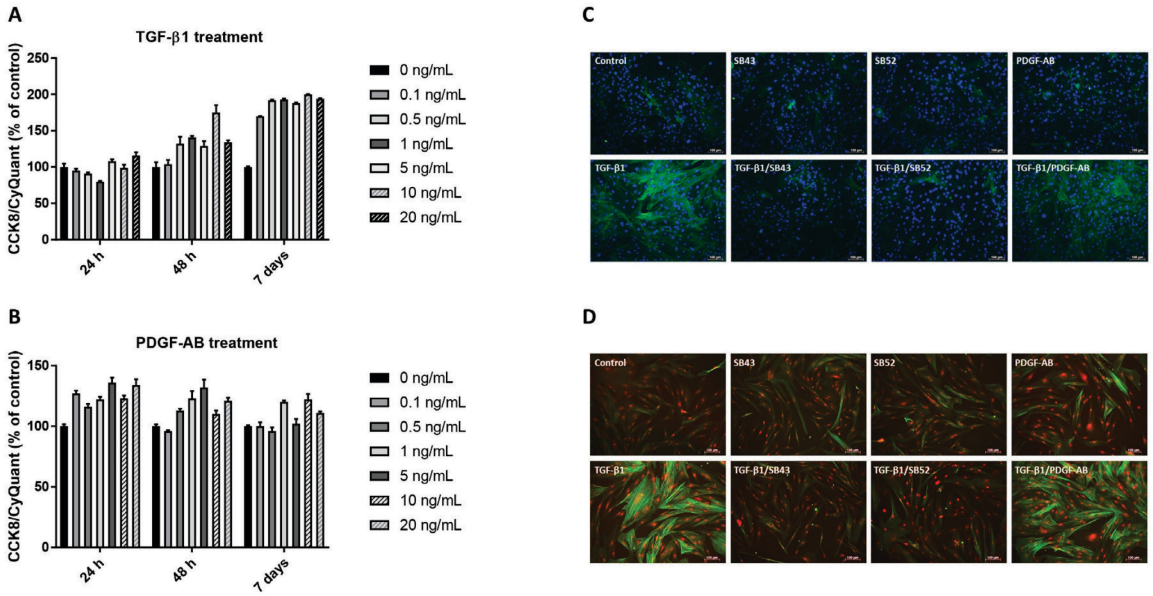

Fig. 1. Effect of TGF-β1 and PDGF-AB on HSC activation and viability. (A-B) Seven concentrations of TGF-β1 (0-20 ng/mL) (A) and PDGF-AB (0-20 ng/mL) (B) were selected and CCK-8 assay was performed to assess cytotoxicity on hTERT-HSC after 24 hours, 48 hours and 7 days. The absorbance was measured at 450 nm with FlexStaion 3 Reader and the values were normalized with the CyQUANT assay. Values are expressed as percentage of control (mean ± SD, N = 3). (C-D) hTERT-HSC cells (C) and human primary HSCs (D) were treated for 48 hours with TGF-β1 (1 ng/mL), SB43 (10 μM), SB52 (1 μM) and/or PDGF-AB (5 ng/mL). After treatment, the cells were fixed and stained against αSMA (green) and nuclei (DAPI, blue in C and Propidium iodite, red in D). The results show an increase in αSMA production after TGF-β1 exposure. SB43 and SB52 significantly inhibited the TGF-β1-induced αSMA. Pictures taken using fluorescence microscopy. Scale bar: 100 μm.

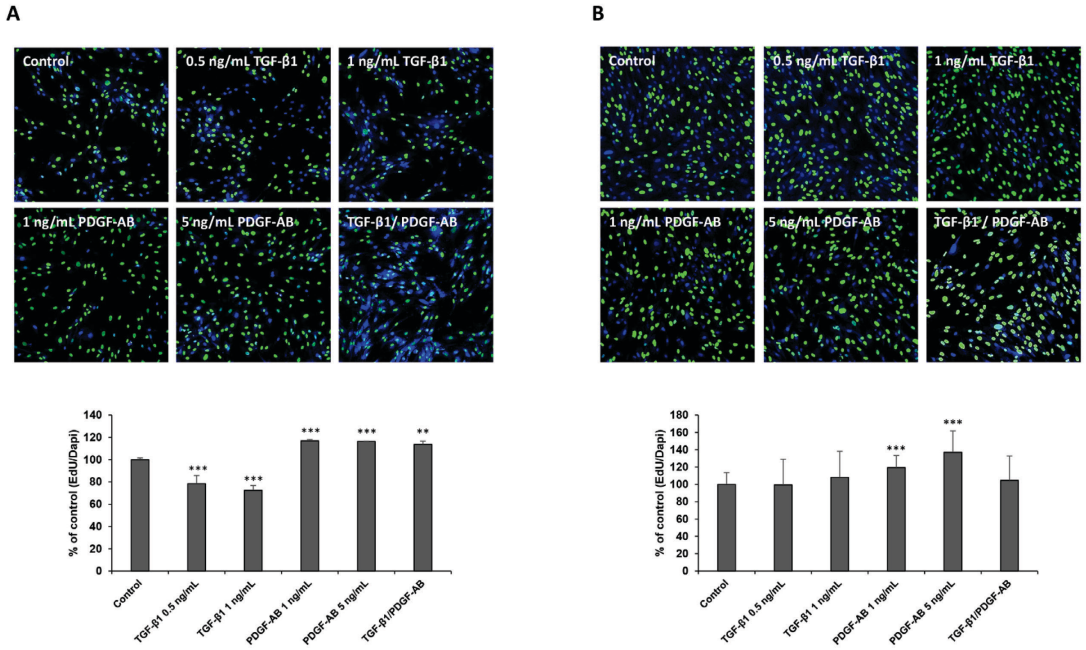

Fig. 2. Effect of TGF-β1 and PDGF-AB on HSC proliferation. hTERT-HSCs (A) and primary HSCs (B) were exposed to TGF-β1 and/or PDGF-AB for 48 hours. EdU was added during the last 30 hours and detected as described in material and methods. The pictures were taken with 10X magnification by using confocal microscopy and nuclei were counted with Image J software. Values are expressed as percentage of control (mean ± SD). **, P ≤ 0.01; *** P ≤ 0.001 vs control. N = 5 for hTERT-HSC (A) and N = 5 different batches (with 5 replicates each) for primary HSC (B).

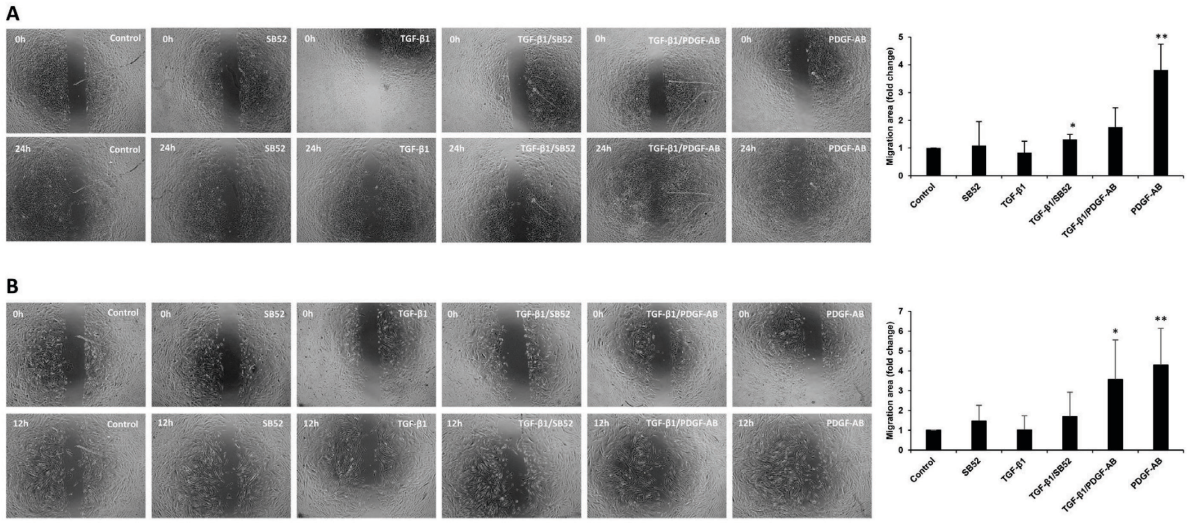

Fig. 3. PDGF-AB-dependent cell migration on HSC. hTERT-HSCs (A) and primary HSCs (B) were seeded into the Culture Insert 2-Well (Ibidi) and exposed to TGF-β1 (1 ng/mL), SB52 (1 μM) and/or PDGF-AB (5 ng/mL) for 48 hours. Pictures were acquired with 4X magnification every hour for a period of 48 hours using Olympus cellVivo incubation system. Pictures of treated and un-treated-samples at 0 hours and 24 hours are showed for hTERT-HSC (A), while 0 and 12 hours

are showed for primary HSCs (B). Migration area was calculated with MRI wound healing tool of Image J software and expressed as fold change of the treated vs control (mean ± SD). *, P ≤ 0.05; **, P ≤ 0.01 vs control. N = 3 for hTERT-HSC (A) and N = 3 different batches (with 2 replicates each) for primary HSC (B).

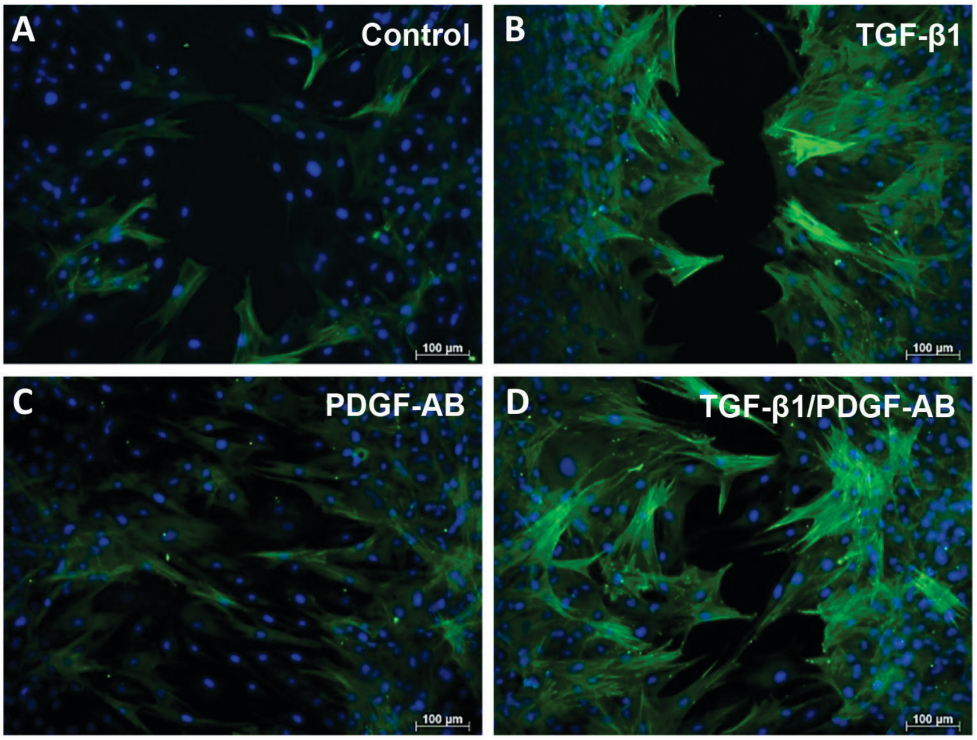

Fig. 4. Immunohistochemical analysis of αSMA during the wound healing process. A wound in hTERT-HSC cells was generated by using Culture-Insert 2 Well and cells were exposed to TGF-β1 and/or PDGF-AB for 48 hours. Immunostaining for αSMA (green) and nuclei (blue) was performed and pictures of the wound area were acquired using fluorescence microscopy. (A) Control cells did not show high migration rate as well as low level of αSMA. (B) TGF-1 did not influence the migratory capacities of HSCs, while significantly induced αSMA production. (C) PDGF-AB leads to widespread migration and no increase in αSMA-positive cells. (D) The combination of both TGF-β1 and PDGF-AB elicited cell migration with a concomitant production of αSMA. Scale bar: 100 µm.

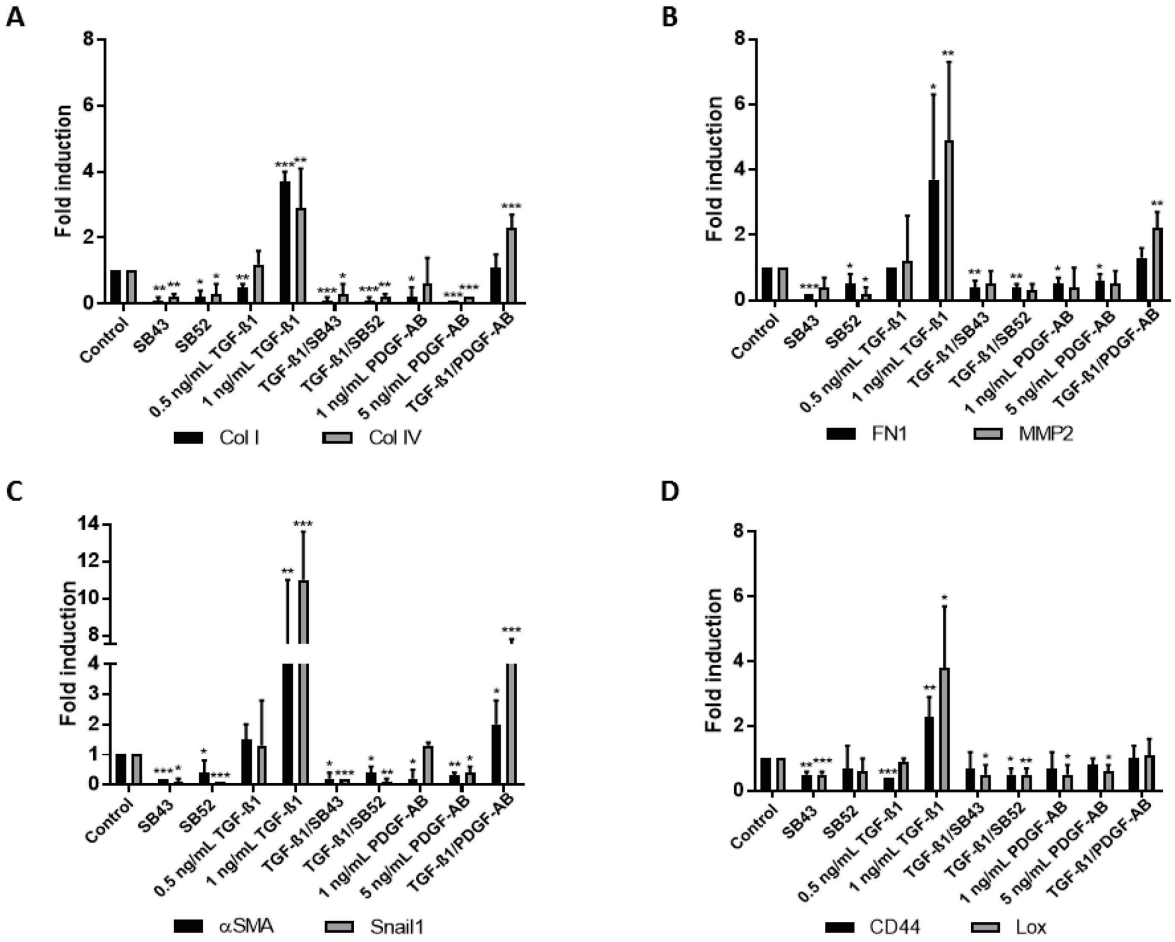

Fig. 5. Gene expression of HSC activation and fibrotic markers of hTERT-HSCs exposed to TGF-β1, SB43, SB52 and/or PDGF-AB. The cells were exposed to 0.5-1 ng/mL TGF-β1, 10 μM SB43, 1 μM SB52 and/or 1-5 ng/mL PDGF-AB for 48 hours. In the co-stimulation 1 and 5 ng/mL were used for TGF-β1 and PDGF-AB respectively. mRNA was extracted using TRIzol conventional procedure and fold induction were calculated as 2^(-ΔΔCT) for each sample and control and expressed as mean fold induction ± SD of three replicates. Beta-2-microglobulin (B2M) was used as reference gene for each sample. (A) Collagen I (black) and Collagen IV (grey); (B) Fibronectin (black) and MMP2 (grey); (C) αSMA (black) and Snail1 (grey); (D) CD44 (black) and Lox (grey). *, P ≤ 0.05; **, P ≤ 0.01; *** P ≤ 0.001 vs control (N = 3).

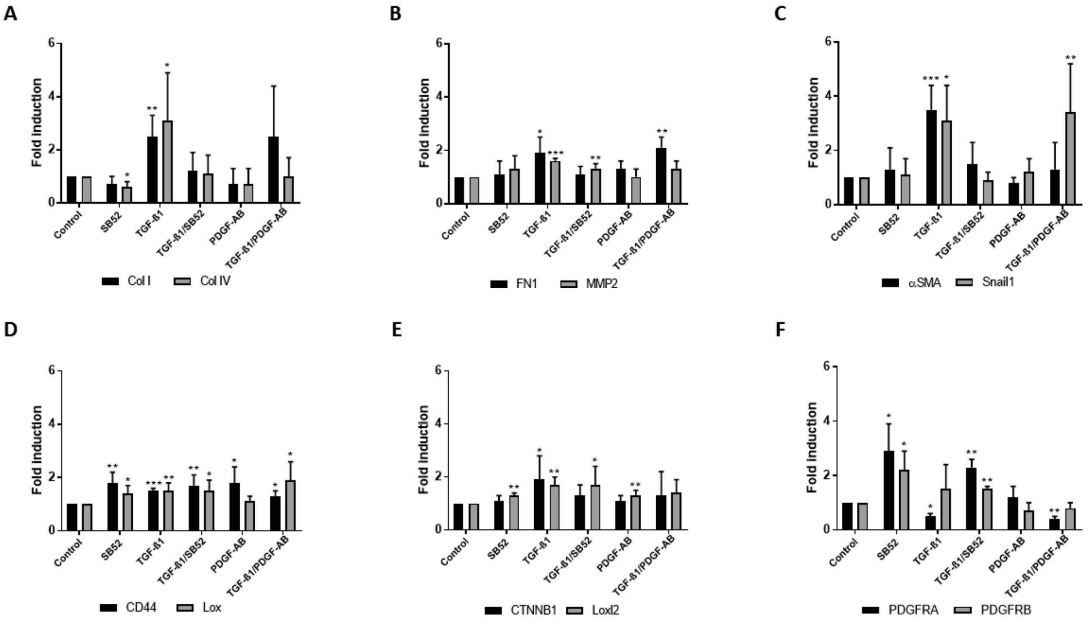

Fig. 6. Gene expression of HSC activation and fibrotic markers of human primary HSCs exposed to TGF-β1, SB52 and/or PDGF-AB. The cells were exposed to 1 ng/mL TGF-β1, 1 μM SB52 and/or 5 ng/mL PDGF-AB for 48 hours. mRNA was extracted using TRIzol conventional procedure and fold induction were calculated as 2^(-ΔΔCT) for each sample and control and expressed as mean fold induction ± SD of three replicates. Beta-2-microglobulin (B2M) was used as reference gene for each sample. (A) Collagen I (black) and Collagen IV (grey); (B) Fibronectin (black) and MMP2 (grey); (C) αSMA (black) and Snail1 (grey); (D) CD44 (black) and Lox (grey); (E) CTNNB1 (black) and Loxl2 (grey); (F) PDGFRA (black) and PDGFRB (grey). *, P ≤ 0.05; **, P ≤ 0.01; *** P ≤ 0.001 vs control (N = 3 from different batches).

4.3 Paper 4

Nrf2 protects stellate cells from Smad-dependent cell activation

Vincenzo Prestigiacomo, Laura Suter-Dick

Published manuscript

Aims: Elucidate the potential role of Nrf2 pathway in HSC trans-differentiation involved in the development of fibrosis.

Results: Nrf2 depletion induces HSC activation, as shown by an increase in αSMA-positive cells and by gene expression induction of ECM components in a TGF-β1/Smad-dependent manner.

Conclusion: These data indicate that Nrf2 limits HSCs activation, through the inhibition of the TGF-β1/Smad pathway in both primary and immortalised HSCs.

PLOS ONE

RESEARCH ARTICLE

Nrf2 protects stellate cells from Smad-dependent cell activation

Vincenzo Prestigiacomo[1,2]*, Laura Suter-Dick[1]

1 University of Applied Sciences Northwestern Switzerland, School of Life Sciences, Muttenz, Switzerland,
2 University of Basel, Department of Pharmaceutical Sciences, Basel, Switzerland

*vincenzo.prestigiacomo@fhnw.ch

Citation: Prestigiacomo V, Suter-Dick L (2018) Nrf2 protects stellate cells from Smad-dependent cell activation. PLoS ONE 13(7): e0201044. https://doi.org/10.1371/journal.pone.0201044

Editor: Partha Mukhopadhyay, National Institutes of Health, UNITED STATES

Received: April 6, 2018

Accepted: July 6, 2018

Published: July 20, 2018

Data Availability Statement: All relevant data are within the paper and its Supporting Information files.

Funding: This work was partly founded by the Swiss Centre for Applied Human Toxicology (SCAHT), and partly funded by the School of Life Sciences (Univers ty of Applied Sciences Northwestern Switzerland). The funder had no role in study design, data collection and analysis, decision to publish, or preparation of the manuscript. This does not alter our adherence to PLOS ONE policies on sharing data and materials.

Abstract

Hepatic stellate cells (HSC) orchestrate the deposition of extracellular matrix (ECM) and are the primary effector of liver fibrosis. Several factors, including TGF-β1, PDGF and oxidative stress, have been shown to trigger HSC activation. However, the involvement of cellular defence mechanisms, such as the activation of antioxidant response by Nrf2/Keap1 in the modulation of HSC activation is not known. The aim of this work was to elucidate the role of Nrf2 pathway in HSC trans-differentiation involved in the development of fibrosis. To this end, we repressed Nrf2 and Keap1 expression in HSC with specific siRNAs. We then assessed activation markers, as well as proliferation and migration, in both primary and immortalised human HSCs exposed to Smad inhibitors (SB-431542 hydrate and SB-525334), TGF-β1 and/or PDGF. Our results indicate that knocking down Nrf2 induces HSC activation, as shown by an increase in αSMA-positive cells and by gene expression induction of ECM components (collagens and fibronectin). HSC with reduced Nrf2-levels also showed an increase in migration and a decrease in proliferation. We could also demonstrate that the activation of Nrf2-deficient HSC involves the TGF-β1/Smad pathway, as the activation was successfully inhibited with the two tested Smad inhibitors. Moreover, TGF-β1 elicited a stronger induction of HSC activation markers in Nrf2 deficient cells than in wild type cells. Thus, our data suggest that Nrf2 limits HSCs activation, through the inhibition of the TGF-β1/Smad pathway in HSCs.

Introduction

Hepatic fibrosis is a scarring process in response to chronic liver injury, and it is charaterized by an accumulation of fibrillar extracellular matrix (ECM) [1]. Following liver injury, hepatic stellate cells (HSCs) undergo activation, a cellular process during which HSCs trans- differentiate into myofibroblasts-like cells [1]. Activated HSC have been recognized as the responsible cells for most of the excess of ECM components in chronic liver fibrosis [1].

HSC activation is triggered by several cytokines; in particular platelet-derived growth factor (PDGF) and transforming growth factor-β1 (TGF-β1), released from platelet and Kupffer cells respectively, have been identified as the main mitogenic and pro-fibrotic mediators for HSCs [1].

Competing interests: The authors have declared that no competing interests exist.

Abbreviations: hTERT-HSC, Immortalised hepatic stellate cells; SB43, SB-431542 hydrate; SB52, SB- 525334; siCON, scrambled siRNA; siNrf2, siRNA targeting Nrf2; siKeap1, siRNA targeting Keap1.

Increasing evidence has shown that oxidative stress may promote fibrosis and HSC activation in the human liver and rodents [2,3]. In many cell types the transcriptional response to oxidative stress is mediated by a cis-acting element termed antioxidant response element (ARE); the nuclear factor E2-related factor 2 (Nrf2) has been identified as the most important transcription factor acting on the ARE for many genes [4–6]. In the human genome, Nrf2 reg- ulates the transcription of more than 500 genes, most of which have a cytoprotective role [6].

A key element for the regulation of the activity of Nrf2 is the Kelch-like ECH-associated protein 1 (Keap1), which acts as a constitutive repressor of Nrf2 [4]. Under normal conditions, Nrf2 is bound to Keap1, which is an adaptor molecule for the Cullin3-based E3 ubiquitin ligase complex, leading to the degradation of Nrf2 via the by ubiquitin-proteasome pathway [5]. In this condition, Nrf2 appears as a highly unstable protein with a half-life of around 15 minutes [4]. Oxidative or electrophilic stress causes the inactivation of Keap1, resulting in Nrf2 stabili- zation, nuclear translocation and subsequent gene induction [5].

Among other organs, Nrf2 plays a predominant role in the liver, since it is a key regulator of the constitutive and inducible expression of some phase II and III detoxification enzymes and antioxidant proteins, such as those involved in glutathione synthesis, in primary hepato- cytes and hepatocyte-like cells [7]. Several studies reported that Nrf2-knockout mice showed an exacerbated cytotoxicity to acetaminophen (APAP) as well as a strongly aggravated liver damage after treatment with CCl4 or ethanol [8–11]. In a similar study, Okawa et al. showed that Keap1-knockout mice were significantly more resistant to APAP than control animals [12]. Concordantly, experiments in mice showed an increase in nuclear translocation of Nrf2 after APAP administration [13]. In addition to its protective role, it has been demonstrated that Nrf2 regulates hepatocyte proliferation by ensuring normal insulin/IGF-1 and Notch1 sig- nalling during liver regeneration [14,15]. Recently, we showed upregulation of both Nrf2 and Keap1 after Methotrexate- and Thioacetamide- induced fibrosis in a 3D human cell culture model, indicating a role of Nrf2 in hepatic fibrosis [16]. Nrf2 has been shown to have antifibro- tic effect in liver, lung and kidney, by promoting the dedifferentiation of fibroblasts [17–19].

Many studies have been conducted on Nrf2-related effects on liver but little is known about its role on HSCs. It has been reported that Nrf2 inhibits the TGF-β1-dependent expression of fibrosis markers in a human stellate cell line [17]. Yang et al. have shown that TGF-β1 reduced the presence of Nrf2 in a rat hepatic stellate cell line [3]. This effect was dependent on the epi- genetic regulation operated by the microRNA-200a. However, although these studies suggest an involvement of Nrf2 in HSC activation, studies conducted on human primary HSCs are still lacking. Here, we report the effects of Nrf2-knockdown on proliferation, migration and activation of human HSCs. Our studies demonstrate that Nrf2-knockdown induces HSC acti- vation in both human primary and immortalised (hTERT) HSCs. Moreover, this activation can be modulated by TGF-β1, PDGF-AB and/or Smad inhibitors. These results may contrib- ute towards studying and developing new successful and advantageous therapies for liver fibrosis.

Material and methods

Reagent, chemicals and antibodies

DMEM High Glucose (41965; Invitrogen), Fetal Bovine Serum (FBS) (10270; Invitrogen), Penicilin-Streptomycin (A8943; Applichem), TGF-β1 (T5050; Sigma), PDGF-AB (P8147; Sigma), SB-431542 hydrate (SB43) (S4317; Sigma), SB-525334 (SB52) (S8822; Sigma), Triton X-100 (T8787; Sigma), Bovine serum albumin (BSA) (05473; Fluka), Lipofectamine1 RNAiMAX Transfection Reagent (13778030; Thermo Fisher), OptiMEM (51985034; Thermo Fisher), αSMA antibody (A5228; Sigma), secondary antibodies Alexa Fluor1 488 (A11017 and A11078; Invitrogen), DAPI (D9542; Sigma), Propidium Iodide (7109; Sigma), anti-β-Actin antibody (sc-47778; Santa Cruz Biotechnology), anti-Nqo1 antibody (Ab2346; Abcam), anti- Nrf2 antibody (16396-1-AP; Proteintech), Anti-α-Tubulin antibody (T8203; Sigma), anti- Keap1 antibody (10503-2-AP; Proteintech), Anti Mouse-AP (4760.1; Roth), Anti-Rabbit Per- oxidase antibody (A6154; Sigma), Anti-Goat Peroxidase antibody (A16008; Invitrogen).

Cell culture and treatments

Human primary HSCs were purchased from iXCells Biotechnologies, USA, (Cat. 10HU-210) or Innoprot, Spain (Cat. P10653). They were cultured in DMEM High Glucose supplemented with 10% FBS and 1% Penicillin-Streptomycin (complete DMEM) and used up to 5 passages. hTERT-HSC were kindly provided by Dr. Bernd Schnabl (UC San Diego, USA)[20] and were cultured in complete DMEM up to 12 passages. The cells were kept in the humidified incuba- tor at 37˚C with 5% CO_2. Cell treatments were performed in serum-free medium for a maxi- mum of 48 hours without changing the medium. Following concentration were used as indicated in the leg- end: 0.5–10 ng/mL TGF-β1, 1–5 ng/mL PDGF-AB, 10 μM SB43, 1 μM SB52.

Nrf2 and Keap1 knockdown

A number of 1.9 x 10^5 HSCs per well were seeded in 12-well plates. The cells were transfected at day zero with siPOOL5 targeting human NFE2L2 (Nrf2) (NM_001145412; siTOOLs Bio- tech) and human Keap1 (NM_012289; siTOOLs Biotech). Briefly, a mixture containing siR- NAs and Lipofectamine was prepared in OptiMEM and added into the well at 1:10 dilution in complete DMEM, in order to achieve a final concentration of 5 nM siRNA and 2 μL Lipofecta- mine per well. The cells were transfected for 72 hours and then detached and used for the next experiments. Scrambled siRNAs were purchased by siTOOLs Biotech and used as negative control (indicated as siCON from now).

Immunocytochemistry analysis

After different treatments, HSCs were fixed in 4% formaldehyde for 15 minutes, followed by per- meabilization with 0.1% Triton-X-100 for 20 minutes. Blocking was performed with 1% BSA in PBS for 60 minutes, followed by incubation with primary antibody against αSMA (dilution 1:200 in blocking solution) or Nqo1 (1:500) for 90 minutes. Incubation with second- ary antibody was per- formed for 60 minutes in blocking solution at a 1:400 dilution. All steps were conducted at room temperature. DAPI and Propidium Iodide were used to stain the nuclei.

Click-iT EdU proliferation assay

The Click-iT1 EdU Alexa Fluor1 488 Imaging Kit (C10637; Invitrogen) was used to measure the proliferation rate of the cells after treatments. After cell transfection, the cells were detached and 3 x 10^4 cells/cm^2 were seeded in 96-well plate format. After overnight attach- ment, the cells were treated with EdU for 30 hours. In a separate experiment, detached cells were seeded and immedi- ately treated with 0.5–1 ng/mL TGF-β1, 1–5 ng/mL PDGF-AB and a mixture with 1 ng/mL TGF-β1 and 5 ng/mL PDGF-AB for 48 hours. EdU dye was added only during the last 30 hours of each experiment and detected following manufacturer's instruc- tions. The pictures were acquired with the Olympus Laser Confocal Scanning Microscope FV1000D spectral type (inverted microscope IX81) and analysed with ImageJ to determinate the proliferation rate.

Gene expression analysis

To determinate the efficiency of transfection, as well as the activation profile of the HSCs, RNA from treated and untreated cells was isolated following TRIzol extraction procedure. RNA was reverse transcribed using a reverse transcriptase (Promega) and oligo dT (Qiagen) and real time PCR was performed using FastStart TaqMan Mix (Roche) and TaqMan probes from Invitrogen. Real time, Taqman qPCR was performed on selected genes (see Table 1). The following qRT-PCR Program was used: 10 minutes denaturation at 95˚C, followed by 40 cycles of 15 seconds at 95˚C and 1 minute at 60˚C. The Ct values were assessed using the Corbett Rotorgene Analysis Software 6000, and B2M was used as an internal standard for the normali- zation of the fold changes of each gene of interest (GOI). Heat map for each gene and condi- tion was obtaining by using the Heatmapper online software (http://www2.heatmapper.ca/ expression/).

Migration assay

The migratory capacity of HSCs was investigated using the Culture-Insert 2 Well (80209; Ibidi) according to the manufacturer's instructions. Briefly, 70 μL of 3 x 10^5 cells/mL suspen- sion were incubated in each chamber in serum-free medium overnight. After cell attachment, the culture insert was gently removed by using sterile tweezers, leaving a cell-free gap of approximatively 500 μm. Medium was slowly aspired and 1 mL/well of serum free DMEM medium was added. Migration of transfected HSCs was evaluated in presence of TGF-β1, PDGF-AB and SB52 inhibitor. The wound healing process was followed during 48 hours by time laps microscopy, using Olympus cellVivo incubation system with 4X magnification. Pic- tures were acquired every hour for a period of 48 hours. Pictures were analysed with ImageJ and migration area was calculated with MRI Wound Healing Tool (http://dev.mri.cnrs.fr/ projects/imagej-macros/wiki/Wound_Healing_Tool) as previously published [21].

Table 1. TaqMan probes used for the research.

Gene of interest	Abbreviation	Invitrogen Ref.nr.
Beta-2-microglobulin (Housekeeping gene)	B2M	Hs00187842_m1
Actin, alpha 2, smooth muscle	ACTA2 (αSMA)	Hs00426835_g1
Activating transcription factor 3	ATF3	Hs00231069_m1
Catenin beta 1	CTNNB1	Hs00355049_m1
Collagen 1 alpha 1	COL1α1	Hs00164004_m1
Collagen 4 alpha 1	COL4α1	Hs00266237_m1
Fibronectin 1	FN1	Hs00415006_m1
Hyaluronic acid receptor	CD44	Hs01075861_m1
Kelch-like ECH-associated protein	Keap1	Hs00202227_m1
Lysyl oxidase	Lox	Hs00942480_m1
Lysyl oxidase like 2	Loxl2	Hs00158757_m1
Metalloproteinase 2	MMP2	Hs01548727_m1
Mitogen-activated protein kinase 8	MAPK8	Hs01548508_m1
Mitogen-activated protein kinase 14	MAPK14	Hs01051152_m1
NAD(P)H quinone dehydrogenase 1	Nqo1	Hs02512143_s1
Nuclear factor (erythroid-derived 2)-like 2	NFE2L2 (Nrf2)	Hs00975961_g1
PDGF receptor alpha	PDGFRA	Hs00998018_m1
PDGF receptor beta	PDGFRB	Hs01019589_m1
Snail family transcriptional repressor 1	Snail1	Hs00195591_m1

https://doi.org/10.1371/journal.pone.0201044.t001

ELISA

The presence of TGF-β1 in the supernatants of transfected HSCs was determined using commercial human ELISA kit (ABIN1979586; Antibodies-online GmbH), strictly following manu- facturer's instructions.

Western blot analysis

Cells were lysed in RIPA lysis buffer (89900; Thermo Fisher) on ice. Whole extracts were prepared and proteins were quantified by using a standard Bradford assay. 30 μg of proteins were separated by SDS-PAGE on Biorad precast anykD gel (456–9033; Biorad) and then blotted onto a nitrocellulose membrane (GE10600004; Sigma). After 60 minutes blocking with Odys- sey1 Blocking Buffer (PBS) (927–40000, LI-COR), the membranes were incubated overnight with primary antibodies diluted in blocking buffer as following: anti-β-Actin antibody (1:500), anti-Nqo1 antibody 1:5000), Anti-α-Tubulin antibody (1:2000), anti-Keap1 antibody (1:2000).

For Nrf2 detection blocking overnight was performed, followed by overnight incubation with anti-Nrf2 antibody (1:750). Horseradish peroxidase conjugated anti-mouse, anti-rabbit and anti-goat antibodies were used as secondary antibodies for 60 minutes in blocking buffer at the dilution of 1:5000. After extensive washing in PBS-T, the membranes were developed by incu- bating for 10 minutes in presence of BCIP and NBT in AP-buffer, and intensities quantified using Image J analysis software as previously published [22].

Statistical analysis

Experiments with primary HSC were conducted with at least 3 batches of cells as indicated in the legend. Data were analysed using GraphPad Prism 7 (GraphPad Software, inc.) and expressed as mean values ± SD as indicating in the legend. The Student's t-test was used for comparison between two groups. Data from three or more groups were analysed by one-way analysis of variance with Tukey's multiple comparisons test. P ≤0.05 was considered significant.

Results

Exposure to TGF-β1 suppresses gene expression of Nrf2 and related genes

Based on our own and previously published data [1,16,23], we exposed the HSCs to TGF-β1 in order to induce HSC activation. At all tested TGF-β1 concentrations, gene expression levels of Nrf2, Keap1 and Nqo1 were significantly downregulated in immortalized HSC (hTERT-HSC) after 48 hours of treatment (Fig 1A). Nrf2 mRNA levels were downregulated in a concentra- tion-dependent manner already after 24 hours (S1A Fig), while Nqo1 showed a significantly downregulation only after 48 hours of exposure (Fig 1A and S1C Fig). Downregulation of Keap1 was observed at all three concentrations of TGF-β1 and at all time points (except 1 ng/ mL at 24 hours) (Fig 1A and S1B Fig). In primary HSC, TGF-β1 significantly decreased the mRNA levels of both Nrf2 and Nqo1after 48 hours of exposure, but no change in expression was observed for Keap1 (Fig 1B). The downregulation of Nrf2 and Nqo1 by TGF-β1 could be prevented by the Smad inhibitor SB52. This inhibitor led to the upregulation of the mRNA lev- els of both Nrf2 and Nqo1, even when applied in combination with TGF-β1, supporting a direct link between TGF-β1 stimulation and Nrf2-repression (Fig 1B).

In addition to the analysis of the mRNA levels of selected markers, we determined the pro- tein levels of Nrf2, Keap1 and Nqo1 after exposure of HSCs to TGF-β1 (Fig 1C–1F). Both human immortalised and primary HSCs (Fig 1C and 1D), showed high basal levels of Nqo1. The downregulation of Nrf2 mRNA caused by exposure to TGF-β1 did not lead to any significant changes in its protein levels at 24h. On the contrary, Nrf2 levels were slightly increased by 1 ng/mL TGF-β1 at 48 hours in both HSCs. An increase in the protein levels of Keap1 was observed after treatments with TGF-β1 in hTERT-HSC in a concentration depen- dent manner at both 24 and 48 hours exposure (Fig 1E). Lower levels of Keap1 were observed in primary HSC compared to hTERT-HSC, and a slight increase after TGF-β1 exposure was observed at 24 hours only (Fig 1F).

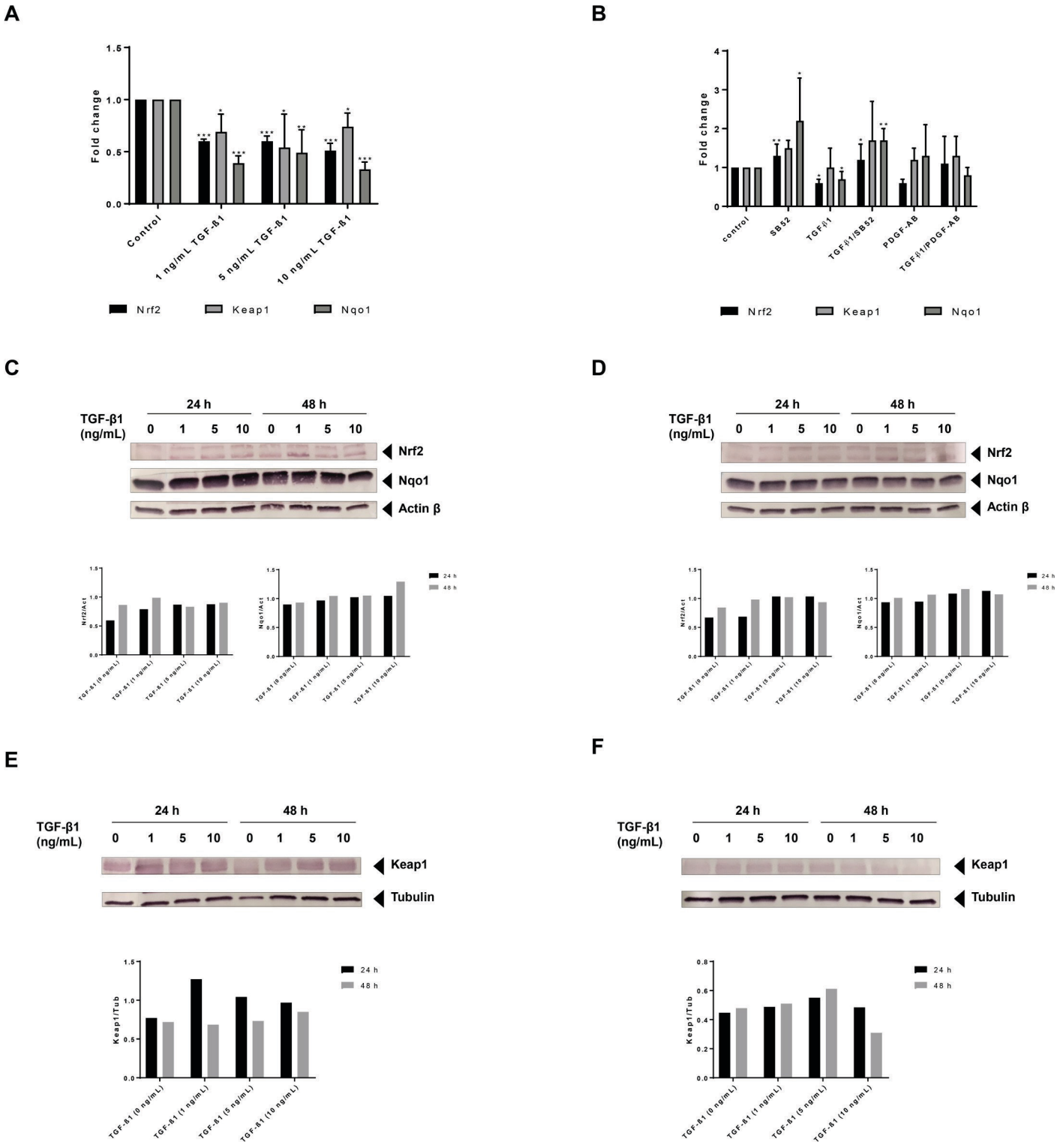

Fig 1. TGF-β1 suppresses mRNA expression of Nrf2 in HSCs. (A) hTERT-HSCs were exposed to 1–5 ng/mL TGF-β1 for 48 hours. mRNA was extracted using TRIzol conventional procedure and fold changes were calculated as 2^(-ΔΔCT) for each sample and control and expressed as mean fold change ± SD (N = 3). Beta- 2-microglobulin (B2M) was used as reference gene for each sample. The results show a significant downregulation of Nrf2, Keap1 and Nqo1 after exposure to TGF- β1. (B) Primary HSCs were exposed to 1 ng/mL TGF-β1, 1 μM SB-525334 (SB52) and/or 5 ng/mL PDGF-AB for 48 hours. mRNA was extracted using TRIzol conventional procedure and fold changes were calculated as 2^(-ΔΔCT) for each sample and control and expressed as mean fold change ± SD (N = 3 different batches). Beta-2-microglobulin (B2M) was used as reference gene for each sample. The results show a significant downregulation of Nrf2, and Nqo1 following exposure to TGF-β1.

SB52 induces upregulation of Nrf2 and Nqo1, efficiently inhibiting the TGF-β1 effect. (C-D) The protein levels of Nrf2, Nqo1 and actin beta were analysed by Western blot analysis after exposure to 0–10 ng/mL TGF-β1 in hTERT-HSC (C) and primary HSCs (D) for 24 and 48 hours. (E-F)

The protein levels of Keap1 and Tubulin were analysed by Western blot analysis after exposure to 0–10 ng/mL TGF-β1 in hTERT-HSC (E) and primary HSCs (F) for 24 and 48 hours.

https://doi.org/10.1371/journal.pone.0201044.g001

Nrf2 knockdown induces stellate cell activation

To further investigate the role of Nrf2 in HSC activation, we performed the knockdown of Nrf2 or Keap1 on HSCs using specific siRNAs (siNrf2 and siKeap1). After 72 hours of incuba- tion with siRNA, we could detect an efficient knockdown in both primary and immortalised HSCs: mRNA of Nrf2 and Nqo1 were significantly downregulated by 80–90% in both primary and hTERT-HSCs after siNrf2 (Fig 2A and 2B). Protein levels were visualised by western blot in hTERT-HSC, show- ing a successful knockdown also at the protein level (Fig 2C). In addi- tion, immunostaining of Nqo1 in hTERT-HSC confirmed the downregulation after exposure to siNrf2 (Fig 2D). The knock- down was maintained for up to 7 days after transfection (data not shown). As expected, siKeap1 induced downregulation of Keap1 mRNA, and a concomi- tant upregulation of Nqo1 mRNA and protein (Fig 2A–2C). In particular, mRNA levels of Nqo1 were upregulated by 4.8- and 3.2-fold changes after siKeap1 in hTERT-HSC and pri- mary HSC, respectively.

Transfection of both immortalised and primary HSCs with siNrf2 caused HSC-activation deter- mined by transcriptional induction of αSMA, Collagens I and IV, and TGF-β1 (Fig 3A and 3B, respectively). Lox, loxl2 and PDGFRB were also upregulated in human primary HSCs (Fig 3B). No significant changes were seen in both scrambled control (siCON) and siKeap1 HSCs. Secreted TGF-β1 was also significantly increased in primary HSC from 20 to 70 pg/mL after siNrf2 transfec- tion (Fig 3E). Additional evidence for the activation of HSCs by siNrf2 is provided by the strong upregulation of αSMA and its organization into stress fibres (Fig 3C and 3D). This effect was inhibited by the Smad inhibitors SB43 and SB52, indicating an involvement of the TGF/Smad pathway. In this experimental set up, stronger inhibition was observed with SB43 rather than SB52 in both primary and immortalised HSCs. As expected, PDGF-AB did not affect αSMA pro- duction, while TGF-β1 further induced αSMA and stress fibres formation in a Smad-dependent manner, as indicated by the immunostaining in pres- ence of TGF-β1 and/or SB inhibitors (Fig 3C and 3D). Interestingly, siKeap1 showed a protec- tive effect against TGF-β1-induced αSMA pro- duction compared to negative control in primary HSCs, suggesting a protective role of Nrf2 against TGF-β1-induced HSC activation (Fig 3F).

Nrf2 knockdown reduces cell proliferation and increases PDGF-induced proliferation rate in HSCs

To explore the proliferative capacities of the transfected HSCs, we performed an EdU prolifer- ation assay (Fig 4). The proliferation rate was around 0.7 for parental hTERT-HSC, and around 0.6 for parental primary HSC. In both HSCs, siNrf2 significantly reduced the prolifera- tion rate by around 30% (Fig 4A and 4B). siCON and siKeap1 did not affect the proliferation rate in the primary HSCs, while they significantly reduced the proliferation in the hTERT- HSC. Nrf2 knockdown cells showed more PDGF-AB-induced cell proliferation than siCON cells (Fig 4C and 4D). Proliferation was in fact increased by 50–100% in both siNrf2 HSCs after exposure to PDGF-AB compared to siCON HSCs where only an increase of 25% was detected. These results suggest that Nrf2 knockdown might drive the cells towards activation, making them more sensitive to stimuli. TGF- β1 did not affect the proliferation rate in primary HSCs, neither with siCON nor with siNrf2 (Fig 4D), while downregulation was measured in hTERT-HSC, with a more pronounced effect after Nrf2 knockdown (Fig 4C).

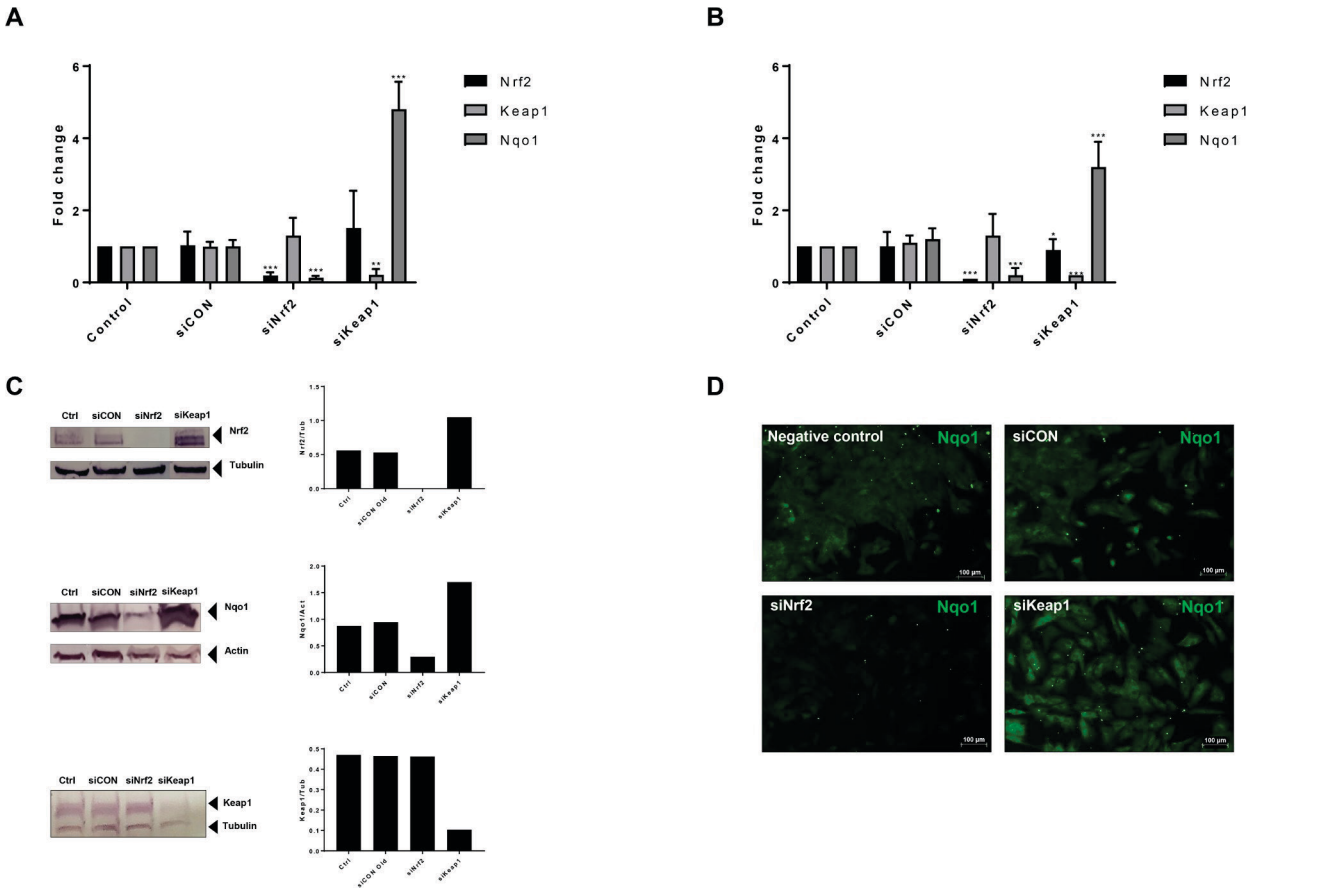

Fig 2. siRNA knockdown of Nrf2 pathway-related genes. (A-B) siRNAs for Nrf2 (siNrf2), Keap1 (siKeap1) and scrambled (siCON) were used to knockdown Nrf2 and Keap1 in hTERT-HSC (A) and primary HSC (B). mRNA level of Nrf2, Keap1 and Nqo1 were then analysed, showing an efficient knockdown of both Nrf2 and Keap1. Fold changes were calculated as 2^(-ΔΔCT) for each sample and control and expressed as mean fold change ± SD. *, P ≤ 0.05; **, P ≤ 0.01; ***; P ≤ 0.001 vs siCON (mean ± SD, N = 4 from independent experiment for hTERT-HSC and N = 6 different batches in primary HSC). (C) Protein levels of Nrf2, Keap1 and Nqo1 were analysed by Western blot in knockdown hTERT-HSC. Ctrl: control samples; siCON: scrambled siRNA; siNrf2: Nrf2 knockdown; siKeap1: Keap1 knockdown. Protein were extracted 72 hours after the transfection. (D) Immunocytochemistry analysis of Nqo1 in hTERT-HSC. Green: Nqo1. siCON: scrambled siRNA; siNrf2: Nrf2 knockdown; siKeap1: Keap1 knockdown.

https://doi.org/10.1371/journal.pone.0201044.g002

Knockdown of Nrf2 induces cell migration in HSCs

Nrf2 knockdown induced a significant increase in cell motility in both hTERT-HSC and pri- mary HSCs while Keap1 knockdown induced a decrease in the migration rate only in primary HSCs (Fig 5). In particular, siNrf2 hTERT-HSC displayed 1.5-fold higher migration than con- trol cells at both 24 and 48 hours (Fig 5A); no changes were measured after siKeap1 and siCON. Primary HSCs showed higher migration than hTERT-HSC, with a complete repair of the wound after 24 hours (data not shown). Thus, the migration rate was calculated at 12 and 24 hours for primary HSCs (Fig 5B). Similarly, to hTERT-HSC, siNrf2-treated primary HSCs displayed higher migra- tion than control cells at 12 hours; no significant changes were mea- sured at 24 hours. The motility of knockdown cells was further affected by TGF-β1 and PDGF-AB (Fig 5C). In fact, transfected primary HSCs showed a PDGF-AB-induced cell migration in both siCON and siNrf2 cells with a synergistic effect of TGF-β1 and PDGF-AB (Fig 5C). TGF-β1 did not affect the migra- tion of control cells (siCON), while a decrease in migration was displayed in the Nrf2 knock- down cells, indicating a stronger response of the cells to the cytokine. No significant effect of SB52 was observed. Similar data were obtained with hTERT-HSC (data not shown).

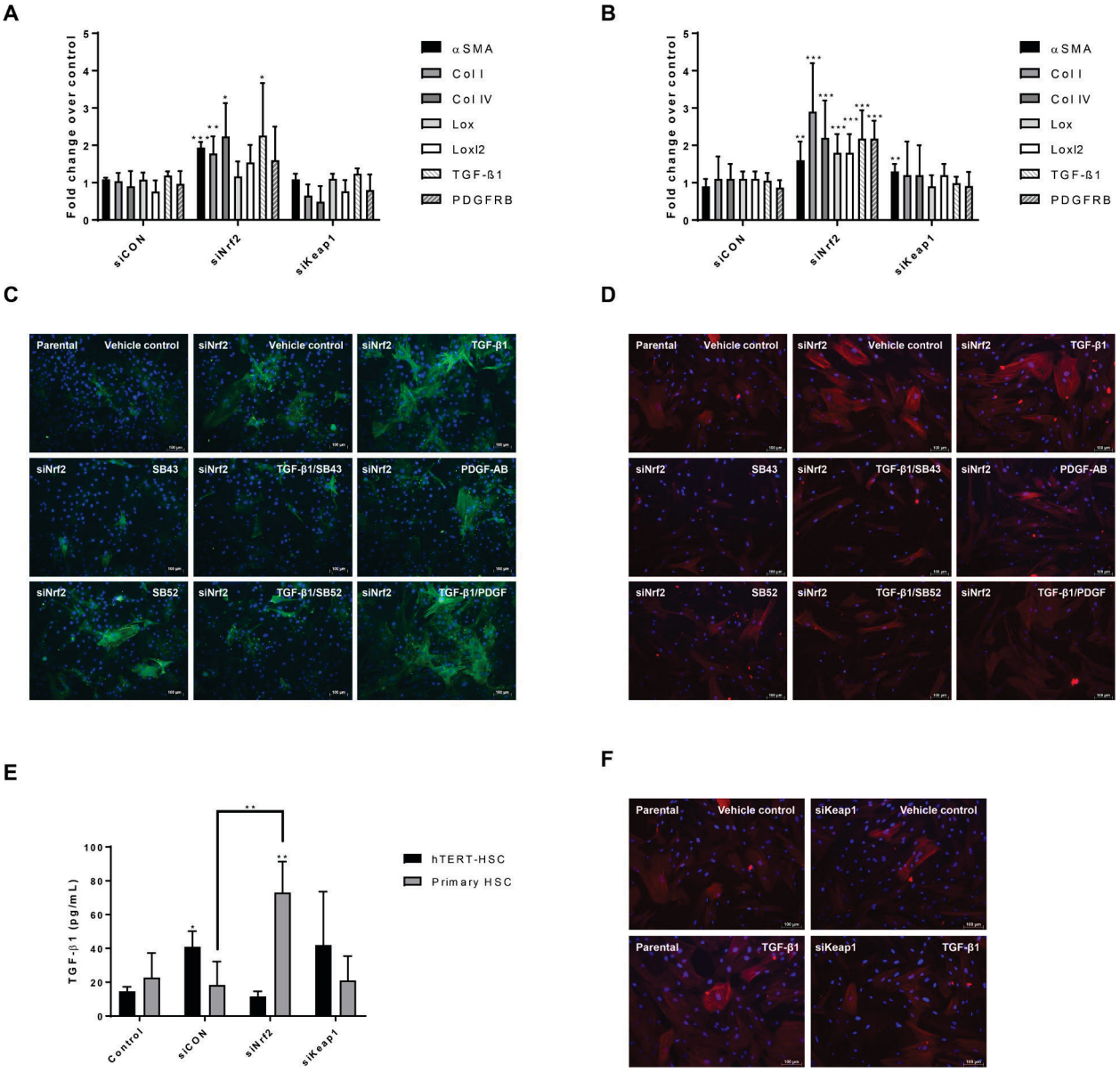

Fig 3. Effect of Nrf2 knockdown on HSC activation and response to stimuli. (A-B) After 72 hours knockdown with siRNAs, mRNA was extracted from hTERT-HSC cells (A) and human primary HSCs (B). Fold change for each gene of interest was calculated as 2^(-ΔΔCT) for each sample and control and expressed as mean fold change ± SD. Beta-2-microglobulin (B2M) was used as reference gene for each sample. *, P ≤ 0.05; **, P ≤ 0.01; ***; P ≤ 0.001 vs Control (mean ± SD, N = 4 from independent experiment for hTERT-HSC and N = 6 different batches for primary HSC). (C-D) hTERT-HSCs (C) and primary HSCs (D) were treated for 48 hours with TGF-β1 (1 ng/mL), SB431542 hydrate (SB43) (10 μM), SB-525334 (SB52) (1 μM) and/or PDGF-AB (5 ng/mL). After treatment, the cells were fixed and stained against αSMA (green in C and red in D) and nuclei (DAPI, blue). The results show an increase in αSMA production in Nrf2 knockdown cells and a further increase after TGF-β1 exposure. SB43 and SB52 significantly inhibited the TGF-β1-induced αSMA. Pictures taken using fluorescence microscopy. siNrf2: Nrf2 knockdown. Scale bar: 100 μm. (E) TGF-β1 release was measured in supernatant medium in both transfected hTERT and primary HSCs by ELISA. siCON: scrambled siRNA; siNrf2: Nrf2 knockdown; siKeap1: Keap1 knockdown. *, P ≤ 0.05; **, P ≤ 0.01 vs Control or siCON (mean ± SD, N = 4 from independent experiments for hTERT-HSC and N = 5 different batches for primary HSC). (F) Immunostaining of αSMA (red) and nuclei (DAPI, blue) in Keap1 knockdown primary HSCs. Knockdown cells show more resistance again TGF-β1 (1 ng/mL) induced activation compared to control cells. siKeap1: Keap1 knockdown.

https://doi.org/10.1371/journal.pone.0201044.g003

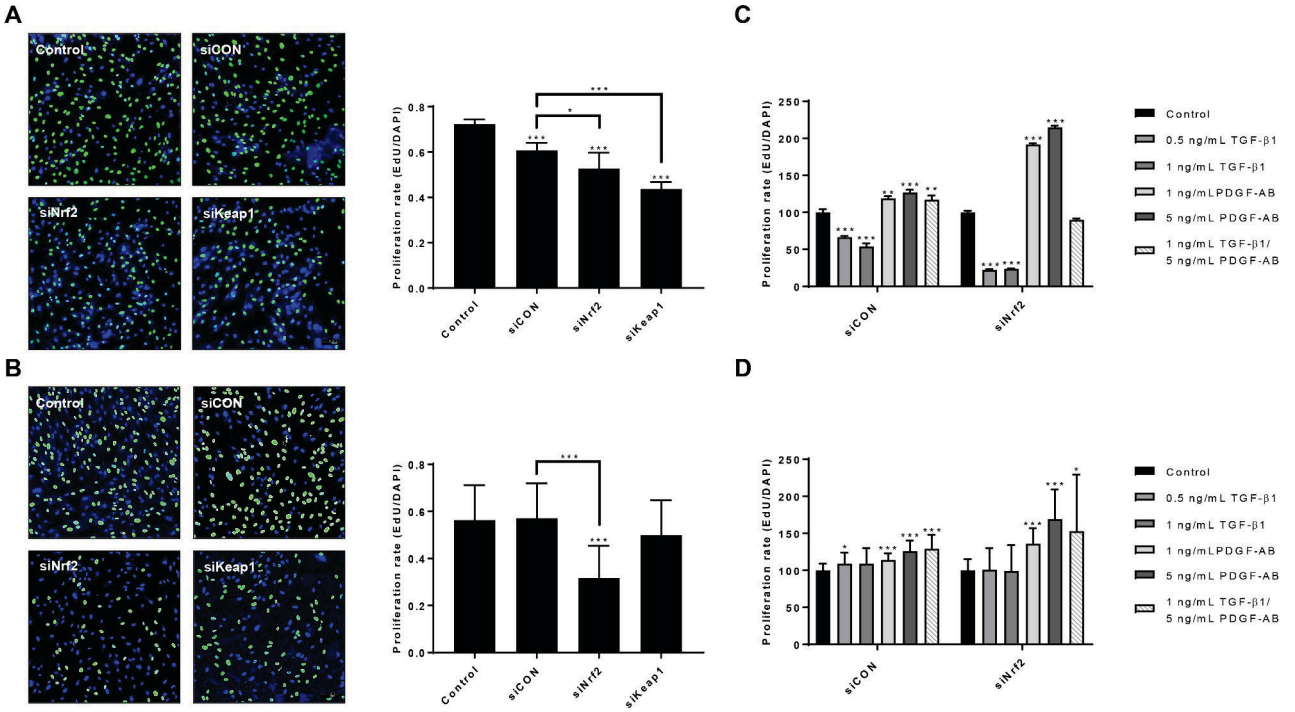

Fig 4. Effect of siRNAs, TGF-β1 and/or PDGF-AB on HSC proliferation. (A-B) hTERT-HSCs (A) and primary HSCs (B) were transfected for 72 hours with siNrf2, siKeap1 or siCON. Cells were then detached and plated for EdU staining as described in Materials and methods section. The pictures were taken with 10X magnification by using confocal microscopy and nuclei were counted with Image J software. siCON: scrambled siRNA; siNrf2: Nrf2 knockdown; siKeap1: Keap1 knockdown. *, P ≤ 0.05; **, P ≤ 0.01; ***; P ≤ 0.001 vs control or siCON. Values are expressed as rate of proliferation (mean ± SD); N = 4 independent experiment with 5 replicates each for hTERT-HSC, and N = 6 different batches with 5 replicates each. (C-D) Proliferation rate of transfected hTERT-HSC (C) and primary HSC (D) after exposure to 0.5–1 ng/mL TGF-β1 and/or 1–5 ng/mL PDGF-AB for 48 hours. EdU was added during the last 30 hours of the experiment. Values are expressed as percentage of proliferation over each control sample. *, P ≤ 0.05; **, P ≤ 0.01; ***; P ≤ 0.001 vs Control (mean ± SD, N = 4 replicates for hTERT-HSC and N = 3 from different batches with 4 replicates each for primary HSC).

https://doi.org/10.1371/journal.pone.0201044.g004

Nrf2 knockdown induces stellate cells activation in a Smad-dependent manner

To elucidate the molecular mechanisms underneath the siNrf2-induced HSC activation, we exposed the transfected cells to TGF-β1, PDGF-AB and/or Smad inhibitors for 48 hours and assessed gene expression of activation and fibrotic markers (Fig 6). In both siCON and siNrf2 hTERT-HSC, SB43 displayed a strong inhibitory effect and decreased the TGF-β1 elicited activation of the cells. The effect of SB52 was similar but less marked. Nrf2 knockdown cells also showed higher response to TGF-β1 than siCON cells, leading to a significant upregulation of all the markers (except collagens) already at 0.5 ng/mL TGF-β1 (Fig 6B). PDGF-AB slightly induced CD44, Lox genes, CTNNB1, MMP2 and Snail1 only in siNrf2 cells. Consistently, the combination of TGF-β1 and PDGF-AB showed stronger gene expression changes in siNrf2 samples than siCON samples (Fig 6). Interestingly, SB43 successfully inhibited the TGF-β1-induced gene induction, with a weaker effect on the siNrf2 cells. SB52, showed a strong inhibitory effect on siCON HSCs, while some of the markers (FN1, CD44, CTNNB1, Lox, Loxl2, MMP2, MAPK8) were still slightly upregulated after TGF-β1/SB52 treatments. These data indicate an anti-activation and anti-fibrotic role of Nrf2 in HSCs.

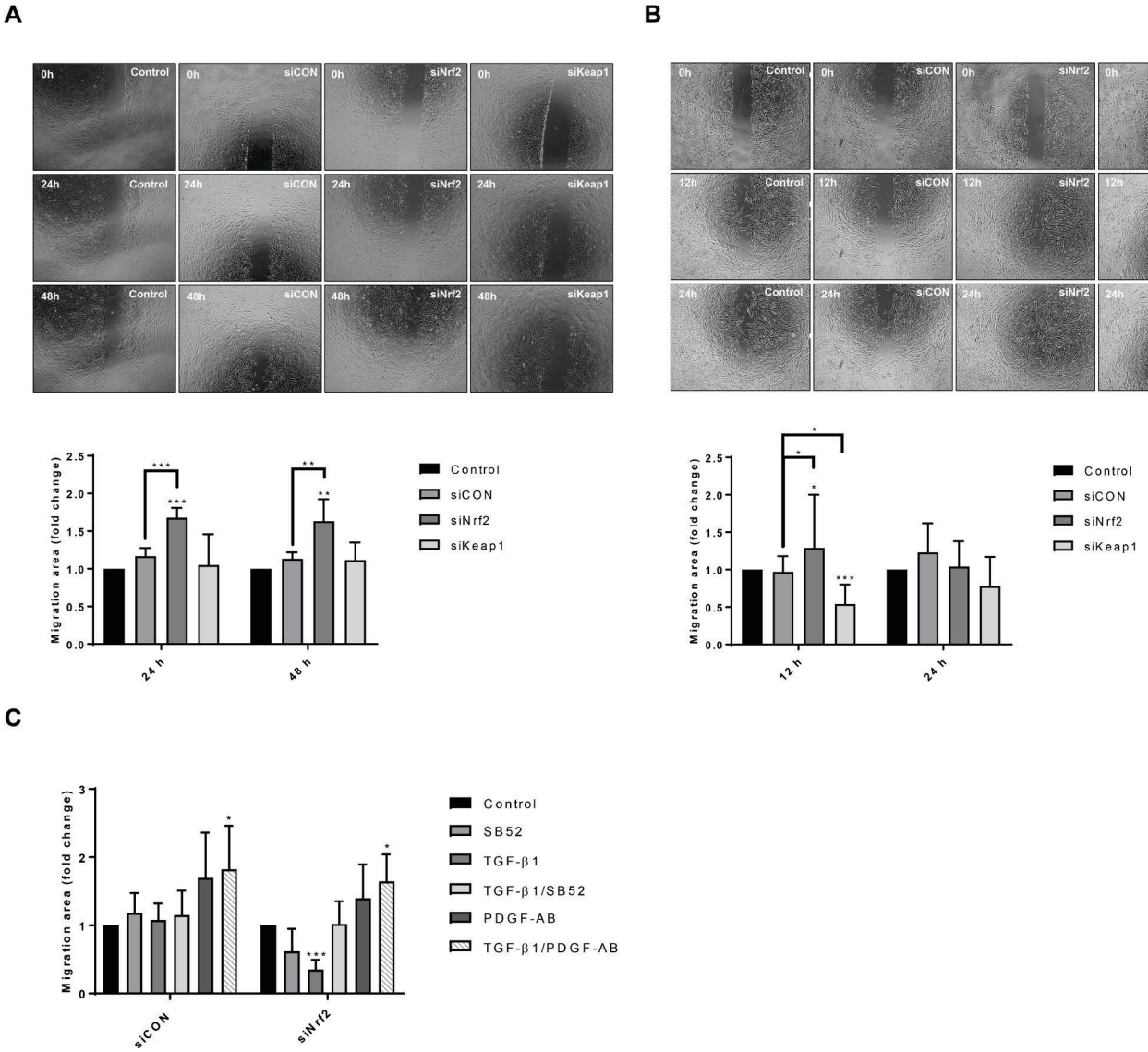

Fig 5. Nrf2 knockdown-dependent migration of HSCs. After 72 hours of knockdown, hTERT-HSCs (A) and primary HSCs (B) were seeded into the Culture Insert 2-Well (Ibidi). Pictures were acquired with 4X magnification every hour for a period of 48 hours using Olympus cellVivo incubation system. Pictures of the samples at 0, 24 and 48 hours are showed for hTERT-HSC (A), while 0,12 and 24 hours are showed for primary HSCs (B). Migration area was calculated with MRI wound healing tool of Image J software and expressed as fold change of the treated vs control (mean ± SD). *, P ≤ 0.05; **, P ≤ 0.01 vs Control. N = 4 independent experiments for hTERT-HSC (A) and N = 6 different batches for primary HSC (B). (C) After transfection, primry HSCs were seeded into the Culture Insert 2-Well and exposed to TGF-β1 (1 ng/mL), SB-525334 (SB52) (1 μM) and/or PDGF-AB (5 ng/mL) for 48 hours. Pictures were acquired with 4X magnification every hour for a period of 48 hours using Olympus cellVivo incubation system. Migration area at 12 hours was calculated with MRI wound healing tool of Image J software and expressed as fold change of the treated vs control (mean ± SD). *, P ≤ 0.05; ***; P ≤ 0.001 vs Control (N = 3 different batches).

https://doi.org/10.1371/journal.pone.0201044.g005

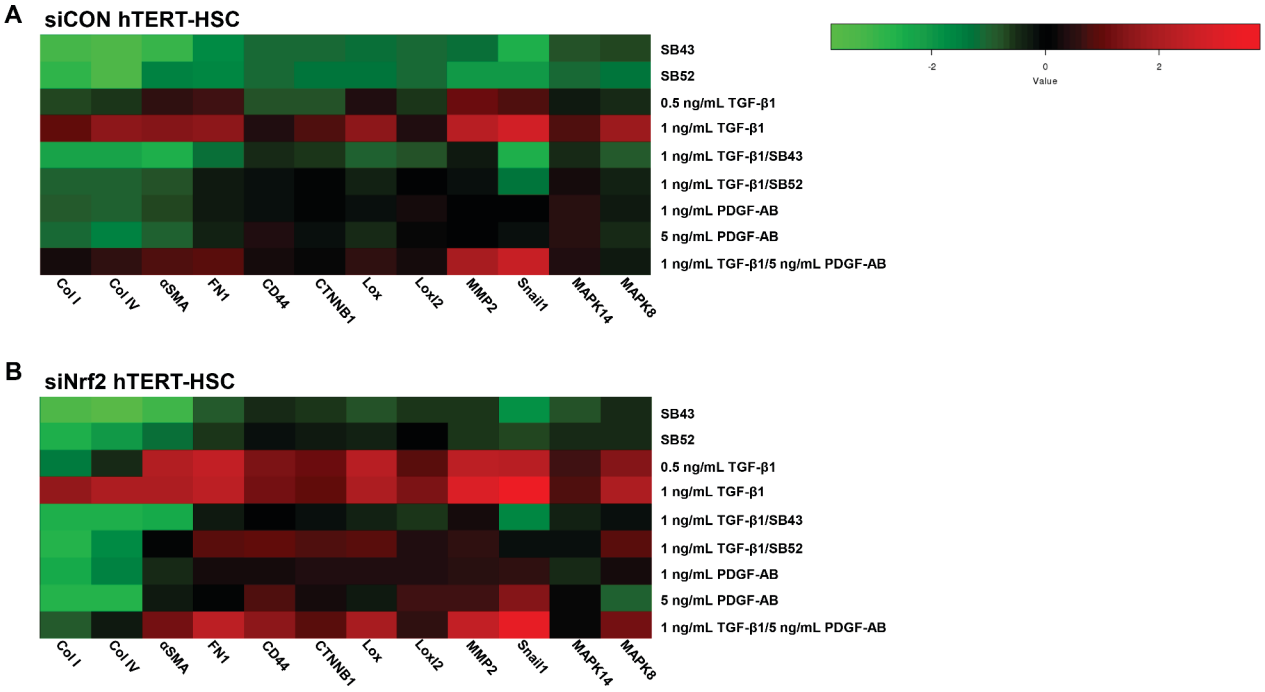

Fig 6. Heat map analysis of gene expression between control and Nrf2 knockdown hTERT-HSC. Heat map analysis showing differential gene expression pattern in siCON transfected hTERT-HSC (A) and siNrf2 transfected hTERT-HSC (B) Heat map was generated on -$Log_2(\Delta\Delta CT)$ by using the Heatmapper online software (http://www2.heatmapper.ca/expression/). Columns represent each gene of interest, while rows indicate each cell treatment. Cells were exposure to the tested compounds for 48 hours prior mRNA extraction.

https://doi.org/10.1371/journal.pone.0201044.g006

Discussion

Recently, Nrf2 has drawn attention to its role as an antifibrotic agent in the liver [17]. However, although Nrf2 has been identified as an important factor in HSC activation [3], the mech- anism through which it acts in HSC remains unclear. In this study, we focused on Nrf2 pathway in both quiescent and activated HSC. Both primary and immortalised HSCs showed high level of Nrf2 and especially of Nqo1 prior treatments (Fig 1), which is consistent with pre- viously published data on rat HSCs showing high Nrf2 content in quiescent cells and lower lev- els after HSCs activation [3]. These high levels of Nrf2 may contribute to maintain HSCs in their quiescent phenotype, as shown by the low level of αSMA before applying the treatments (Fig 3C and 3D). In our study, we demonstrated that TGF-β1-induced HSC activation signifi- cantly reduced the mRNA levels of both Nrf2 and Nqo1 in a concentration and time-depen- dent manner in human HSCs. However, TGF-β1 exposure did not significantly affect the protein levels of Nrf2 or Nqo1. A potential explanation for the changes in the mRNA level may be due to a loss of Nrf2 function rather than a decrease in protein quantity. Consistent with this hypothesis, we detected an upregulation of ATF3 after TGF-β1 exposure (S1D Fig). It has been reported that TGF-β1-induced ATF3 binds Nrf2, resulting in a strong repression of an ARE reporter, without directly affecting the Nrf2 protein level [24,25]. Nrf2 may also be anchored to the cytoskeleton by Keap1, as suggested by the increase in Keap1 protein amount after TGF-β1 exposure (Fig 1E and 1F).

Our results strongly support the direct involvement of Nrf2 in limiting HSC activation. We could show that decreased levels of Nrf2 induced a significant upregulation of genes involved either in HSC activation (αSMA, Lox, Loxl2) or ECM remodelling (Collagens I and IV) (Fig 3A and 3B). The upregulation of TGF-β1 and PDGFRB are relevant hallmarks of HSC activation, due to the involvement of these proteins in maintaining a positive loop towards activation [23,26]. Primary HSCs displayed a stronger response to siNrf2 based on the stronger upregulation of marker genes.

Decreased levels of Nrf2 in HSC also led to increased production and release of TGF-β1-levels suggesting that the HSC activation was at least partly TGF-β1/Smad-dependent. In support of this theory, the two Smad inhibitors SB43 and SB52 efficiently reduced the TGF- β1-induced increase in αSMA production and the induction of mRNA levels of most of the activation markers in siNrf2 HSCs (Fig 3C and 3D and Fig 6). The less marked activation phe- notype observed with the inhibitors alone may be due to the blocking of basal activation of the Smad pathway (e.g. through endogenous TGF-ß1). On the other hand, Nrf2 accumulation in siKeap1-HSCs led to a milder activation by TGF-β1, based on induction of αSMA (Fig 3F).

These results indicate that the high amount of Nrf2 in quiescent HSCs is essential to maintain- ing a repressed phenotype, suggesting a new role of Nrf2 as anti-fibrogenic factor in HSCs.

Migration and proliferation are important hallmarks of activated HSC as well as of cancer progression in many tissues, and they have been often related to Nrf2 pathway [1,27–30]. Here we report that Nrf2 inhibits migration and induces proliferation in quiescent HSCs. The deple- tion of Nrf2 significantly increased cell motility, while Keap1 knockdown significantly reduced motility in primary HSCs (Fig 5). Cell migration was not correlated to cell proliferation, as indicated by the decrease in the proliferation rate of the siNrf2 cells (Fig 4). No release of PDGF-AB was detected in either HSCs, indicating that the effects on migration and prolifera- tion are not directly correlated to PDGF (data not shown). Similarly, the two Smad inhibitors SB43 and SB52 did not affect neither proliferation nor migration of HSCs, suggesting a Smad- independent regulatory mechanism of these two cellular processes (data not shown). Nrf2 has been shown to interact with the PI3K-AKT signalling pathway and NF-kB in regulating anti- oxidant- as well as proliferation- and migration-related genes in many tissues [31–33]. The antagonistic effect of Nrf2 to NF-kB may be one of the mechanisms through Nrf2 inhibits migration and invasiveness in the HSCs, as it has been shown for human embryonic kidney cells [33]. Similarly, an interaction with AKT may be acting in HSCs and regulates prolifera- tion. AKT has been shown to play an important role in the early activation of HSC and in their protection against apoptosis [34,35]. On the other hand, the promotion of proliferation oper- ated by Nrf2 may be correlated to its inhibitory effect on the TGF-β1 pathway, as the anti-pro- liferative effect of this cytokine has been widely documented on smooth muscle cells and epithelial cells [36–39]. Concordantly, our results show that TGF-β1 decreased HSC prolifera- tion of the HSC-line and that this response was further enhanced in Nrf2-deficient cells.

Depletion of Nrf2 also led to a more pronounced PDGF-AB-induced proliferation, whereas only minor effects on cell migration were observed (Fig 4C and 4D and Fig 5C).

Our evidence provides insight into a novel role of Nrf2 in HSCs. Fig 7 illustrates the Nrf2 signalling pathway and its interplay with the TGF-β1/Smad pathway. We showed high level of both Nrf2 and Nqo1 prior TGF-β1 induction in HSCs. Nrf2, as well as Nqo1, have been identi- fied as the most important genes involved in the oxidative response against reactive oxygen species (ROS) [40]. The high amount of Nrf2 in the HSCs may inhibit the Smad2/3 protein by inducing the gene expression of phosphatases (such as PPM1A), which may reduce the phos- phorylation of Smad2/3 as previously published [41]. This would result in a low amount of active Smad2/3, favouring a proliferative status rather than the induction of the genes involved in HSC activation and motility. This is concordant with the phenotype of control HSCs observed in our experiments, characterized by low levels of activation markers (αSMA and TGF-β1). Nrf2 has also been shown to bind Smad proteins in cancer cell lines, acting as a tran- scriptional repressor by competing with Smad complex for the co-transcriptional activator p300/CBP [27]. These observations point out Nrf2 as a key factor in maintaining a repressed phenotype in HSC, which is in agreement with the activation elicited in the Nrf2 knockdown experiments.

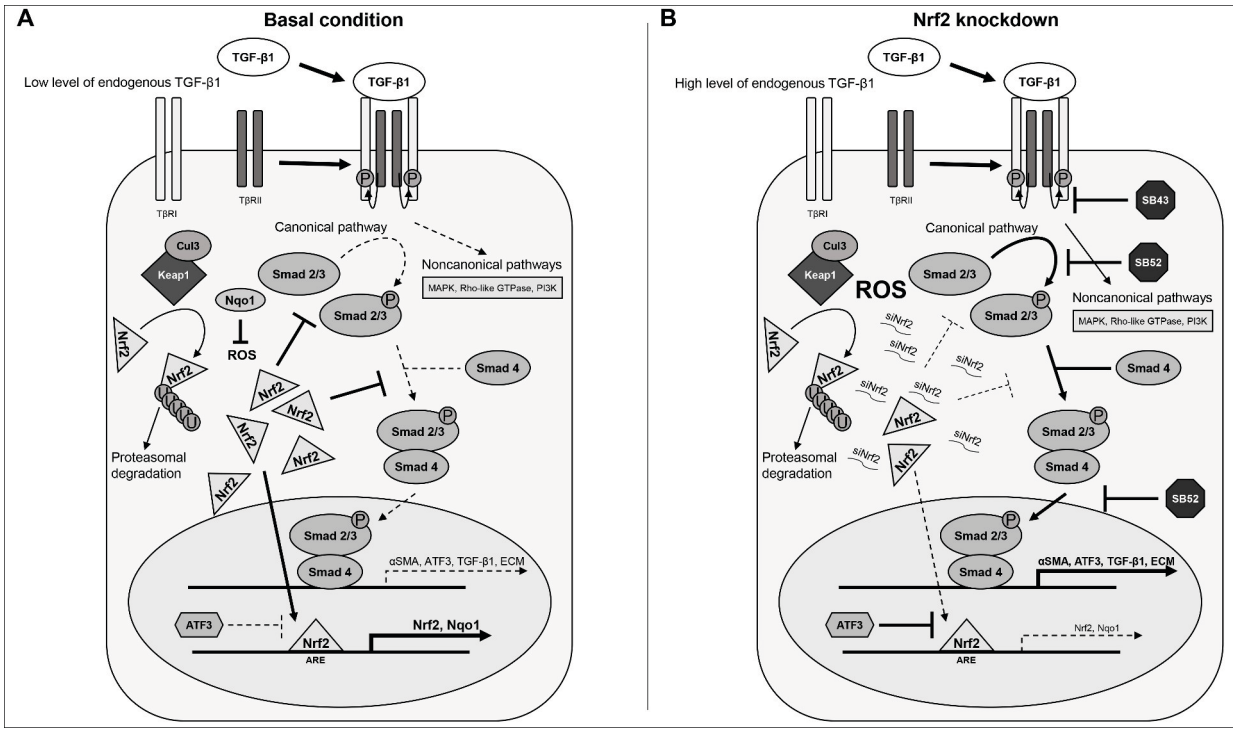

Fig 7. Nrf2 intervention into the TGF-β1/Smad signalling pathway. Panel A, basal condition: HSCs express high levels of both Nrf2 and its target genes (e.g. Nqo1), thereby controlling reactive oxygen species (ROS) level. Nrf2 also inhibits Smad pathway by binding directly to Smad protein or through the action of phosphatases [41]. In these conditions, the TGF-β1/Smad pathway has a low activity, resulting in low level of αSMA, collagens and TGF-β1. Thus, HSC cells exhibit a quiescent phenotype. Panel B, Nrf2 knockdown: we have found out that Nrf2 knockdown, with a consequent decrease of its target genes, induces stellate cells activation. Decrease in Nrf2 was in fact associated with an increase in the levels of Extracellular matrix (ECM) components as well as αSMA and TGF-β1. TGF-β1 further induces the expression of ATF3, which acts as functional repressor of Nrf2. We found out that this siNrf2-induced stellate cell activation may be regulated by the Smad inhibitors SB-431542 hydrate (SB43) and SB-525334 (SB52), confirming the role of Nrf2 in relation to the Smad pathway.

https://doi.org/10.1371/journal.pone.0201044.g007

Following Nrf2 knockdown (Fig 7B), Nqo1 levels in the cytoplasm decrease quickly, which may result in an increase of ROS and its inhibitory effect of PPM1A [41]. Thus, Smad2/3 could bind Smad4 and translocate to the nucleus, resulting in a strong induction of HSC activation markers, induction of migration and inhibition of proliferation. In line with this hypothesis, Smad inhibitors could modulate siNrf2-induced HSC activation, confirming the involvement of the TGF-β1/Smad pathway. Interestingly, SB43 showed a stronger inhibition than SB52, both alone and in combination with TGF-β1. This may be related to their different inhibition mechanism. SB43 has been shown to inhibit the TGF-β type I receptor (TβRI), acting more upstream on the pathway compared to SB52, which inhibits Smad3 phosphorylation and nuclear translocation [42–44]. Nrf2 knockdown (and TGF-β1 release), as well as the addition of exogenous TGF-β1, lead to high amount of phosphorylated Smad2/3 which implies SB52 to be ineffective at fully repressing TGF-β1-induced gene expression. New synthesized ATF3 could further contribute to the Nrf2 inhibition, exacerbating more the TGF-β1-induced HSC activation.

In conclusion, our data provide clear proof of the direct involvement of Nrf2 in HSC activation. This underlines the importance of Nrf2 in non-parenchymal liver cells in addition to its already known cytoprotective role in hepatocytes. Our data also provide insights into the mechanisms by which Nrf2 decreases HSC activation, highlighting a new role of Nrf2 as anti- fibrotic molecule in HSCs. Indeed, the depletion of Nrf2 may be a contributing factor to HSC activation *in vitro* as well as *in vivo*. Intervention on Nrf2 pathway in HSC may be a new per- spective therapy for liver fibrosis.

Supporting information

S1 Fig. TGF-β1 effects on Nrf2 pathway's component. (A-C) hTERT-HSCs were exposed to 1–5 ng/mL TGF-β1 for 24, 48 and 72 hours. mRNA was extracted using TRIzol conventional procedure and fold changes were calculated as 2^(-ΔΔCT) for each sample and control and expressed as mean fold change ± SD (N = 3). Beta-2-microglobulin (B2M) was used as refer- ence gene for each sample. The results show a significant downregulation of Nrf2, Keap1 and Nqo1 after exposure to TGF-β1 in a time- and concentration-dependent manner. (A) Nrf2 mRNA levels; (B) Keap1 mRNA levels; (C) Nqo1 mRNA levels. (D) mRNA levels of ATF3 were analysed in both hTERT-HSC and primary HSC after exposure to 1 ng/mL TGF-β1 for 48 hours. Fold induction were calculated as 2^(-ΔΔCT) for each sample and control and expressed as mean fold induction ± SD (N = 3 for hTERT-HSC and N = 5 different batches for primary HSC). *, $P \leq 0.05$; **, $P \leq 0.01$; ***; $P \leq 0.001$ vs Control.

(TIF)

Acknowledgments

We are very thankful to Dr. B. Schnabl for making the hTERT-HSC available for our research.

Author Contributions

Conceptualization: LauraSuterDick.

Data curation: Vincenzo Prestigiacomo.

Formal analysis: Vincenzo Prestigiacomo, Laura Suter-Dick.

Funding acquisition: Laura Suter-Dick.

Investigation: Vincenzo Prestigiacomo.

Methodology: Vincenzo Prestigiacomo.

Project administration: Vincenzo Prestigiacomo, Laura Suter-Dick.

Resources: Vincenzo Prestigiacomo.

Supervision: Laura Suter-Dick.

Validation: Vincenzo Prestigiacomo.

Visualization: Vincenzo Prestigiacomo.

Writing – original draft: Vincenzo Prestigiacomo.

Writing – review & editing: Vincenzo Prestigiacomo, Laura Suter-Dick.

References

1. Lee UE, Friedman SL. Mechanisms of Hepatic Fibrogenesis. Best Pract Res Clin Gastroenterol. 2011; 25: 195–206. https://doi.org/10.1016/j.bpg.2011.02.005 PMID: 21497738
2. Mormone E, Lu Y, Ge X, Fiel MI, Nieto N. Fibromodulin, an oxidative stress-sensitive proteoglycan, reg- ulates the fibrogenic response to liver injury in mice. Gastroenterology. 2012; 142: 612–621.e5. https:// doi.org/10.1053/j.gastro.2011.11.029 PMID: 22138190

3. Yang J-J, Tao H, Hu W, Liu L-P, Shi K-H, Deng Z-Y, et al. MicroRNA-200a controls Nrf2 activation by target Keap1 in hepatic stellate cell proliferation and fibrosis. Cell Signal. 2014; 26: 2381–2389. https:// doi.org/10.1016/j.cellsig.2014.07.016 PMID: 25049078
4. Nguyen T, Nioi P, Pickett CB. The Nrf2-antioxidant response element signaling pathway and its activa- tion by oxidative stress. J Biol Chem. 2009; 284: 13291–13295. https://doi.org/10.1074/jbc. R900010200 PMID: 19182219
5. Taguchi K, Motohashi H, Yamamoto M. Molecular mechanisms of the Keap1–Nrf2 pathway in stress response and cancer evolution. Genes Cells Devoted Mol Cell Mech. 2011; 16: 123–140. https://doi. org/10.1111/j.1365-2443.2010.01473.x PMID: 21251164
6. Pall ML, Levine S. Nrf2, a master regulator of detoxification and also antioxidant, anti-inflammatory and other cytoprotective mechanisms, is raised by health promoting factors. Sheng Li Xue Bao. 2015; 67: 1–18. PMID: 25672622
7. Sison-Young RLC, Mitsa D, Jenkins RE, Mottram D, Alexandre E, Richert L, et al. Comparative Proteo- mic Characterization of 4 Human Liver-Derived Single Cell Culture Models Reveals Significant Variation in the Capacity for Drug Disposition, Bioactivation, and Detoxication. Toxicol Sci Off J Soc Toxicol. 2015; 147: 412–424. https://doi.org/10.1093/toxsci/kfv136 PMID: 26160117
8. Chan K, Han XD, Kan YW. An important function of Nrf2 in combating oxidative stress: detoxification of acetaminophen. Proc Natl Acad Sci U S A. 2001; 98: 4611–4616. https://doi.org/10.1073/pnas. 081082098 PMID: 11287661
9. Enomoto A, Itoh K, Nagayoshi E, Haruta J, Kimura T, O'Connor T, et al. High sensitivity of Nrf2 knock- out mice to acetaminophen hepatotoxicity associated with decreased expression of ARE-regulated drug metabolizing enzymes and antioxidant genes. Toxicol Sci Off J Soc Toxicol. 2001; 59: 169–177.
10. Xu W, Hellerbrand C, Köhler UA, Bugnon P, Kan Y-W, Werner S, et al. The Nrf2 transcription factor pro- tects from toxin-induced liver injury and fibrosis. Lab Investig J Tech Methods Pathol. 2008; 88: 1068– 1078. https://doi.org/10.1038/labinvest.2008.75 PMID: 18679376
11. Lamlé J, Marhenke S, Borlak J, von Wasielewski R, Eriksson CJP, Geffers R, et al. Nuclear factor-eythroid 2-related factor 2 prevents alcohol-induced fulminant liver injury. Gastroenterology. 2008; 134: 1159–1168. https://doi.org/10.1053/j.gastro.2008.01.011 PMID: 18395094
12. Okawa H, Motohashi H, Kobayashi A, Aburatani H, Kensler TW, Yamamoto M. Hepatocyte-specific deletion of the keap1 gene activates Nrf2 and confers potent resistance against acute drug toxicity. Bio- chem Biophys Res Commun. 2006; 339: 79–88. https://doi.org/10.1016/j.bbrc.2005.10.185 PMID: 16293230
13. Goldring CEP, Kitteringham NR, Elsby R, Randle LE, Clement YN, Williams DP, et al. Activation of hepatic Nrf2 in vivo by acetaminophen in CD-1 mice. Hepatol Baltim Md. 2004; 39: 1267–1276. https:// doi.org/10.1002/hep.20183 PMID: 15122755
14. Beyer TA, Xu W, Teupser D, auf dem Keller U, Bugnon P, Hildt E, et al. Impaired liver regeneration in Nrf2 knockout mice: role of ROS-mediated insulin/IGF-1 resistance. EMBO J. 2008; 27: 212–223. https://doi.org/10.1038/sj.emboj.7601950 PMID: 18059474
15. Wakabayashi N, Shin S, Slocum SL, Agoston ES, Wakabayashi J, Kwak M- K, et al. Regulation of notch1 signaling by nrf2: implications for tissue regeneration. Sci Signal. 2010; 3: ra52. https://doi.org/ 10.1126/scisignal.2000762 PMID: 20628156
16. Prestigiacomo V, Weston A, Messner S, Lampart F, Suter-Dick L. Pro-fibrotic compounds induce stel- late cell activation, ECM-remodelling and Nrf2 activation in a human 3D-multicellular model of liver fibro- sis. PLOS ONE. 2017; 12: e0179995. https://doi.org/10.1371/journal.pone.0179995 PMID: 28665955
17. Oh CJ, Kim J-Y, Min A-K, Park K-G, Harris RA, Kim H-J, et al. Sulforaphane attenuates hepatic fibrosis via NF-E2-related factor 2-mediated inhibition of transforming growth factor-β/Smad signaling. Free Radic Biol Med. 2012; 52: 671–682. https://doi.org/10.1016/j.freeradbiomed.2011.11.012 PMID: 22155056
18. Artaud-Macari E, Goven D, Brayer S, Hamimi A, Besnard V, Marchal-Somme J, et al. Nuclear factor erythroid 2-related factor 2 nuclear translocation induces myofibroblastic dedifferentiation in idiopathic pulmonary fibrosis. Antioxid Redox Signal. 2013; 18: 66–79. https://doi.org/10.1089/ars.2011.4240 PMID: 22703534
19. Ryoo I, Ha H, Kwak M-K. Inhibitory Role of the KEAP1-NRF2 Pathway in TGFβ1-Stimulated Renal Epi- thelial Transition to Fibroblastic Cells: A Modulatory Effect on SMAD Signaling. PLOS ONE. 2014; 9: e93265. https://doi.org/10.1371/journal.pone.0093265 PMID: 24691097
20. Schnabl B, Purbeck CA, Choi YH, Hagedorn CH, Brenner D. Replicative senescence of activated human hepatic stellate cells is accompanied by a pronounced inflammatory but less fibrogenic pheno- type. Hepatol Baltim Md. 2003; 37: 653–664. https://doi.org/10.1053/jhep.2003.50097 PMID: 12601363
21. Hauck PM, Wolf ER, Olivos DJ, Batuello CN, McElyea KC, McAtarsney CP, et al. Early-Stage Metasta- sis Requires Mdm2 and Not p53 Gain of Function. Mol Cancer Res. 2017; https://doi.org/10.1158/1541- 7786.MCR-17-0174 PMID: 28784612
22. Pennock R, Bray E, Pryor P, James S, McKeegan P, Sturmey R, et al. Human cell dedifferentiation in mesenchymal condensates through controlled autophagy. Sci Rep. 2015; 5: 13113. https://doi.org/10. 1038/srep13113 PMID: 26290392

23. Li H-Y, Ju D, Zhang D-W, Li H, Kong L-M, Guo Y, et al. Activation of TGF-β1-CD147 positive feedback loop in hepatic stellate cells promotes liver fibrosis. Sci Rep. 2015; 5: 16552. https://doi.org/10.1038/ srep16552 PMID: 26559755

24. Bakin AV, Stourman NV, Sekhar KR, Rinehart C, Yan X, Meredith MJ, et al. Smad3–ATF3 signaling mediates TGF-β suppression of genes encoding Phase II detoxifying proteins. Free Radic Biol Med. 2005; 38: 375–387. https://doi.org/10.1016/j.freeradbiomed.2004.10.033 PMID: 15629866

25. Brown SL, Sekhar KR, Rachakonda G, Sasi S, Freeman ML. Activating Transcription Factor 3 Is a Novel Repressor of the Nuclear Factor Erythroid-Derived 2–Related Factor 2 (Nrf2)–Regulated Stress Pathway. Cancer Res. 2008; 68: 364–368. https://doi.org/10.1158/0008-5472.CAN-07-2170 PMID: 18199529

26. Wong L, Yamasaki G, Johnson RJ, Friedman SL. Induction of beta-platelet-derived growth factor recep- tor in rat hepatic lipocytes during cellular activation in vivo and in culture. J Clin Invest. 1994; 94: 1563– 1569. https://doi.org/10.1172/JCI117497 PMID:7929832

27. Rachakonda G, Sekhar KR, Jowhar D, Samson PC, Wikswo JP, Beauchamp RD, et al. Increased Cell Migration and Plasticity in Nrf2 Deficient Cancer Cell Lines. Oncogene. 2010; 29: 3703–3714. https:// doi.org/10.1038/onc.2010.118 PMID: 20440267

28. Chien M-H, Lee W-J, Hsieh F-K, Li C-F, Cheng T-Y, Wang M-Y, et al. Keap1–Nrf2 Interaction Sup- presses Cell Motility in Lung Adenocarcinomas by Targeting the S100P Protein. Clin Cancer Res. 2015; 21: 4719–4732. https://doi.org/10.1158/1078-0432.CCR-14-2880 PMID: 26078391

29. Shen H, Yang Y, Xia S, Rao B, Zhang J, Wang J. Blockage of Nrf2 suppresses the migration and inva- sion of esophageal squamous cell carcinoma cells in hypoxic microenvironment. Dis Esophagus. 2014; 27: 685–692. https://doi.org/10.1111/dote.12124 PMID: 24028437

30. Fan Z, Wirth A-K, Chen D, Wruck CJ, Rauh M, Buchfelder M, et al. Nrf2-Keap1 pathway promotes cell proliferation and diminishes ferroptosis. Oncogenesis. 2017; 6: e371. https://doi.org/10.1038/oncsis. 2017.65 PMID: 28805788

31. Murakami S, Motohashi H. Roles of Nrf2 in cell proliferation and differentiation. Free Radic Biol Med. 2015; 88, Part B: 168–178. https://doi.org/10.1016/j.freeradbiomed.2015.06.030 PMID: 26119783

32. Potteti HR, Tamatam CR, Marreddy R, Reddy NM, Noel S, Rabb H, et al. Nrf2-AKT interactions regu- late heme oxygenase 1 expression in kidney epithelia during hypoxia and hypoxia-reoxygenation. Am J Physiol Renal Physiol. 2016; 311: F1025–F1034. https://doi.org/10.1152/ajprenal.00362.2016 PMID: 27582105

33. Cuadrado A, Mart´ın-Moldes Z, Ye J, Lastres-Becker I. Transcription Factors NRF2 and NF-κB Are Coordinated Effectors of the Rho Family, GTP-binding Protein RAC1 during Inflammation. J Biol Chem. 2014; 289: 15244–15258. https://doi.org/10.1074/jbc.M113.540633 PMID: 24759106

34. Cai CX, Buddha H, Castelino-Prabhu S, Zhang Z, Britton RS, Bacon BR, et al. Activation of Insulin- PI3K/Akt-p70S6K Pathway in Hepatic Stellate Cells Contributes to Fibrosis in Nonalcoholic Steatohepa- titis. Dig Dis Sci. 2017; 62: 968–978. https://doi.org/10.1007/s10620-017-4470-9 PMID: 28194671

35. Wang Y, Jiang X-Y, Liu L, Jiang H-Q. Phosphatidylinositol 3-kinase/Akt pathway regulates hepatic stel- late cell apoptosis. World J Gastroenterol WJG. 2008; 14: 5186–5191. https://doi.org/10.3748/wjg.14. 5186 PMID: 18777595

36. Churchman AT, Anwar AA, Li FYL, Sato H, Ishii T, Mann GE, et al. Transforming growth factor-beta1 elicits Nrf2-mediated antioxidant responses in aortic smooth muscle cells. J Cell Mol Med. 2009; 13: 2282–2292. https://doi.org/10.1111/j.1582-4934.2009.00874.x PMID: 19674192

37. Okita Y, Kamoshida A, Suzuki H, Itoh K, Motohashi H, Igarashi K, et al. Transforming growth factor-β induces transcription factors MafK and Bach1 to suppress expression of the heme oxygenase-1 gene. J Biol Chem. 2013; 288: 20658–20667. https://doi.org/10.1074/jbc.M113.450478 PMID: 23737527

38. Robson CN, Gnanapragasam V, Byrne RL, Collins AT, Neal DE. Transforming growth factor-beta1 up- regulates p15, p21 and p27 and blocks cell cycling in G1 in human prostate epithelium. J Endocrinol. 1999; 160: 257–266. PMID: 9924195

39. Griswold-Prenner I, Kamibayashi C, Maruoka EM, Mumby MC, Derynck R. Physical and Functional Interactions between Type I Transforming Growth Factor β Receptors and Bα, a WD-40 Repeat Subunit of Phosphatase 2A. Mol Cell Biol. 1998; 18: 6595–6604. PMID: 9774674

40. Bataille AM, Manautou JE. Nrf2: a potential target for new therapeutics in liver disease. Clin Pharmacol Ther. 2012; 92: 340–348. https://doi.org/10.1038/clpt.2012.110 PMID: 22871994

41. Lin X, Duan X, Liang Y-Y, Su Y, Wrighton KH, Long J, et al. PPM1A functions as a Smad phosphatase to terminate TGFbeta signaling. Cell. 2006; 125: 915-928. https://doi.org/10.1016/j.cell.2006.03.044 PMID: 16751101

42. Laping NJ, Grygielko E, Mathur A, Butter S, Bomberger J, Tweed C, et al. Inhibition of Transforming Growth Factor (TGF)-β1–Induced Extracellular Matrix with a Novel Inhibitor of the TGF-β Type I Recep- tor Kinase Activity: SB-431542. Mol Pharmacol. 2002; 62: 58–64. https://doi.org/10.1124/mol.62.1.58 PMID: 12065755

43. Inman GJ, Nicolás FJ, Callahan JF, Harling JD, Gaster LM, Reith AD, et al. SB-431542 Is a Potent and Specific Inhibitor of Transforming Growth Factor-β Superfamily Type I Activin Receptor-Like Kinase (ALK) Receptors ALK4, ALK5, and ALK7. Mol Pharmacol. 2002; 62: 65–74. https://doi.org/10.1124/ mol.62.1.65 PMID: 12065756

44. Grygielko ET, Martin WM, Tweed C, Thornton P, Harling J, Brooks DP, et al. Inhibition of gene markers of fibrosis with a novel inhibitor of transforming growth factor-beta type I receptor kinase in puromycin- induced nephritis. J Pharmacol Exp Ther. 2005; 313: 943–951. https://doi.org/10.1124/jpet.104.082099 PMID: 15769863

4.4 Conclusion

In this chapter, a deep characterization of HSC activation has been presented. Particularly, the first paper (Prestigiacomo et al., under review 2018) aimed to elucidate the role of PDGF and TGF-β1 on HSC activation. Both primary and hTERT-HSC were characterized in terms of their activation, proliferative and migratory capacities. Upon exposure to TGF-β1, HSCs transdifferentiated into myofibroblasts-like cells, showing strong production of αSMA and increase expression of Lox genes, collagens, and other ECM components (such as fibronectin and MMP2). A successful inhibition of this fibrogenic effect of TGF-β1 was achieved by using Smad inhibitors (SB431542 hydrate and SB525334), confirming the role of TGF-β1/Smad pathway on HSC activation. The data show that similar mechanisms are valid *in vitro* in primary HSCs as well as in hTERT-HSCs. TGF-β1 also significantly decreased the proliferation rate of hTERT-HSC in a concentration-dependent manner, suggesting an involvement of Non-Smad pathways in the regulation of HSC proliferation as previously reported for epithelial cells [133]. In contrast, PDGF-treatment induced proliferation and cell migration in a concentration-dependent manner without eliciting activation and fibrogenesis. Simultaneous exposure of HSCs to both compounds showed a synergistic effect leading to a myofibroblasts-like phenotype of activated HSC, which show increase in αSMA amount, ECM deposition, and migration. Furthermore, these data show that hTERT-HSC react likewise primary HSC, identifying them as a well-suited surrogated of primary HSCs for activation studies *in vitro*. This study elucidates the effect of these two relevant cytokines on key aspects that characterize HSC activation, making clear that both factors are essential to achieve a fully activated phenotype *in vitro*.

The second and main study carried out on this chapter (Prestigiacomo V and Suter-Dick L, PLoS ONE 2018) describes a novel and crucial role of Nrf2 in HSCs. Nrf2 was found to be highly expressed in quiescent HSCs, where it may contribute to the maintaining of a repressed phenotype. Nrf2 stabilization, achieved by means of Keap1 knockdown, significantly reduced the TGF-β1-induced αSMA production, suggesting a protective role of Nrf2 against HSC activation. Consistently, Nrf2 knockdown induced HSC activation in both primary and immortalised HSCs, as shown by the increase in αSMA production as well as the induction of gene expression of ECM components (collagens and fibronectin). Hence, Nrf2 is shown not only to act as a protective molecule against ROS but also as a repressive factor for HSC activation. In addition, the Nrf2 knockdown-induced HSC activation indicated an involvement of the TGF-β1/Smad pathway. In particular, we observed that Nrf2 depletion induced TGF-β1 release and Smad-dependent HSC activation, as suggested by the successful inhibition with Smad inhibitors (SB431542 hydrate and SB525334). Moreover, Nrf2 knockdown exacerbated the TGF-β1-induced activation as indicated by the stronger gene induction of fibrotic and activation markers. These data led to the identification of

Nrf2 as a “safeguard” of HSCs, and its depletion may be a contributing factor to HSC activation and fibrosis progression.

5. Scientific impact, limitations and future perspectives of current research

The research carried out during this thesis addressed some limiting factors, which are faced when attempting to study liver fibrotic diseases. These limitations include the lack of a suitable 3D model as well as the scarcity of therapeutic intervention able to revert HSC activation and restore liver homeostasis during fibrosis. Therefore, the aim of the first two studies was the development of a rat primary cell-based and a human cell line-based liver model. While the other two studies aimed at elucidating the molecular mechanisms behind HSC activation, focusing in particular on the interplay of PDGF and TGF-β1 and on the potential role of Nrf2. The 3D model systems developed in these studies were able to recapitulate the cellular events leading to fibrosis: hepatocellular injury, antioxidant defence response, activation of Kupffer cells and activation of HSC leading to deposition of ECM. The rat model generated included the three relevant cell types involved in fibrosis and was able to elicit a fibrotic phenotype after exposure to TGF-β1. Moreover, the human cell line-based model showed the ability to physiologically respond to pro-fibrotic drugs, indicating this system as a suitable model to study liver injury disease induced by clinically relevant compounds. The cell line-based model also represents a suited alternative to human primary cell-based models, due to the stability and easy handling of cell lines compared to primary cells. However, although these models hold a large amount of potential, an analogous model with human primary cells may be required to corroborate the data obtained. Moreover, the lack of LSEC represent another key limitation of these models. Although the LSECs are not the primary effectors of liver fibrosis, there is growing evidence that they play modulatory effects. Future developments to further improve and validate the system should aim at including LSECs, as well as at testing other liver toxicants (e.g. acetaminophen, bile acids or lipid overloading) and/or at using a microfluidic design that may give an additional increment to the reliability of the model. Thereafter, the system may be used for the detection of potential pro-fibrotic compounds and for replacing used animal models. It may also allow testing of anti-fibrotic compounds in a physiological relevant *in vitro* system, providing researchers a novel tool to study inhibition of fibrosis progression.

In addition to the development of a suitable *in vitro* model, this thesis also addressed specific mechanisms involved in the activation of HSCs. In particular, we aimed to further characterize HSC activation following exposure to PDGF and TGF-β1. Our data confirmed the involvement of these cytokines in the activation of HSCs and provided additional evidence supporting the hypothesis that both signals act synergistically during HSCs activation. The results also indicated that both cytokines are required in order to elicit a complete activated phenotype in HSCs. Mechanistic *in vivo* and *in vitro* studies are required to better understand the potential interconnection between these two pathways. Future research should include studies with inhibitors of the PDGF pathway that may be useful to characterize the cascade of events occurring after PDGF signalling. Furthermore, the results presented on both human primary and immortalised HSCs point out

the hTERT-HSC as a reliable cell line to further investigate these pathways, and represents a more accessible model than primary HSCs.

Both primary and hTERT-HSCs were also utilized to investigate the role of Nrf2 in HSC activation. The most exciting result of this research was the identification of Nrf2 as a crucial protective factor against HSC activation. We could show that Nrf2 inhibits HSC activation acting through the inhibition of the TGF-β1/Smad pathway. Additional studies are required to evaluate its potential interference with Non-Smad pathway as well as PDGF regulation pathway. Nevertheless, our data suggest that an intervention on Nrf2 pathway in HSC may be a new therapeutic approach for the prevention and/or reduction of HSC activation. An additional line of investigation that might be pursued in light of our results is the study of the involvement of Nrf2 in fibrosis using the multicellular, 3D culture model. Nrf2 has already been shown to promote liver regeneration and hepatocyte growth [78,79], so together with the data obtained in the current research, a strategy aiming to Nrf2 induction and/or stabilization may result in a safer and effective therapy to heal fibrotic diseases.

In conclusion, the studies presented in this thesis provide encouraging data that may contribute to the design and the identification of novel therapeutic approach for liver fibrosis. The 3D liver models here generated may give a pulse to study fibrosis development and to test novel drugs, in order to consolidate *in vivo* data in an inexpensive and productive way. Furthermore, the newly found role of the Nrf2 defence pathway in HSCs, together with the well-known role it plays in hepatocytes, may boost the research on liver towards a therapeutic strategy based on the stimulation and/or stabilization of Nrf2.

6. Acknowledgements

My immeasurable appreciation and deepest gratitude for the help and support go to the following persons who in one way or another have contributed in enriching me scientifically and personally during my PhD studies.

I owe my deepest gratitude to my professor and supervisor at the Fachhochschule Nordwestschweiz Prof. Dr. Laura Suter-Dick for the continuous support and motivating words during the time I conducted my Master and PhD thesis in her laboratory. She trusted me and let me grow with my own head, leading me, with her contagious enthusiasm, to achieve all the set goals during this research. I also thank her for supervising my thesis and giving me the opportunity to present my work in many scientific events, which led to interesting scientific exchanges and experiences for my career.

I would like to thank my faculty representative at the University of Basel Prof. Dr. Alex Odermatt and my co-referee from the University of Liverpool Prof. Dr. Christopher Goldring for their stimulating discussions and for their critical evaluation of my work.

I would like to thank all past and present members of my research group for their support, for maintaining an enjoyable work atmosphere and for being more than colleagues. Particularly, I would like to thank Anna Weston, Franziska Lampart and Chiara Bongiovanni for contributing to some of my research. Special thanks to Catherine Pilling for her support and advice during my last period of work as well as for having critically read parts of this thesis.

I would also like to thank Dr. Jens M. Kelm and Dr. Simon Messner from InSphero for their fruitful advice and for kindly providing the plates used for the first part of the research. Thanks to Dr. Franziska Boess from Roche and to Prof. Dr. Bernd Schnabl from UC San Diego for kindly providing the rat cells and hTERT-HSC used in this research.

Thank also to the Fachhochschule Nordwestschweiz, the Swiss Centre for Applied Human Toxicology and the Swiss Commission for Toxicology and Innovation for their financial support during this research.

I would like to thank all my family for the incommensurable support during all my endeavours. In particular, I am deeply grateful to my wife Rosy for always believing in me and for standing by me in my life. She has always been there with her love encouraging me during the most challenging times. I cannot thank her enough.

Finally yet importantly, I thank my friends and all the other people that have believed in me during all my studies.

Thank you.

7. References

1. Iredale JP. Models of liver fibrosis: exploring the dynamic nature of inflammation and repair in a solid organ. J Clin Invest. 2007;117: 539–548. doi:10.1172/JCI30542

2. Zhang C-Y, Yuan W-G, He P, Lei J-H, Wang C-X. Liver fibrosis and hepatic stellate cells: Etiology, pathological hallmarks and therapeutic targets. World J Gastroenterol. 2016;22: 10512–10522. doi:10.3748/wjg.v22.i48.10512

3. Malik R, Selden C, Hodgson H. The role of non-parenchymal cells in liver growth. Semin Cell Dev Biol. 2002;13: 425–431. doi:10.1016/S1084952102001301

4. Svegliati-Baroni G, De Minicis S, Marzioni M. Hepatic fibrogenesis in response to chronic liver injury: novel insights on the role of cell-to-cell interaction and transition. Liver Int Off J Int Assoc Study Liver. 2008;28: 1052–1064. doi:10.1111/j.1478-3231.2008.01825.x

5. Safadi R, Friedman SL. Hepatic fibrosis--role of hepatic stellate cell activation. MedGenMed Medscape Gen Med. 2002;4: 27.

6. Bataller R, Brenner DA. Liver fibrosis. J Clin Invest. 2005;115: 209–218. doi:10.1172/JCI24282

7. Evon DM, Amador J, Stewart P, Reeve BB, Lok AS, Sterling RK, et al. Psychometric properties of the PROMIS short form measures in a U.S. cohort of 961 patients with chronic hepatitis C prescribed direct acting antiviral therapy. Aliment Pharmacol Ther. : n/a-n/a. doi:10.1111/apt.14531

8. Friedman SL. Liver fibrosis – from bench to bedside. J Hepatol. 2003;38: 38–53. doi:10.1016/S0168-8278(02)00429-4

9. Ismail MH, Pinzani M. Reversal of Liver Fibrosis. Saudi J Gastroenterol Off J Saudi Gastroenterol Assoc. 2009;15: 72–79. doi:10.4103/1319-3767.45072

10. Mokdad AA, Lopez AD, Shahraz S, Lozano R, Mokdad AH, Stanaway J, et al. Liver cirrhosis mortality in 187 countries between 1980 and 2010: a systematic analysis. BMC Med. 2014;12. doi:10.1186/s12916-014-0145-y

11. Mallat A, Lotersztajn S. Cellular mechanisms of tissue fibrosis. 5. Novel insights into liver fibrosis. Am J Physiol Cell Physiol. 2013;305: C789-799. doi:10.1152/ajpcell.00230.2013

12. Eom YW, Kim G, Baik SK. Mesenchymal stem cell therapy for cirrhosis: Present and future perspectives. World J Gastroenterol WJG. 2015;21: 10253–10261. doi:10.3748/wjg.v21.i36.10253

13. Fallowfield JA, Iredale JP. Targeted treatments for cirrhosis. Expert Opin Ther Targets. 2004;8: 423–435. doi:10.1517/14728222.8.5.423

14. Godoy P, Hewitt NJ, Albrecht U, Andersen ME, Ansari N, Bhattacharya S, et al. Recent advances in 2D and 3D in vitro systems using primary hepatocytes, alternative hepatocyte sources and non-parenchymal liver cells and their use in investigating mechanisms of hepatotoxicity, cell signaling and ADME. Arch Toxicol. 2013;87: 1315–1530. doi:10.1007/s00204-013-1078-5

15. Mescher AL. Junqueira's Basic Histology: Text & Atlas. New York: McGraw Hill; 2010.

16. Kmieć Z. Cooperation of liver cells in health and disease. Adv Anat Embryol Cell Biol. 2001;161: III–XIII, 1-151.

17. Braet F, Wisse E. Structural and functional aspects of liver sinusoidal endothelial cell fenestrae: a review. Comp Hepatol. 2002;1: 1. doi:10.1186/1476-5926-1-1

18. Adams DH, Eksteen B. Aberrant homing of mucosal T cells and extra-intestinal manifestations of inflammatory bowel disease. Nat Rev Immunol. 2006;6: 244–251. doi:10.1038/nri1784

19. Poonkhum R, Showpittapornchai U, Pradidarcheep W. Collagen arrangement in space of Disse correlates with fluid flow in normal and cirrhotic rat livers. Microsc Res Tech. 2015;78: 187–193. doi:10.1002/jemt.22460

20. Schuppan D, Ruehl M, Somasundaram R, Hahn EG. Matrix as a modulator of hepatic fibrogenesis. Semin Liver Dis. 2001;21: 351–372. doi:10.1055/s-2001-17556

21. Friedman SL. Molecular regulation of hepatic fibrosis, an integrated cellular response to tissue injury. J Biol Chem. 2000;275: 2247–2250.

22. Friedman SL. Hepatic stellate cells: protean, multifunctional, and enigmatic cells of the liver. Physiol Rev. 2008;88: 125–172. doi:10.1152/physrev.00013.2007

23. Lee UE, Friedman SL. Mechanisms of Hepatic Fibrogenesis. Best Pract Res Clin Gastroenterol. 2011;25: 195–206. doi:10.1016/j.bpg.2011.02.005

24. Weiskirchen R, Tacke F. Cellular and molecular functions of hepatic stellate cells in inflammatory responses and liver immunology. Hepatobiliary Surg Nutr. 2014;3: 344–363. doi:10.3978/j.issn.2304-3881.2014.11.03

25. Marra F. Hepatic stellate cells and the regulation of liver inflammation. J Hepatol. 1999;31: 1120–1130.

26. Canbay A, Taimr P, Torok N, Higuchi H, Friedman S, Gores GJ. Apoptotic body engulfment by a human stellate cell line is profibrogenic. Lab Investig J Tech Methods Pathol. 2003;83: 655–663.

27. Gressner AM. Cytokines and cellular crosstalk involved in the activation of fat-storing cells. J Hepatol. 1995;22: 28–36.

28. Yu Q, Stamenkovic I. Cell surface-localized matrix metalloproteinase-9 proteolytically activates TGF-beta and promotes tumor invasion and angiogenesis. Genes Dev. 2000;14: 163–176.

29. Rockey DC, Friedman SL. Chapter 6 - Hepatic Fibrosis and Cirrhosis. In: by E, Boyer TD, Wright TL, Manns MP, Editor C, Zakim D, editors. Zakim and Boyer's Hepatology (Fifth Edition). Edinburgh: W.B. Saunders; 2006. pp. 87–109. doi:10.1016/B978-1-4160-3258-8.50011-5

30. Holt AP, Salmon M, Buckley CD, Adams DH. Immune interactions in hepatic fibrosis. or "Leucocyte-stromal interactions in hepatic fibrosis." Clin Liver Dis. 2008;12: 861–x. doi:10.1016/j.cld.2008.07.002

31. Li H-Y, Ju D, Zhang D-W, Li H, Kong L-M, Guo Y, et al. Activation of TGF-β1-CD147 positive feedback loop in hepatic stellate cells promotes liver fibrosis. Sci Rep. 2015;5: 16552. doi:10.1038/srep16552

32. Robert S, Gicquel T, Bodin A, Lagente V, Boichot E. Characterization of the MMP/TIMP Imbalance and Collagen Production Induced by IL-1β or TNF-α Release from Human Hepatic Stellate Cells. PLoS ONE. 2016;11. doi:10.1371/journal.pone.0153118

33. Liu Y, Wen XM, Lui ELH, Friedman SL, Cui W, Ho NPS, et al. Therapeutic targeting of the PDGF and TGF-beta-signaling pathways in hepatic stellate cells by PTK787/ZK22258. Lab Investig J Tech Methods Pathol. 2009;89: 1152–1160. doi:10.1038/labinvest.2009.77

34. Liu C, Li J, Xiang X, Guo L, Tu K, Liu Q, et al. PDGF receptor-α promotes TGF-β signaling in hepatic stellate cells via transcriptional and posttranscriptional regulation of TGF-β receptors. Am J Physiol - Gastrointest Liver Physiol. 2014;307: G749–G759. doi:10.1152/ajpgi.00138.2014

35. Marra F. Chemokines in liver inflammation and fibrosis. Front Biosci J Virtual Libr. 2002;7: d1899-1914.

36. Iizuka M, Murata T, Hori M, Ozaki H. Increased contractility of hepatic stellate cells in cirrhosis is mediated by enhanced Ca2+-dependent and Ca2+-sensitization pathways. Am J Physiol Gastrointest Liver Physiol. 2011;300: G1010-1021. doi:10.1152/ajpgi.00350.2010

37. Elpek GÖ. Cellular and molecular mechanisms in the pathogenesis of liver fibrosis: An update. World J Gastroenterol. 2014;20: 7260–7276. doi:10.3748/wjg.v20.i23.7260

38. Gressner AM, Weiskirchen R, Breitkopf K, Dooley S. Roles of TGF-beta in hepatic fibrosis. Front Biosci J Virtual Libr. 2002;7: d793-807.

39. Poli G. Pathogenesis of liver fibrosis: role of oxidative stress. Mol Aspects Med. 2000;21: 49–98. doi:10.1016/S0098-2997(00)00004-2

40. Lee J, Giordano S, Zhang J. Autophagy, mitochondria and oxidative stress: cross-talk and redox signalling. Biochem J. 2012;441: 523–540. doi:10.1042/BJ20111451

41. Cichoż-Lach H, Michalak A. Oxidative stress as a crucial factor in liver diseases. World J Gastroenterol WJG. 2014;20: 8082–8091. doi:10.3748/wjg.v20.i25.8082

42. Ghatak S, Biswas A, Dhali GK, Chowdhury A, Boyer JL, Santra A. Oxidative stress and hepatic stellate cell activation are key events in arsenic induced liver fibrosis in mice. Toxicol Appl Pharmacol. 2011;251: 59–69. doi:10.1016/j.taap.2010.11.016

43. Svegliati-Baroni G, Ridolfi F, Di Sario A, Saccomanno S, Bendia E, Benedetti A, et al. Intracellular signaling pathways involved in acetaldehyde-induced collagen and fibronectin gene expression in human hepatic stellate cells. Hepatology. 2001;33: 1130–1140. doi:10.1053/jhep.2001.23788

44. Ambade A, Mandrekar P. Oxidative stress and inflammation: essential partners in alcoholic liver disease. Int J Hepatol. 2012;2012: 853175. doi:10.1155/2012/853175

45. Bouchard G, Yousef IM, Barriault C, Tuchweber B. Role of glutathione and oxidative stress in phalloidin-induced cholestasis. J Hepatol. 2000;32: 550–560.

46. Mormone E, Lu Y, Ge X, Fiel MI, Nieto N. Fibromodulin, an oxidative stress-sensitive proteoglycan, regulates the fibrogenic response to liver injury in mice. Gastroenterology. 2012;142: 612–621.e5. doi:10.1053/j.gastro.2011.11.029

47. Yang J-J, Tao H, Hu W, Liu L-P, Shi K-H, Deng Z-Y, et al. MicroRNA-200a controls Nrf2 activation by target Keap1 in hepatic stellate cell proliferation and fibrosis. Cell Signal. 2014;26: 2381–2389. doi:10.1016/j.cellsig.2014.07.016

48. Nieto N. Ethanol and fish oil induce NFkappaB transactivation of the collagen alpha2(I) promoter through lipid peroxidation-driven activation of the PKC-PI3K-Akt pathway. Hepatol Baltim Md. 2007;45: 1433–1445. doi:10.1002/hep.21659

49. Nieto N, Friedman SL, Cederbaum AI. Stimulation and proliferation of primary rat hepatic stellate cells by cytochrome P450 2E1-derived reactive oxygen species. Hepatol Baltim Md. 2002;35: 62–73. doi:10.1053/jhep.2002.30362

50. Edeas M, Attaf D, Mailfert A-S, Nasu M, Joubet R. Maillard reaction, mitochondria and oxidative stress: potential role of antioxidants. Pathol Biol (Paris). 2010;58: 220–225. doi:10.1016/j.patbio.2009.09.011

51. Majima HJ, Indo HP, Suenaga S, Matsui H, Yen H-C, Ozawa T. Mitochondria as possible pharmaceutical targets for the effects of vitamin E and its homologues in oxidative stress-related diseases. Curr Pharm Des. 2011;17: 2190–2195.

52. Mao G, Kraus GA, Kim I, Spurlock ME, Bailey TB, Beitz DC. Effect of a mitochondria-targeted vitamin E derivative on mitochondrial alteration and systemic oxidative stress in mice. Br J Nutr. 2011;106: 87–95. doi:10.1017/S0007114510005830

53. Nguyen T, Nioi P, Pickett CB. The Nrf2-antioxidant response element signaling pathway and its activation by oxidative stress. J Biol Chem. 2009;284: 13291–13295. doi:10.1074/jbc.R900010200

54. Taguchi K, Motohashi H, Yamamoto M. Molecular mechanisms of the Keap1–Nrf2 pathway in stress response and cancer evolution. Genes Cells Devoted Mol Cell Mech. 2011;16: 123–140. doi:10.1111/j.1365-2443.2010.01473.x

55. Pall ML, Levine S. Nrf2, a master regulator of detoxification and also antioxidant, anti-inflammatory and other cytoprotective mechanisms, is raised by health promoting factors. Sheng Li Xue Bao. 2015;67: 1–18.

56. Zou Y, Lee J, Nambiar SM, Hu M, Rui W, Bao Q, et al. Nrf2 Is Involved in Maintaining Hepatocyte Identity during Liver Regeneration. PLoS ONE. 2014;9. doi:10.1371/journal.pone.0107423

57. Lee J-M, Li J, Johnson DA, Stein TD, Kraft AD, Calkins MJ, et al. Nrf2, a multi-organ protector? FASEB J Off Publ Fed Am Soc Exp Biol. 2005;19: 1061–1066. doi:10.1096/fj.04-2591hyp

58. Padmanabhan B, Tong KI, Ohta T, Nakamura Y, Scharlock M, Ohtsuji M, et al. Structural basis for defects of Keap1 activity provoked by its point mutations in lung cancer. Mol Cell. 2006;21: 689–700. doi:10.1016/j.molcel.2006.01.013

59. Nioi P, Nguyen T. A mutation of Keap1 found in breast cancer impairs its ability to repress Nrf2 activity. Biochem Biophys Res Commun. 2007;362: 816–821. doi:10.1016/j.bbrc.2007.08.051

60. Hendrix ND, Wu R, Kuick R, Schwartz DR, Fearon ER, Cho KR. Fibroblast growth factor 9 has oncogenic activity and is a downstream target of Wnt signaling in ovarian endometrioid adenocarcinomas. Cancer Res. 2006;66: 1354–1362. doi:10.1158/0008-5472.CAN-05-3694

61. Chen X, Cheung ST, So S, Fan ST, Barry C, Higgins J, et al. Gene expression patterns in human liver cancers. Mol Biol Cell. 2002;13: 1929–1939. doi:10.1091/mbc.02-02-0023.

62. Wurmbach E, Chen Y, Khitrov G, Zhang W, Roayaie S, Schwartz M, et al. Genome-wide molecular profiles of HCV-induced dysplasia and hepatocellular carcinoma. Hepatol Baltim Md. 2007;45: 938–947. doi:10.1002/hep.21622

63. Venugopal R, Jaiswal AK. Nrf2 and Nrf1 in association with Jun proteins regulate antioxidant response element-mediated expression and coordinated induction of genes encoding detoxifying enzymes. Oncogene. 1998;17: 3145–3156. doi:10.1038/sj.onc.1202237

64. Venugopal R, Jaiswal AK. Nrf1 and Nrf2 positively and c-Fos and Fra1 negatively regulate the human antioxidant response element-mediated expression of NAD(P)H:quinone oxidoreductase1 gene. Proc Natl Acad Sci U S A. 1996;93: 14960–14965.

65. Chien M-H, Lee W-J, Hsieh F-K, Li C-F, Cheng T-Y, Wang M-Y, et al. Keap1–Nrf2 Interaction Suppresses Cell Motility in Lung Adenocarcinomas by Targeting the S100P Protein. Clin Cancer Res. 2015;21: 4719–4732. doi:10.1158/1078-0432.CCR-14-2880

66. Ramos-Gomez M, Kwak MK, Dolan PM, Itoh K, Yamamoto M, Talalay P, et al. Sensitivity to carcinogenesis is increased and chemoprotective efficacy of enzyme inducers is lost in nrf2 transcription factor-deficient mice. Proc Natl Acad Sci U S A. 2001;98: 3410–3415. doi:10.1073/pnas.051618798

67. Xu C, Huang M-T, Shen G, Yuan X, Lin W, Khor TO, et al. Inhibition of 7,12-dimethylbenz(a)anthracene-induced skin tumorigenesis in C57BL/6 mice by sulforaphane is mediated by nuclear factor E2-related factor 2. Cancer Res. 2006;66: 8293–8296. doi:10.1158/0008-5472.CAN-06-0300

68. Khor TO, Huang M-T, Prawan A, Liu Y, Hao X, Yu S, et al. Increased susceptibility of Nrf2 knockout mice to colitis-associated colorectal cancer. Cancer Prev Res Phila Pa. 2008;1: 187–191. doi:10.1158/1940-6207.CAPR-08-0028

69. Coulouarn C, Factor VM, Thorgeirsson SS. Transforming growth factor-beta gene expression signature in mouse hepatocytes predicts clinical outcome in human cancer. Hepatol Baltim Md. 2008;47: 2059–2067. doi:10.1002/hep.22283

70. Shin SM, Yang JH, Ki SH. Role of the Nrf2-ARE Pathway in Liver Diseases. Oxid Med Cell Longev. 2013;2013. doi:10.1155/2013/763257

71. Chan K, Han XD, Kan YW. An important function of Nrf2 in combating oxidative stress: detoxification of acetaminophen. Proc Natl Acad Sci U S A. 2001;98: 4611–4616. doi:10.1073/pnas.081082098

72. Enomoto A, Itoh K, Nagayoshi E, Haruta J, Kimura T, O'Connor T, et al. High sensitivity of Nrf2 knockout mice to acetaminophen hepatotoxicity associated with decreased expression of ARE-regulated drug metabolizing enzymes and antioxidant genes. Toxicol Sci Off J Soc Toxicol. 2001;59: 169–177.

73. Okawa H, Motohashi H, Kobayashi A, Aburatani H, Kensler TW, Yamamoto M. Hepatocyte-specific deletion of the keap1 gene activates Nrf2 and confers potent resistance against acute drug toxicity. Biochem Biophys Res Commun. 2006;339: 79–88. doi:10.1016/j.bbrc.2005.10.185

74. Goldring CEP, Kitteringham NR, Elsby R, Randle LE, Clement YN, Williams DP, et al. Activation of hepatic Nrf2 in vivo by acetaminophen in CD-1 mice. Hepatol Baltim Md. 2004;39: 1267–1276. doi:10.1002/hep.20183

75. Xu W, Hellerbrand C, Köhler UA, Bugnon P, Kan Y-W, Werner S, et al. The Nrf2 transcription factor protects from toxin-induced liver injury and fibrosis. Lab Investig J Tech Methods Pathol. 2008;88: 1068–1078. doi:10.1038/labinvest.2008.75

76. Lamlé J, Marhenke S, Borlak J, von Wasielewski R, Eriksson CJP, Geffers R, et al. Nuclear factor-eythroid 2-related factor 2 prevents alcohol-induced fulminant liver injury. Gastroenterology. 2008;134: 1159–1168. doi:10.1053/j.gastro.2008.01.011

77. Sison-Young RLC, Mitsa D, Jenkins RE, Mottram D, Alexandre E, Richert L, et al. Comparative Proteomic Characterization of 4 Human Liver-Derived Single Cell Culture Models Reveals Significant Variation in the Capacity for Drug Disposition, Bioactivation, and Detoxication. Toxicol Sci Off J Soc Toxicol. 2015;147: 412–424. doi:10.1093/toxsci/kfv136

78. Beyer TA, Xu W, Teupser D, auf dem Keller U, Bugnon P, Hildt E, et al. Impaired liver regeneration in Nrf2 knockout mice: role of ROS-mediated insulin/IGF-1 resistance. EMBO J. 2008;27: 212–223. doi:10.1038/sj.emboj.7601950

79. Wakabayashi N, Shin S, Slocum SL, Agoston ES, Wakabayashi J, Kwak M-K, et al. Regulation of notch1 signaling by nrf2: implications for tissue regeneration. Sci Signal. 2010;3: ra52. doi:10.1126/scisignal.2000762

80. Zou Y, Hu M, Lee J, Nambiar SM, Garcia V, Bao Q, et al. Nrf2 is essential for timely M phase entry of replicating hepatocytes during liver regeneration. Am J Physiol-Gastrointest Liver Physiol. 2014;308: G262–G268. doi:10.1152/ajpgi.00332.2014

81. Oh CJ, Kim J-Y, Min A-K, Park K-G, Harris RA, Kim H-J, et al. Sulforaphane attenuates hepatic fibrosis via NF-E2-related factor 2-mediated inhibition of transforming growth factor-β/Smad signaling. Free Radic Biol Med. 2012;52: 671–682. doi:10.1016/j.freeradbiomed.2011.11.012

82. Artaud-Macari E, Goven D, Brayer S, Hamimi A, Besnard V, Marchal-Somme J, et al. Nuclear factor erythroid 2-related factor 2 nuclear translocation induces myofibroblastic dedifferentiation in idiopathic pulmonary fibrosis. Antioxid Redox Signal. 2013;18: 66–79. doi:10.1089/ars.2011.4240

83. Ryoo I, Ha H, Kwak M-K. Inhibitory Role of the KEAP1-NRF2 Pathway in TGFβ1-Stimulated Renal Epithelial Transition to Fibroblastic Cells: A Modulatory Effect on SMAD Signaling. PLOS ONE. 2014;9: e93265. doi:10.1371/journal.pone.0093265

84. Rachakonda G, Sekhar KR, Jowhar D, Samson PC, Wikswo JP, Beauchamp RD, et al. Increased Cell Migration and Plasticity in Nrf2 Deficient Cancer Cell Lines. Oncogene. 2010;29: 3703–3714. doi:10.1038/onc.2010.118

85. Marques TG, Chaib E, da Fonseca JH, Lourenço ACR, Silva FD, Ribeiro MAF, et al. Review of experimental models for inducing hepatic cirrhosis by bile duct ligation and carbon tetrachloride injection. Acta Cir Bras. 2012;27: 589–594.

86. Suk KT, Kim DJ. Staging of liver fibrosis or cirrhosis: The role of hepatic venous pressure gradient measurement. World J Hepatol. 2015;7: 607–615. doi:10.4254/wjh.v7.i3.607

87. Edmondson R, Broglie JJ, Adcock AF, Yang L. Three-dimensional cell culture systems and their applications in drug discovery and cell-based biosensors. Assay Drug Dev Technol. 2014;12: 207–218. doi:10.1089/adt.2014.573

88. Messner S, Agarkova I, Moritz W, Kelm JM. Multi-cell type human liver microtissues for hepatotoxicity testing. Arch Toxicol. 2013;87: 209–213. doi:10.1007/s00204-012-0968-2

89. Sato M, Kojima N, Miura M, Imai K, Senoo H. Induction of cellular processes containing collagenase and retinoid by integrin-binding to interstitial collagen in hepatic stellate cell culture. Cell Biol Int. 1998;22: 115–125. doi:10.1006/cbir.1998.0234

90. Kawada N, Seki S, Inoue M, Kuroki T. Effect of antioxidants, resveratrol, quercetin, and N-acetylcysteine, on the functions of cultured rat hepatic stellate cells and Kupffer cells. Hepatol Baltim Md. 1998;27: 1265–1274. doi:10.1002/hep.510270512

91. van Grunsven LA. 3D in vitro models of liver fibrosis. Adv Drug Deliv Rev. 2017;121: 133–146. doi:10.1016/j.addr.2017.07.004

92. Kostadinova R, Boess F, Applegate D, Suter L, Weiser T, Singer T, et al. A long-term three dimensional liver co-culture system for improved prediction of clinically relevant drug-induced hepatotoxicity. Toxicol Appl Pharmacol. 2013;268: 1–16. doi:10.1016/j.taap.2013.01.012

93. Lauschke VM, Hendriks DFG, Bell CC, Andersson TB, Ingelman-Sundberg M. Novel 3D Culture Systems for Studies of Human Liver Function and Assessments of the Hepatotoxicity of Drugs and Drug Candidates. Chem Res Toxicol. 2016;29: 1936–1955. doi:10.1021/acs.chemrestox.6b00150

94. Landry J, Bernier D, Ouellet C, Goyette R, Marceau N. Spheroidal aggregate culture of rat liver cells: histotypic reorganization, biomatrix deposition, and maintenance of functional activities. J Cell Biol. 1985;101: 914–923.

95. Abu-Absi SF, Friend JR, Hansen LK, Hu W-S. Structural polarity and functional bile canaliculi in rat hepatocyte spheroids. Exp Cell Res. 2002;274: 56–67. doi:10.1006/excr.2001.5467

96. Bell CC, Hendriks DFG, Moro SML, Ellis E, Walsh J, Renblom A, et al. Characterization of primary human hepatocyte spheroids as a model system for drug-induced liver injury, liver function and disease. Sci Rep. 2016;6: 25187. doi:10.1038/srep25187

97. Friedman SL, Rockey DC, McGuire RF, Maher JJ, Boyles JK, Yamasaki G. Isolated hepatic lipocytes and Kupffer cells from normal human liver: morphological and functional characteristics in primary culture. Hepatol Baltim Md. 1992;15: 234–243.

98. Feaver RE, Cole BK, Lawson MJ, Hoang SA, Marukian S, Blackman BR, et al. Development of an in vitro human liver system for interrogating nonalcoholic steatohepatitis. JCI Insight. 2016;1: e90954. doi:10.1172/jci.insight.90954

99. Leite SB, Roosens T, El Taghdouini A, Mannaerts I, Smout AJ, Najimi M, et al. Novel human hepatic organoid model enables testing of drug-induced liver fibrosis in vitro. Biomaterials. 2016;78: 1–10. doi:10.1016/j.biomaterials.2015.11.026

100. Marra F, Choudhury GG, Pinzani M, Abboud HE. Regulation of platelet-derived growth factor secretion and gene expression in human liver fat-storing cells. Gastroenterology. 1994;107: 1110–1117.

101. Kikuchi A, Monga SP. PDGFRα in liver pathophysiology: emerging roles in development, regeneration, fibrosis, and cancer. Gene Expr. 2015;16: 109–127. doi:10.3727/105221615X14181438356210

102. Fredriksson L, Li H, Eriksson U. The PDGF family: four gene products form five dimeric isoforms. Cytokine Growth Factor Rev. 2004;15: 197–204. doi:10.1016/j.cytogfr.2004.03.007

103. Ostman A, Thyberg J, Westermark B, Heldin CH. PDGF-AA and PDGF-BB biosynthesis: proprotein processing in the Golgi complex and lysosomal degradation of PDGF-BB retained intracellularly. J Cell Biol. 1992;118: 509–519.

104. Li X, Pontén A, Aase K, Karlsson L, Abramsson A, Uutela M, et al. PDGF-C is a new protease-activated ligand for the PDGF alpha-receptor. Nat Cell Biol. 2000;2: 302–309. doi:10.1038/35010579

105. Bergsten E, Uutela M, Li X, Pietras K, Ostman A, Heldin CH, et al. PDGF-D is a specific, protease-activated ligand for the PDGF beta-receptor. Nat Cell Biol. 2001;3: 512–516. doi:10.1038/35074588

106. Heldin C-H. Targeting the PDGF signaling pathway in tumor treatment. Cell Commun Signal CCS. 2013;11: 97. doi:10.1186/1478-811X-11-97

107. Wong L, Yamasaki G, Johnson RJ, Friedman SL. Induction of beta-platelet-derived growth factor receptor in rat hepatic lipocytes during cellular activation in vivo and in culture. J Clin Invest. 1994;94: 1563–1569.

108. Kocabayoglu P, Lade A, Lee YA, Dragomir A-C, Sun X, Fiel MI, et al. β-PDGF receptor expressed by hepatic stellate cells regulates fibrosis in murine liver injury, but not carcinogenesis. J Hepatol. 2015;63: 141–147. doi:10.1016/j.jhep.2015.01.036

109. Yan X, Liu Z, Chen Y. Regulation of TGF-beta signaling by Smad7. Acta Biochim Biophys Sin. 2009;41: 263–272.

110. Khalil N. TGF-beta: from latent to active. Microbes Infect. 1999;1: 1255–1263.

111. Zhang YE. Non-Smad pathways in TGF-beta signaling. Cell Res. 2009;19: 128–139. doi:10.1038/cr.2008.328

112. Khimji A-K, Shao R, Rockey DC. Divergent transforming growth factor-beta signaling in hepatic stellate cells after liver injury: functional effects on ECE-1 regulation. Am J Pathol. 2008;173: 716–727. doi:10.2353/ajpath.2008.071121

113. Schnabl B, Bradham CA, Bennett BL, Manning AM, Stefanovic B, Brenner DA. TAK1/JNK and p38 have opposite effects on rat hepatic stellate cells. Hepatol Baltim Md. 2001;34: 953–963. doi:10.1053/jhep.2001.28790

114. Masamune A, Satoh M, Kikuta K, Sakai Y, Satoh A, Shimosegawa T. Inhibition of p38 mitogen-activated protein kinase blocks activation of rat pancreatic stellate cells. J Pharmacol Exp Ther. 2003;304: 8–14. doi:10.1124/jpet.102.040287

115. Morin P, Wickman G, Munro J, Inman GJ, Olson MF. Differing contributions of LIMK and ROCK to TGFβ-induced transcription, motility and invasion. Eur J Cell Biol. 2011;90: 13–25. doi:10.1016/j.ejcb.2010.09.009

116. Ji H, Tang H, Lin H, Mao J, Gao L, Liu J, et al. Rho/Rock cross-talks with transforming growth factor-β/Smad pathway participates in lung fibroblast-myofibroblast differentiation. Biomed Rep. 2014;2: 787–792. doi:10.3892/br.2014.323

117. Horbelt D, Denkis A, Knaus P. A portrait of Transforming Growth Factor β superfamily signalling: Background matters. Int J Biochem Cell Biol. 2012;44: 469–474. doi:10.1016/j.biocel.2011.12.013

118. Pohlers D, Brenmoehl J, Löffler I, Müller CK, Leipner C, Schultze-Mosgau S, et al. TGF-beta and fibrosis in different organs - molecular pathway imprints. Biochim Biophys Acta. 2009;1792: 746–756. doi:10.1016/j.bbadis.2009.06.004

119. Lee JI, Wright JH, Johnson MM, Bauer RL, Sorg K, Yuen S, et al. Role of Smad3 in platelet-derived growth factor-C-induced liver fibrosis. Am J Physiol - Cell Physiol. 2016;310: C436–C445. doi:10.1152/ajpcell.00423.2014

120. Dooley S, ten Dijke P. TGF-β in progression of liver disease. Cell Tissue Res. 2012;347: 245–256. doi:10.1007/s00441-011-1246-y

121. Roy SG, Nozaki Y, Phan SH. Regulation of alpha-smooth muscle actin gene expression in myofibroblast differentiation from rat lung fibroblasts. Int J Biochem Cell Biol. 2001;33: 723–734.

122. Hu B, Wu Z, Phan SH. Smad3 mediates transforming growth factor-beta-induced alpha-smooth muscle actin expression. Am J Respir Cell Mol Biol. 2003;29: 397–404. doi:10.1165/rcmb.2003-0063OC

123. Krstić J, Trivanović D, Mojsilović S, Santibanez JF. Transforming Growth Factor-Beta and Oxidative Stress Interplay: Implications in Tumorigenesis and Cancer Progression. In: Oxidative Medicine and Cellular Longevity [Internet]. 2015 [cited 23 Feb 2018]. doi:10.1155/2015/654594

124. Ruef J, Rao GN, Li F, Bode C, Patterson C, Bhatnagar A, et al. Induction of rat aortic smooth muscle cell growth by the lipid peroxidation product 4-hydroxy-2-nonenal. Circulation. 1998;97: 1071–1078.

125. Albright CD, Salganik RI, Craciunescu CN, Mar M-H, Zeisel SH. Mitochondrial and microsomal derived reactive oxygen species mediate apoptosis induced by transforming growth factor-β1 in immortalized rat hepatocytes. J Cell Biochem. 2003;89: 254–261. doi:10.1002/jcb.10498

126. Herrera B, Murillo MM, Álvarez-Barrientos A, Beltrán J, Fernández M, Fabregat I. Source of early reactive oxygen species in the apoptosis induced by transforming growth factor-β in fetal rat hepatocytes. Free Radic Biol Med. 2004;36: 16–26. doi:10.1016/j.freeradbiomed.2003.09.020

127. Liu R-M, Gaston Pravia KA. Oxidative stress and glutathione in TGF-β-mediated fibrogenesis. Free Radic Biol Med. 2010;48: 1–15. doi:10.1016/j.freeradbiomed.2009.09.026

128. Arsalane K, Dubois CM, Muanza T, Bégin R, Boudreau F, Asselin C, et al. Transforming Growth Factor- β1 Is a Potent Inhibitor of Glutathione Synthesis in the Lung Epithelial Cell Line A549: Transcriptional Effect on the GSH Rate-limiting Enzyme γ -Glutamylcysteine Synthetase. Am J Respir Cell Mol Biol. 1997;17: 599–607. doi:10.1165/ajrcmb.17.5.2833

129. Bakin AV, Stourman NV, Sekhar KR, Rinehart C, Yan X, Meredith MJ, et al. Smad3–ATF3 signaling mediates TGF-β suppression of genes encoding Phase II detoxifying proteins. Free Radic Biol Med. 2005;38: 375–387. doi:10.1016/j.freeradbiomed.2004.10.033

130. Corcoran A, Cotter TG. Redox regulation of protein kinases. FEBS J. 2013;280: 1944–1965. doi:10.1111/febs.12224

131. Lin X, Duan X, Liang Y-Y, Su Y, Wrighton KH, Long J, et al. PPM1A functions as a Smad phosphatase to terminate TGFbeta signaling. Cell. 2006;125: 915–928. doi:10.1016/j.cell.2006.03.044

132. Whalen R, Rockey DC, Friedman SL, Boyer TD. Activation of rat hepatic stellate cells leads to loss of glutathione S-transferases and their enzymatic activity against products of oxidative stress. Hepatol Baltim Md. 1999;30: 927–933. doi:10.1002/hep.510300404

133. Griswold-Prenner I, Kamibayashi C, Maruoka EM, Mumby MC, Derynck R. Physical and Functional Interactions between Type I Transforming Growth Factor β Receptors and Bα, a WD-40 Repeat Subunit of Phosphatase 2A. Mol Cell Biol. 1998;18: 6595–6604.